A CYTOTOXIC ANTIBODY AGAINST HUMAN EMBRYONIC STEM CELLS

TAN HENG LIANG
B.Eng in Chemical Engineering (Hons.), National University of Singapore
M.Sc. in Chemical Engineering (with Specialization in Biopharmaceutical Engineering), National University of Singapore

A THESIS SUBMITTED
FOR THE DEGREE OF DOCTOR OF PHILOSOPHY

NATIONAL UNIVERSITY OF SINGAPORE
2011

A CYTOTOXIC ANTIBODY AGAINST HUMAN EMBRYONIC STEM CELLS

Supervisors:

Prof Lee Eng Hin
Prof Miranda Yap
A/P Andre Choo

Specially Dedicated to Prof Miranda Yap

To my family and friends

ACKNOWLEDGEMENT

This thesis is dedicated to everyone who have supported and believed in me through these arduous past 5 years. First, I would like to thank both supervisors Prof Lee and Prof Yap for their confidence in me, their continuous guidance and words of wisdom. My most sincere appreciation (no amount of words can describe it) to Andre who put his total trust in me to work on this project. He is both a great mentor and a great friend. I would like to thank him for his enormous amount of patience, constant guidance and for teaching me all the valuable research techniques for the past 8 years. As a friend, he is always willing to lend a listening ear and extend his help.

I would also like to thank all colleagues (past and present) in Bioprocessing Technology Institute for their assistance and making the institute an enjoyable place to work in. I would also like to express special thanks and gratitude to Jayanthi (also known as the Mama of Stem Cells) and Angela for their endless support and guidance through the 8 years in the Stem Cells Group, not forgetting Wey Jia and Vanessa. You girls, including Andre, are like a family to me!

Finally, I would like to give a big hug of appreciation to my family and friends for their support and patience. To Mom and Dad, thanks for taking care of the crazy dogs, settling all miscellaneous stuff on my behalf, providing all the emotional support and also for preparing my daily breakfast which I bring to work. To all my friends who stood by me and making my life fun, exciting and enjoyable, thank you!

TABLE OF CONTENTS

SUMMARY

Human embryonic stem cells (hESCs), derived from the inner cell mass of the blastocyst, are pluripotent and can differentiate into any tissue from the 3 germ layers. At the same time, these cells can proliferate indefinitely *in vitro* in the undifferentiated state under appropriate conditions. In recent years, stem cells have gained prominence because they potentially can be a source for replacement of cells and tissues that have been damaged in the course of disease, infection, trauma or congenital abnormalities.

Despite the immense potential hESCs hold for regenerative medicine, one of the most pertinent concerns using differentiated cells from hESCs is the presence of residual undifferentiated cells, which carry the risk of teratoma formation. Numerous studies have shown that undifferentiated hESCs can form teratomas in SCID mouse models. Furthermore, because the differentiation process is not 100% efficient, residual hESCs may remain in the differentiated cell product

To produce therapeutically useful cells, we need to characterize and understand hESCs through the identification of cellular components and pathways that govern their proliferation and differentiation. One of the ways to identify the receptors or antigens involved in hESC regulation is to utilize antibodies against hESC surface markers. Routinely, hESCs are characterized using antibodies targeting cell surface markers such as stage-specific embryonic antigen (SSEA-3 and -4), TRA-1-60 and TRA-1-81. However, these antibodies are not unique to hESCs as they were raised against 4- to 8-cell stage mouse embryos or embryonal carcinomas (EC).

Consequently, our group generated a panel of monoclonal antibodies (mAbs) targeting cell surface markers on undifferentiated hESCs by immunizing mice with intact live hESCs as the immunogen. These mAbs can potentially be used in the following ways:

(1) To discover novel hESC surface markers,

(2) To characterize the hESC populations and

(3) To separate the undifferentiated cells from the differentiated cells.

One of the antibodies from the panel, mAb 84 which is an IgM, is a novel cytotoxic monoclonal antibody, which selectively kills undifferentiated pluripotent stem cells (hESC and iPS cells) and not differentiated cells within 45 min of incubation *in vitro*.

By mass spectrometry, the antigen target of mAb 84 was identified as podocalyxin-like protein-1 precursor (PODXL), a highly glycosylated sialomucin with an apparent molecular weight of ~ 200 kDa. mAb 84 killing of hESCs was found to be independent of complement and temperature but was dependent on incubation time and concentration of antibody used. Upon incubation of hESCs with other antibodies to PODXL, we found that though all the mAbs bind to hESCs, only mAb 84 was cytotoxic. In addition, it was determined that mAb 84 binds to O-linked glycans on PODXL.

In SCID (Severe Combined Immunodeficiency) mice models, we showed that teratoma formation by hESCs *in vivo* was eliminated following treatment with mAb 84. This is compared to untreated cells which formed teratomas after 6-9 weeks post-injection. Concommitantly, when undifferentiated hESCs were treated with other hESC-specific mAbs from our panel *in vitro* and injected into SCID mice, teratomas formed as early as 7

weeks post-injection. These results suggest that the cytotoxic properties of mAb 84 on hESCs are epitope specific and not based only on binding to PODXL or to any surface antigens on hESCs. Preliminary studies also showed that treatment of spontaneously differentiating cells with mAb 84 was able to significantly delay the onset of tumor formation.

Mechanistically, treatment of hESCs with mAb 84 did not induce apoptosis because elevation of caspase activity and DNA fragmentation was not observed. Instead mAb 84 kills hESCs via a process similar to oncosis. Cell death was preceded by cell aggregation and examination of the cell surface by scanning electron microscopy (SEM) revealed the presence of pores and the aggregation of PODXL after mAb 84 treatment. Additionally, we hypothesize that the pore formation on the cell surface membrane was a consequence of the degradation of several cytoskeleton-associated proteins within 10 min of mAb treatment.

This is the first study on antibody-mediated oncosis which utilizes hESCs as a model. The significance of these findings is that this antibody can be used to eliminate contaminating hESCs and iPS cells from the differentiated cell population prior to clinical applications because teratoma formation *in vivo* would severely compromise the success of the transplant. This “clean-up” step prior to transplantation will increase the safety of this procedure and alleviate concerns over the use of hESCs and iPS cells as the starting cell population for cell therapy.

LIST OF TABLES

LIST OF FIGURES

CHAPTER 1 INTRODUCTION

1.1 Background

Human embryonic stem cells (hESCs) hold immense potential for regenerative medicine as they possess the dual properties of proliferating indefinitely and differentiating into cell types representing the 3 germ layers [1,2]. Studies have demonstrated that these cells can be differentiated to lineage-specific cell types, such as cardiomyocytes [3,4], insulin-producing cells [5-7], and neural–like cells [8-10]. However, there are several problems and safety concerns associated with the use of hESCs for cell-based therapies [1,11]. Firstly, hESCs have to be reproducibly differentiated into the specific cell types under a controlled environment. Subsequently, as the differentiation process is not 100% efficient, the cell type of interest has to be separated from residual cells prior to transplantation that are partially differentiated or remain undifferentiated. In the latter situation, the presence of residual undifferentiated hESCs in the transplant can potentially result in teratoma formation *in vivo* [1,11-13].

To produce therapeutically useful cells, we need to characterize and understand hESCs through the identification of cellular components and pathways that govern their proliferation and differentiation [14,15]. One of the ways to identify the receptors or antigens involved in hESC regulation is to utilize antibodies against hESC surface markers. Routinely, hESC are characterized using antibodies targeting cell surface markers such as stage-specific embryonic antigen (SSEA-3 and -4), TRA-1-60 and TRA-1-81. However, these antibodies are not unique to hESCs as they were raised

against 4- to 8-cell stage mouse embryos or embryonal carcinomas (EC) [16,17]. Consequently, our group generated a panel of monoclonal antibodies (mAbs) targeting cell surface markers on undifferentiated hESCs by immunizing mice with intact live hESCs as the immunogen. These mAbs can potentially be used in the following ways:

(1) To discover novel hESC surface markers,

(2) To characterize the hESC populations and

(3) To separate the undifferentiated cells from the differentiated cells.

One of the antibodies from the panel, mAb 84 which is an IgM, was found not only to bind but also kill undifferentiated hESCs. The ability of mAb 84 to selectively kill undifferentiated hESCs is extremely beneficial as mAb 84 can potentially be used to remove residual undifferentiated hESCs from differentiated cells prior to therapeutic applications.

1.2 Thesis Objective

As mentioned above, our group previously generated a panel of mAbs targeting cell surface markers on undifferentiated hESCs. From this panel of antibodies, mAb 84 which is an IgM, was identified to bind and kill undifferentiated hESC.

Having identified mAb 84 as a potentially good candidate to eliminate undifferentiated hESCs, further characterization of mAb 84 is essential before it can be effectively used. The objective of the research for this thesis is therefore to further define mAb 84 in the following areas:

(1) *In vitro* characterization of mAb 84,

(2) *In vivo* characterization of mAb 84 and,

(3) Elucidation of death mechanism of mAb 84.

1.2.1 *In vitro* characterization of mAb 84

First, the identity of the antigen target on hESCs will be identified through immuno-precipitation with mAb 84 followed by mass spectrometry analysis. Subsequently, other antibodies to the identified antigen will be tested to determine if these other antibodies are also cytotoxic to undifferentiated hESC. Work will also be carried out to investigate the effect of complement, temperature and concentration of antibody used on the cytotoxicity of mAb 84 on hESCs. The kinetics of mAb 84 killing on hESCs will also be studied. The specificity of mAb 84 will be assessed by comparing the binding and cytotoxicity of mAb 84 on undifferentiated hESCs and spontaneously differentiated hESCs either cultured in the absence of FGF-2 or as hESC-derived embryoid bodies (EBs). We will also proceed to investigate if the binding of mAb 84 to the identified antigen is dependent on post-translational modifications, namely; N-linked and O-linked glycosylation. Lastly, we will determine if mAb 84 is also cytotoxic to iPS cells.

1.2.2 *In vivo* characterization of mAb 84

Here, we will investigate if treatment of undifferentiated hESCs with mAb 84 *in vitro* will eliminate its ability to form teratomas *in vivo*. Other mAbs in our panel will also be compared to determine if the specificity to eliminate teratoma formation *in vivo* is unique to mAb 84. Apart from homogenous populations of hESCs, mixed cell populations of differentiated and undifferentiated hESCs generated either by differentiating hESCs into 5 day

EBs or culturing hESCs without FGF-2 for 12 days will also be evaluated for tumor formation and susceptibility to mAb 84.

1.2.3 Elucidation of death mechanism of mAb 84

The mechanism responsible for hESC-killing by mAb 84 will be elucidated. Briefly, we will determine if mAb 84 kills hESCs via apoptosis or oncosis and the hallmarks of cell death. Subsequently, the events that occur in mAb 84-mediated killing of hESCs will be identified.

1.3 Thesis Organization

The thesis comprises of seven chapters.

Chapter 1 describes the background and objectives of this research.

Chapter 2 is a review of literature and focuses on 4 main areas: (1) the importance of hESCs, (2) the concerns and safety issues of using hESC-derived cell products, (3) the various antibodies that induce cell death and (4) the different modes of cell death, namely; apoptosis and oncosis.

Chapter 3 details the materials and methods of the various experiments performed in this thesis.

Chapter 4 presents results on the characterization of mAb 84 *in vitro*. The antigen target of mAb 84 was identified as PODXL. The cytotoxicity of mAb 84 was independent of complement and temperature but dependent on incubation time and concentration of antibody used. Results also showed that mAb 84 killed iPS cells.

Chapter 5 presents data on the characterization of mAb 84 *in vivo*. The data showed that SCID mice injected with mAb 84-treated hESCs failed to

form teratomas compared to the untreated control or hESCs treated with other antibodies, where teratomas were observed after 7 weeks post-injection.

Chapter 6 elucidates the mechanism responsible for mAb 84 killing of hESC. Mechanistically, mAb 84 kills hESCs via oncosis.

Chapter 7 summarizes the results and conclusions of the thesis and discusses the possible directions and future work to be conducted.

CHAPTER 2 LITERATURE REVIEW

2.1 Origin and Application of Human Embryonic Stem Cells

Human embryonic stem cells (hESCs), derived from the inner cell mass of the blastocyst, are pluripotent stem cells and can potentially differentiate into any tissue representative of the 3 germ layers (Figure 2.1) [1,2,14,18]. At the same time, these cells can proliferate indefinitely *in vitro* in the undifferentiated state under the appropriate conditions [19,20]. In recent years, stem cells have come into prominence due to their abilities to proliferate and differentiate into specialized cells.

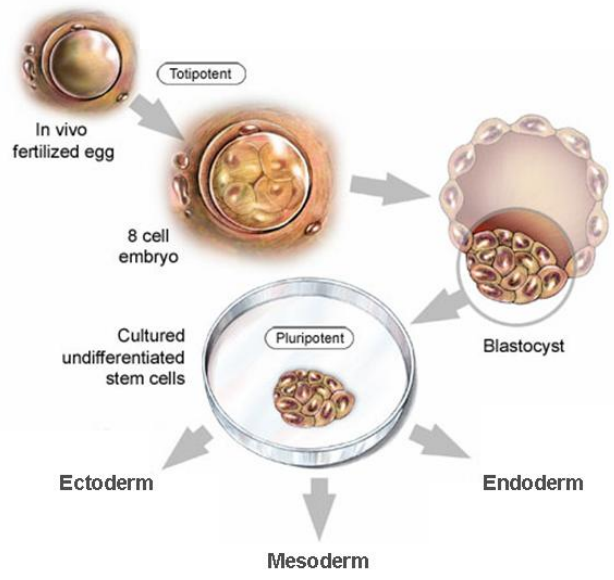

Figure 2.1 Origin of hESCs and their cell fate. Human embryonic stem cells are derived from the inner cell mass of the blastocyst. These cells have the capacity to differentiate into the three germ layers, namely; endoderm, mesoderm and ectoderm.

Potentially, stem cells may be a source of replacement for cells and tissues that have been damaged in the course of disease, infection or causes due to congenital abnormalities [1,2,14,18]. Studies by various groups have shown that hESCs can be differentiated into various cell types with the goal of using these hESC derivatives in transplantation to replace cells that have been terminated or crippled by diseases such as chronic heart disease, diabetes and Parkinson's disease. Some examples include cardiomyocytes, insulin-producing cells and neurons. He *et. al.* and Snir *et. al.* were able to reproducibly differentiate hESCs into cardiomyocytes [3,4] and these cells exhibited cardio-like characteristics such as action potential and ultra-structural maturation. Studies by D'Amour *et. al.* demonstrated that hESCs can be differentiated into insulin-expressing cells with an insulin content approaching that of adult islets [6]. Although their results were preliminary, these findings are critical steps for the development of a renewable source of cells for the treatment of diabetes. Several groups have also successfully differentiated hESCs into neurons with the aim of using these hESC-derived neurons for the treatment of neurological disorders [8-10]. Recently, Geron proceeded with the first human clinical trial using hESC-derived cells (http://www.geron.com) [21]. The therapeutic product, GRNOPC1, contains hESC–derived oligodendrocyte progenitor cells that have demonstrated remyelinating and nerve growth-stimulating properties leading to restoration of function in animal models with acute spinal cord injury [21,22]. Work is also being carried out to evaluate GRNOPC1 in various neuronal diseases such as Alzheimer's disease and Multiple Sclerosis.

These various studies using hESC-derivatives and Geron's clinical trial with GRNOPC1 highlight the immense potential of hESCs for regenerative therapy. However, numerous studies have shown that there are safety issues associated with the use of hESCs for cell-base therapies [1,11]. These safety concerns will be discussed in the following section.

More recently, an alternative source of pluripotent stem cells was reported by Takahashi *et. al.* and Yu *et. al.* [23,24]. Known as induced pluripotent stem (iPS) cells, these cells have the potential to proliferate indefinitely in culture and still retain their capacity for differentiation into a wide variety of cells [23,24]. Human fibroblasts are reprogrammed to iPS cells by transient over-expression of a small number of transcription factors [23,24]. In addition, these iPS cells have been shown to be comparable to hESCs in morphology, pluripotent marker expression and differentiation potential, including teratoma formation [23-27]. The derivation of iPS cells can potentially overcome two important obstacles associated with the use of hESC: immune rejection after transplantation and ethical concerns regarding the use of human embryos [25,26]. Like hESC, the presence of residual undifferentiated iPS cells in transplants can potentially result in teratoma formation *in vivo.*

2.2 Safety Concerns with hESC-based Therapies

Despite the immense potential hESCs hold for regenerative medicine, there remain safety concerns associated with the presence of residual hESCs in the differentiated cell product. Numerous studies have shown that undifferentiated hESCs can form teratomas in SCID mouse models

[1,2,13,19,20,28,29]. A study carried out by Hentze *et. al.* has shown that as few as 245 undifferentiated hESCs is sufficient for teratoma formation in SCID mice [12].

During differentiation, because the process is not 100% efficient, residual hESCs may remain in the differentiated cell product. In cell-based therapies utilizing hESC-derivatives, these residual hESCs contaminants could result in the formation of teratomas post transplant or grafting [1,11,21,30]. A study by Fujikawa *et. al.* showed that ES cell-derived insulin-expressing cells, when transplanted into SCID mice, formed teratomas leading to the failure of treatment for Type I diabetes [30]. In Geron's clinical trial with GRNOPC1, the process was placed on clinical hold after microscopic cysts were observed in animals post treatment (http://www.geron.com/GRNOPC1Trial/grnopc1-sec3.html). The presence of these cysts in the animals transplanted with GRNOPC1 caused much concern especially the possibility of teratoma formation [21]. In a prominent case study, a group of Israeli researchers reported that a boy with ataxia telangiectasia who had received several fetal neural stem cell transplants developed tumors in his brain and spinal cord four years after treatment [21,31]. This case study highlights the possibility of tumor formation not just from embryonic stem cells but also from other sources of stem cells (including fetal neural stem cells) and may prove to be a major stumbling block for cell-based therapies.

2.3 Solutions to Remove Residual hESCs from hESC-derivatives

As mentioned, hESCs exhibit potentially unlimited proliferation capacity combined with pluripotent differentiation capacity thus making them an attractive source of material for cell therapy applications [1,2,11]. One prerequisite for use in cell therapy is the enrichment of the desired cell type from unwanted lineages and the removal of potentially tumorigenic cells [1,11]. In a review by Hentze *et. al*., the various methods to eliminate unwanted cells and enrich for the desired cell type were summarized (Figure 2.2) [11]. One of the methods proposed is the use of specific antibodies to positively or negatively enrich for the desired cell population. An alternate method is to use of cytotoxic antibodies to directly kill residual undifferentiated hESCs. The following section provides examples on the use of cytotoxic antibodies to eliminate the respective target cells.

Selection Method	Principle	Advantages	Disadvantages	Example	Ref
(a) Positive selection					
Genetically engineered hESC	Transfection with a fusion gene consisting of a desired tissue-specific promoter driving a resistance gene	Stringent selection, many examples for proof-of-principle in mESC	Genetic manipulation introduces another level of complexity – regulatory concerns	α-cardiac myosin heavy chain promoter driving a neomycin resistance gene for cardiomyocyte enrichment from mESC	[41]
Selection by specific ectopic marker expression	Purification of the desired cell type with antibodies against specific cell surface markers	Highly stringent selection for clinical use	Antibody specificity is crucial, costs	FACS or MACS® sorting of $CD34^+$ human hematopoetic progenitor cells	[92]
Purification on physical properties	Separation of cells by density gradient centrifugation or differences in cell adherence	Easy to perform, inexpensive,fast	Low specificity and low yields of enrichment	Enrichment of cardiomyocytes derived from hESC	[93]
(b) Negative selection					
Genetically engineered hESC	Transfection with a fusion gene consisting of an undesired phenotype-specific promoter (e.g. *Oct-4*) driving a suicide gene	Highly selective elimination of undifferentiated, potentially harmful cells	Genetic manipulation introduces another level of complexity – regulatory concerns	Cell ablation by thymidine kinase expression in a non-selective manner	[78, 85]
Selection on specific ectopic marker expression	Removal of the undesired cell type with antibodies against specific cell surface markers	Highly selective elimination of undifferentiated, potentially harmful cells	Ensuring high sensitivity, costs	Use of well-characterized hESC surface antigens such as SSEA-4 and TRA-60, to remove pluripotent cells	[87]
Targeted elimination by cytotoxic antibodies	Incubation with antibodies targeting and eliminating only undifferentiated cells	Highly selective (depending on the antibody), simple to perform, no additional steps involved	Ensuring high sensitivity, costs	Use of new, cell death-related hESC-specific epitopes	[a]
Purification on physical properties	Separation of cells by density gradient centrifugation or by differences in cell adherence	Easy to perform, inexpensive, fast	Low specificity and low yields of enrichment	Undifferentiated cells eliminated by discontinuous gradient centrifugation	[94]
Elimination of pluripotent cells by cytotoxic drugs	Undifferentiated cells with high proliferation rate targeted by drugs (e.g. nucleoside analogues)	Easy to perform, inexpensive, fast	Only applicable to finally differentiated cell populations, dormant stem cells not targeted	Ceramide analogues induce apoptosis in pluripotent cells	[95]
(c) General manipulation					
Mitotical inactivation of the cell therapy product	Mitomycin C treatment blocks mitosis of the entire cell population	Easy to perform, inexpensive	Effects on the desired cell population unclear (e.g. integration into host tissue, long term survival)	ES cells differentiated to dopamine neurons and treated with Mitomycin C were in rodents and primates	[96]
Inducing differentiation of the remaining undifferentiated cells	Extended differentiation or an additional differentiation step by chemical induction to deplete remaining hESC (e.g. by retinoic acid)	Easy to perform, inexpensive	Efficiency of differentiation critical; undesired cell types are generated and might need to be removed	Unproven concept, but prolonged *in vitro* differentiation was shown to reduce teratoma formation	[83]

[a]Personal communication, A. Choo, BTI Singapore.

Figure 2.2 Various methods to eliminate unwanted cells and enrich for desired cell type.

2.4 Use of Cytotoxic Antibodies to Eliminate Target Cells

The use of various cytotoxic antibodies to eliminate target cells has been reported in many studies. The mAb, MEM-59, recognizes CD43 on hematopoietic progenitor cells (HPC) and kills the cells after 48 h of

incubation [32]. Another antibody, Rituximab, upon hyper-crosslinking with goat anti-human (GAH) secondary antibody induces cell death in non-hodgkin's lymphomas after 20 h of incubation [33]. There are also potent cytotoxic antibodies such as RAV12 which kills COLO 205 colon tumour cells within 30 min [34]. The mAb 14F7 kills L1210 murine tumour cell line within 3 h while anti-Porimin kills Jurkat cells within 20 mins of incubation [35,36]. Although these antibodies possess cytotoxic properties on their target cells, the death mechanisms induced are different. MEM-59 and Rituximab induce apoptosis while the RAV12, 14F7 and anti-Porimin caused the cells to die via oncosis. These different mechanisms of cell death will be described in greater detail in the later sections.

2.5 Various Phases and Modes of Cell Death

Cell death is important for normal development of an organism and is essential in the maintenance of tissue homeostasis [37,38]. Following a lethal injury, cells undergo 3 phases of cell death [39]:

(1) the 'pre-lethal' phase which is often reversible;

(2) the 'point-of-no-return' or cell death; and

(3) postmortem autolytic and degradative changes.

Following an injury, cells undergo a series of responses that collectively form a disease process. Many injuries to cells are sub-lethal in which the cells are able to survive in some altered or new steady state. Examples include vacuolization from dilatation of lysosomes and triglyceride accumulation. On the other hand, certain injuries, e.g. complete ischemia, are often lethal to cells and following a period of reversible reactions (pre-lethal

phase), the cells die and undergo a series of degradative reactions. The 2 common modes of cell death are apoptosis and oncosis [38-43].

2.6 Apoptosis

Apoptosis plays an essential role in the normal development and function of multicellular organisms such as cell deletion during embryonic development and balancing cell numbers in continuously renewing tissues. Dysregulation of apoptosis has been implicated in the development of several diseases like Alzheimers, cancer and auto-immune diseases [44].

The term ‘apoptosis’ was first introduced by John Kerr in 1972. This mode of cell death is associated with a distinct set of physical and biochemical changes to the cytoplasm, nucleus and the plasma membrane. Cells undergoing apoptosis exhibit a reduction in size and become granular. Changes to the plasma membrane (formation of ‘membrane blebs’) and cytoskeleton lead to the formation of apoptotic bodies that enclose fragments of nucleus and cytoplasm. The apoptotic bodies display phagocytic signals on the outer membrane and are subsequently engulfed and digested by phagocytes and neighbouring endothelial cells. Consequently, these cell corpses are cleared from the tissue and no inflammatory response is triggered during this process. The absence of inflammation is considered as the most characteristic feature of apoptosis compared to other modes of cell death [38,40,42,45].

2.6.1 Characteristics of apoptosis

Apoptosis is an organized and tightly controlled process. In most apoptosis models, cell death begins 12 to 24 h after the initiation of a trigger [41]. Cells undergoing apoptosis exhibit several biochemical modifications such as protein cleavage, protein cross-linking, DNA breakdown, and phagocytic recognition [38,42,45]. Table 2.1 summarizes the hallmarks of apotosis and the assays that can be carried out.

Table 2.1 Hallmarks of apoptosis and their respective assays.

Hallmarks	Assays
Caspase activation	**Measure of various caspase activity**
Phosphatidylserine externalization	**Annexin V detection**
DNA fragmentation	**TUNEL assay**

2.6.1.1 Activation of caspases

Caspases are widely expressed as inactive proenzymes in most cells. They have proteolytic activity and are able to cleave proteins at aspartic acid residues, although different caspases have different specificities involving recognition of neighboring amino acids [44-48]. Once activated, these caspases can activate other procaspases. Some procaspases can also aggregate and autoactivate. This proteolytic cascade, in which one caspase activate other caspases, amplifies the apoptotic signaling pathway and leads

to rapid cell death. Once caspases are activated, irreversible commitment towards cell death is inevitable. Caspases have also been identified and broadly categorized into initiators (caspase-2,-8,-9,-10) and effectors or executioners (caspase-3,-6,-7).

2.6.1.2 Exposure of phosphatidylserine (PS)

Another biochemical feature of apoptosis is the expression of cell surface markers that result in the early phagocytic recognition of apoptotic cells [45,49]. PS, normally sequestered in the inner plasma membrane, is externalized and displayed on the outer plasma membrane during apoptosis. PS can be detected with Annexin V, a recombinant PS-binding protein that interacts strongly and specifically with PS residues. Annexin V has been commonly used for the detection of early apoptosis [49,50].

2.6.1.3 Fragmentation of DNA

The formation of distinct DNA fragements is a biochemical hallmark of late apoptosis as depicted in Figure 2.3a [44,45,51,52]. The caspase-activated DNase (CAD) is inactivated when it is bound to the inhibitor, iCAD (Figure 2.3b). During apoptosis, iCAD is cleaved by caspases which leads to the release of the active endonuclease CAD. CAD enters the nucleus where it degrades the chromosomal DNA and produces the characteristic internucleosomal DNA cleavage or ‘laddering’ of DNA on agarose gel electrophoresis [44,52,53].

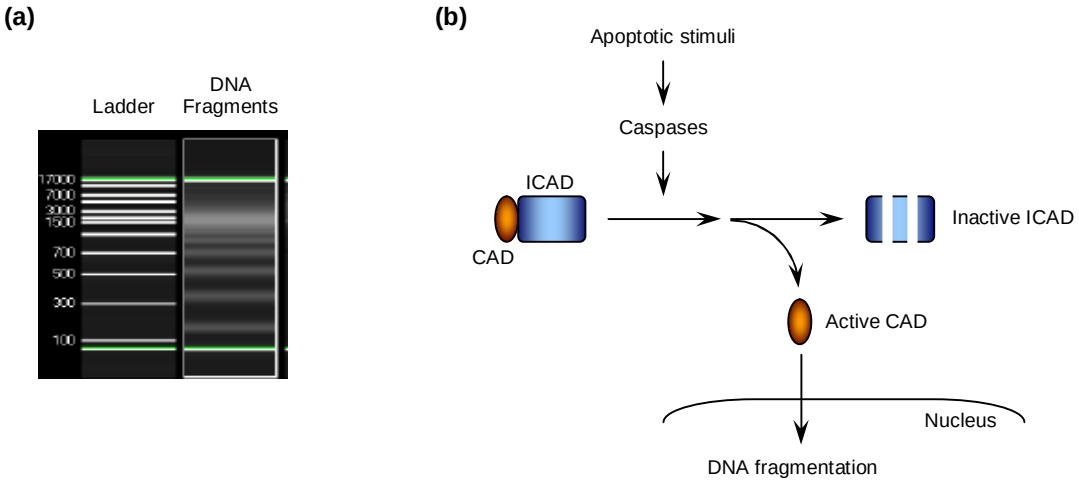

Figure 2.3 DNA fragmentation during apoptosis. (a) Laddering of DNA fragments on an agarose gel electrophoresis. (b) CAD is cleaved from iCAD by caspases during apoptosis. Activated CAD translocates to the nucleus and degrades chromosomal DNA.

Terminal deoxynucleotidyl transferase dUTP nick end labeling (TUNEL) is a common method for detecting DNA fragmentation that results from apoptotic signaling cascades [54]. The assay relies on the presence of nicks in the DNA which enables the enzyme, terminal deoxynucleotidyl transferase (TDT), to catalyze the addition of dUTPs that are secondarily labeled with a marker.

2.7 Apoptosis and Programmed Cell Death

Apoptosis has been used synonymously with programmed cell death. However, programmed cell death is strictly not apoptosis [42]. Programmed cell death received its name before apoptosis and it refers to situations in which cells are programmed to die at a fixed time. As pointed out by Majno and Joris, not all cell death occurring in the course of normal animal development have apoptotic features [37]. Thus, as originally intended, programmed cell death describes the inclusive phenomena of all cell deaths

that occur normally in the development of a species, with highly reproducible timing and location [41]. In other words, when programmed cell death occurs, the death mode can be either apoptosis or oncosis.

2.8 Oncosis

Oncosis (derived from the word “onkos” which means swelling) was proposed in 1910 by von Reckling-hausen to describe a form of cell death distinct from apoptosis [42,55,56]. It generally represents a response to gross injury and can be induced by an overdose of cytotoxic agents [55,56]. Oncosis usually occurs within seconds to minutes following application of the injury and the early changes include marked alterations in cell shape and volume [39,57]. Oncotic cell death is characterized by cell swelling, organelle swelling, vacuolization and increase in membrane permeability [39,42,55,57]. The molecular and biochemical mechanisms underlying oncosis are still unclear. Some studies have shown that oncosis is caused by failure of the ionic pumps of the plasma membrane and decreased levels of cellular ATP [37,39,42,55,57].

2.8.1 Characteristic of oncosis

The characteristics of oncotic cell death are summarized in Table 2.2.

Table 2.2 Hallmarks of oncosis and their respective assays.

Hallmarks	Assays
Rapid cell death, occurs within seconds to minutes	**-**
Progressive increase in membrane permeability	**Uptake of trypan blue/propidium iodide; uptake of dextran beads of various molecular weights (MW)**
Leakage of intracellular constituents	**Change in lactate dehydrogenase (LDH) concentration**
Cytoskeleton protein denaturation	**Detection of cytoskeleton proteins - western blotting**
Pore formation of plasma membrane	**Scanning electron microscopy**

2.8.1.1 Rapid cell death

In apoptosis, cell death occurs between 12 h to 24 h post initiation [41]. Koopman *et. al*. showed that when B cells were induced to undergo apoptosis upon culture at low serum concentration, subpopulation of the cells were stained positive for Annexin V after 56 h, indicating the start of apoptosis [50]. In another study by Zhang *et. al.*, hyper-crosslinking of Rituximab with goat anti-human (GAH) secondary antibody or with Dynabeads or dextran polymer,

induced apoptosis in non-Hodgkin's lymphomas [33]. The incubation time required was between 18-20 h.

On the contrary, in oncosis, cell death can occur as fast as seconds or minutes [39,57]. When renal proximal tubules (RPT) were incubated under anoxia, PI uptake occurred as fast as 5 min and the release of LDH from the cells was observed as quickly as 15 min [58]. The mAb, anti-Porimin, kills Jurkat cells via oncosis and cell death occurs within 20 min of incubation [36].

2.8.1.2 Increase in membrane permeability

During oncosis, the cells experience progressive increase in membrane permeability [42,58,59]. Chen *et al.* demonstrated 3 different permeability phases in freshly isolated rabbit renal proximal tubules (RPT) subjected to anoxia. Their results demonstrated that anoxia increases the permeability of the plasma membrane in a time- and size- dependent manner. The first phase allowed the entry of propidium iodide (PI, a cell-impermeable DNA dye, MW 668 Da). The second phase allowed the entry of dextrans up to 3 kDa, and the last phase allowed the entry of 70-kDa dextrans and the release of cytosolic enzymes, such as LDH (MW=130 kDa). Similar plasma membrane permeability changes were observed in Madin-Darby canine kidney (MDCK) cells and hepatic sinusoidal endothelial cells when they were exposed to chemical hypoxia [60,61]. As a consequence of the increase in membrane permeability during oncotic cell death, release of intracellular constituents such as LDH was observed [58,59,62]. Similar LDH releases during oncosis were also reported by Ma *et. al.* and Liu *et. al.* [57].

2.8.1.3 Protein denaturation

During oncosis, protein hydrolysis and/or denaturation occurs [42]. Recent studies have linked the progressive membrane permeability changes during oncosis to proteolysis of cytoskeletal proteins, such as α-actinin, paxillin, talin and vinculin [55]. In a study by Liu et. al., when RPT cells were exposed to hypoxia for 30 min or treated with antimycin A for 30 min, degradation of α-actinin, paxillin, talin and vinculin was observed [62]. In addition, there are growing evidences that the proteolysis of these cytoskeletal proteins are mediated by calpains, a family of 14 Ca^{2+}-activated cysteine proteases [38,55,62-65].

2.9 Apoptosis, Oncosis and Necrosis

In the review by Majno and Joris, they described that necrosis is not a form of cell death, but refers to the morphological alterations secondary to cell death by any mechanism, including apoptosis [38,40,42]. In other words, necrosis defines the postmortem cellular changes [39]. On the other hand, oncosis and apoptosis are 2 forms of cell death, which leads to necrosis [38,40,42]. Apoptosis and oncosis are therefore pre-mortal processes, while necrosis is a post-mortal condition. Figure 2.4 illustrates the relationship between apoptosis, oncosis and nerosis [38].

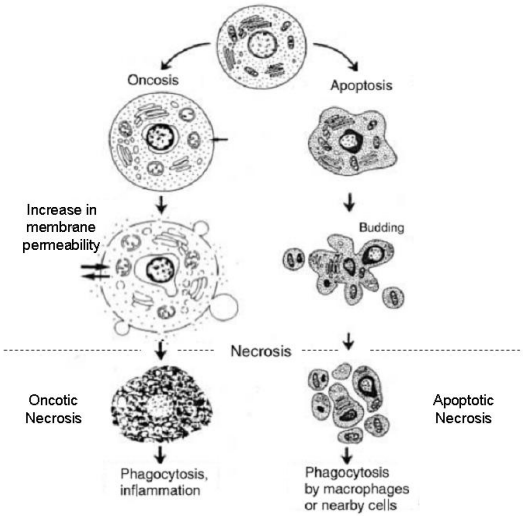

Figure 2.4 Illustration of apoptosis and oncosis as described by Majno and Joris. Apoptosis and oncosis are 2 forms of cell death; whereas necrosis is the end stage of either cell death. At necrosis, cell death by apoptosis or oncosis is termed as apoptotic necrosis or oncotic necrosis respectively.

2.10 Apoptosis Versus Oncosis

Recent studies have demonstrated that in response to a given death stimulus, there is often a continuum of apoptosis and necrosis. Many insults induce apoptosis at lower doses and necrosis at higher doses. Even in response to a certain dose of death-inducing agent, features of both apoptosis and necrosis may coexist in the same cell [37]. Nonetheless, apoptosis and oncosis are 2 forms of cell death which bear distinct different characteristics. Table 2.3 summarizes the differences between apoptosis and oncosis [37,45].

Table 2.3 Differences between apoptosis and oncosis.

Apoptosis	Oncosis
Cell death occurs between 12-24 hr	Rapid cell death, occurs within seconds to minutes
Cell shrinkage	Cell swelling
Plasma membrane integrity maintained	Plasma membrane integrity lost
Ordered DNA degradation	Random DNA degradation
Cytoplasm retained in apoptotic bodies	Cytoplasm released
No inflammation	Inflammation usually present

2.11 Antibody-induced Cell Death

Many reports have shown that cell death can be induced when cells are incubated with specific antibodies (Section 2.4). The mechanism of these antibody-mediated cell deaths can be either apoptosis or oncosis which are described in the following sections.

2.11.1 Antibody-induced apoptosis

Bazil *et. al.* showed that the monoclonal antibody, MEM-59, induced apoptosis in hematopoietic progenitor cells (HPC) after incubation [32]. MEM-59 recognizes CD43, an adhesion molecule highly expressed on HPC. After

48 h of incubation with the antibody, the phenotype of HPC was characteristics of apoptosis such as cell shrinkage and DNA fragmentation (Figure 2.5).

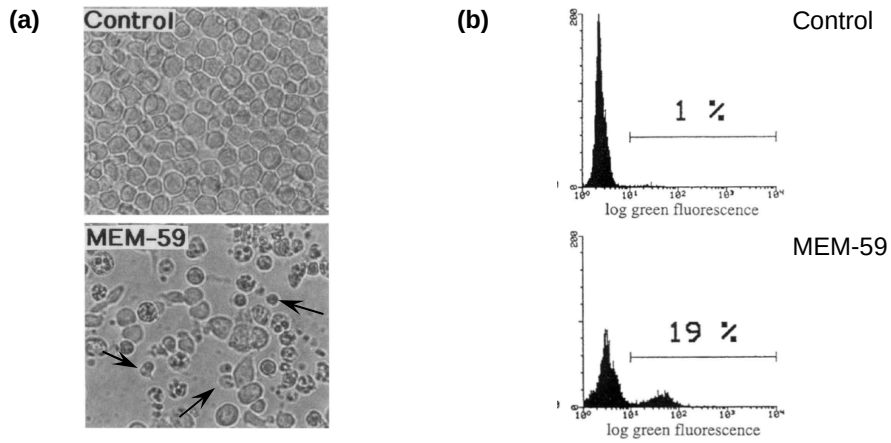

Figure 2.5 MEM-59 induces apoptosis in HPC [32]. After 48 h incubation with MEM-59, HPC shows characteristic of apoptosis. Apoptotic HPC (a) undergoes cell shrinkage as indicated by the black arrows, (b) shows marked increase in DNA fragmentation (increase in fluorescence level) via terminal deoxynucleotidyl transferase assay.

In another study by Zhang *et. al.*, hyper-crosslinking of Rituximab with goat anti-human (GAH) secondary antibody or with Dynabeads or dextran polymer, induced apoptosis in non-Hodgkin's lymphomas [33]. The incubation time required was between 18-20 h and the cells exhibited apoptotic characteristics such as PS exposure (as detected by Annexin V), DNA fragmentation and increase in caspase-3 activity (Figure 2.6). In addition, Rituximab hyper-crosslinked with dextran polymer was able to cause marked tumour regression in their xenograft model (Figure 2.7).

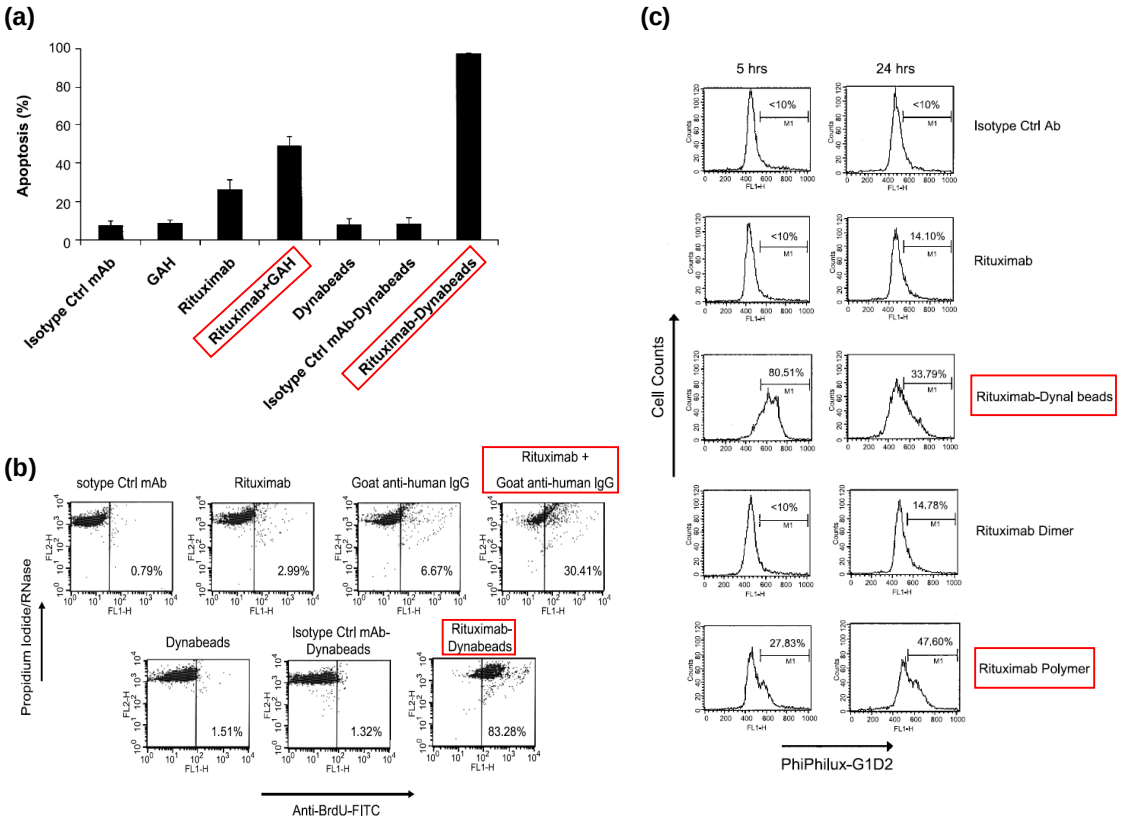

Figure 2.6 Hyper-crosslinked Rituximab induces apoptosis in non-Hodgkin's lymphomas [33]. After 18-20 h incubation with hyper-crosslinked Rituximab, non-Hodgkin's lymphomas show characteristic of apoptosis. Treatment with hyper-crosslinked Rituximab are boxed in red. (a) Apoptotic cells as determined by PS exposure. (b) DNA fragmentation via TUNEL. (c) Measure of caspase-3 activity.

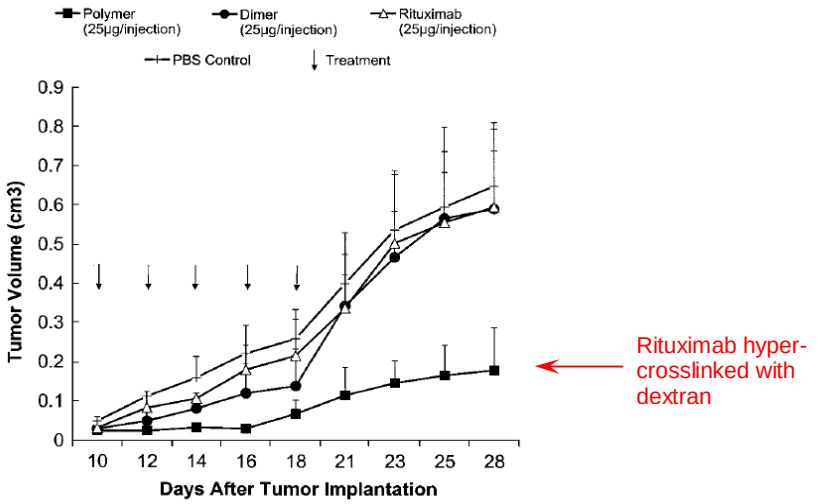

Figure 2.7 Rituximab hyper-crosslinked with dextran causes tumour regression in xenografts [33].

2.11.2 Antibody-induced oncosis

There are also reports of antibodies inducing oncotic cell death. RAV12 (IgG1 subclass) is a chimeric mAb derived from the parental mAb KID3. Both antibodies exhibit potent cytotoxic activity *in vitro* against COLO 205 colon tumor cells [34]. Interestingly, RAV12-mediated cytotoxicity requires the cross-linking of cellular components: Fab fragments of RAV12 did not induce cytotoxicity, whereas cross-linking of the Fab fragments with a secondary antibody restored the cytotoxic activity to the level of the intact antibody.

Following RAV12 and KID3 treatment of COLO 205 cells *in vitro,* the cells undergo oncosis. Microscopic examination revealed that there was rapid swelling within 1 h following RAV12 treatment (Figure 2.8a). Double staining for RAV12 and filamentous-actin showed that RAV12 associated with the plasma membrane and treatment with RAV12 caused disruption of the actin cytoskeleton (Figure 2.8a). Time-lapse microscopy also revealed that cellular swelling led to membrane leakage following treatment with KID3 (Figure

2.8b). Consequently, elevated LDH was detected in the medium within 30 min of antibody treatment, indicative of membrane rupture. In addition, RAV12 was able to inhibit tumour growth *in vivo*.

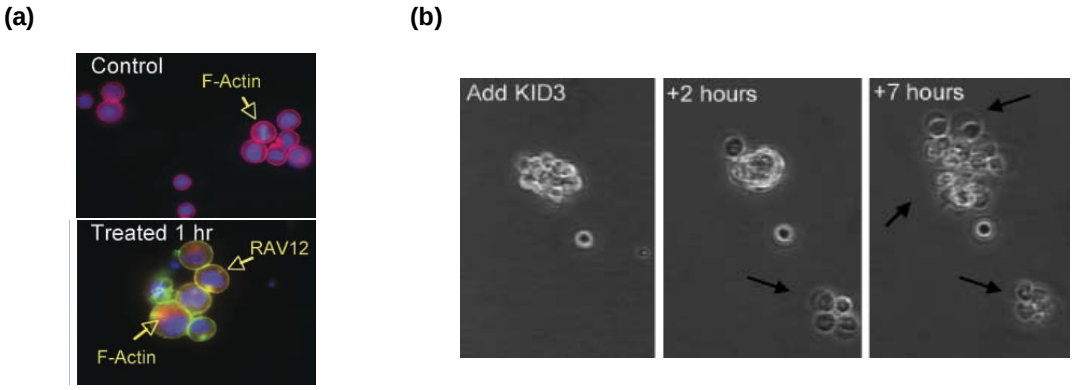

Figure 2.8 RAV12 and KID3 induces oncosis in COLO 205 colon tumour cells [34]. (a) Swelling of cells and disruption of actin after 1 h treatment with RAV12. (b) KID3 causes cell swelling as indicated by the arrows.

The cell death following KID3 treatment did not exhibit markers of apoptotic cell death. The KID3 treated cells did not exhibit Annexin V staining and DNA fragmentation or changes in cell cycle.

Two other examples of antibodies that kill cells via oncosis [35,36] are mAbs 14F7 and anti-Porimin. The mAb 14F7 kills L1210 murine tumour cell line within 3 h of incubation while anti-Porimin kills Jurkat cells within 20 min of incubation. In both studies, the cell death mechanism was independent of complement and did not resemble apoptosis (no DNA fragmentation or caspase activation was observed). However, both antibodies caused increase in cell membrane permeability as evident from PI uptake. Interestingly, cells treated with the two antibodies underwent rapid and apparent cell aggregation and the formation of pores on the cell membrane were visualized under scanning electron microscope (SEM) (Figure 2.9). Similar to RAV12, the mAb

14F7-induced cell death also involved the re-arrangement of cytoskeletal proteins.

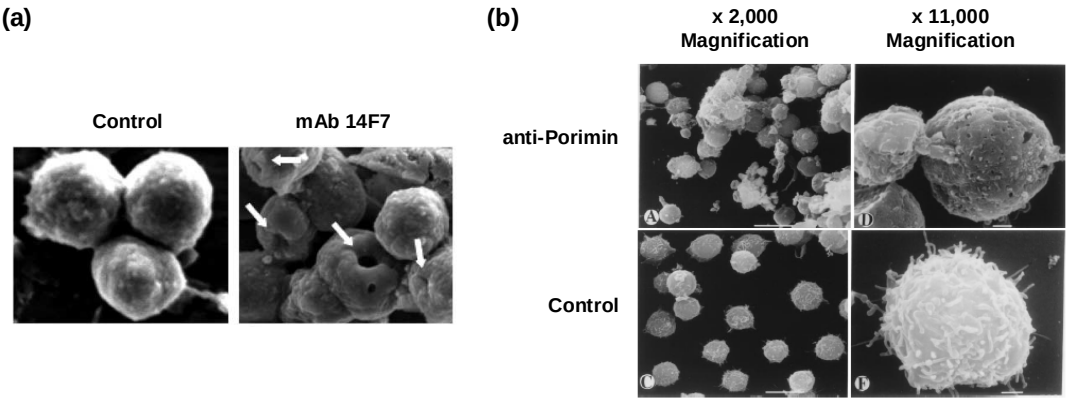

Figure 2.9 Formation of pores through cell membrane and cell aggregation during oncosis. In both studies, cells treated with antibodies experienced rapid and apparent cell aggregation, and formation of pores through the cell membrane as opposed to the control. (a) L1210 murine tumour cell line after treatment with mAb 14F7 [35]. (b) Jurkat cells after treatment with anti-Porimin [36].

2.12 Summary

Despite the immense potential hESCs hold for regenerative medicine, safety concerns associated with the presence of residual hESCs in the differentiated cell product remains. Studies have shown that undifferentiated hESCs can form teratomas in SCID mouse models and as few as 245 undifferentiated hESCs is sufficient for teratoma formation in SCID mouse [12]. To make hESC-derivative products safer for cell-based therapies, several methods were proposed. One of the methods proposed is to use specific antibodies to positively or negatively select for the desired cell population. An alternate method is to use cytotoxic antibodies to directly kill residual undifferentiated hESCs. Cytotoxic antibodies that kill cells via apoptosis or oncosis have been used to eliminate undesired cells in many studies.

CHAPTER 3 MATERIALS AND METHODS

3.1 Cell Culture

3.1.1 Human embryonic stem cells and induced pluripotent stem cells

Human embryonic stem cells line, HES-3 (46 X,X) was obtained from ES Cell International (ESI). The cells were cultured at 37^{o}C/5% CO_2 on matrigel-coated culture dishes supplemented with conditioned media (CM) from immortalized mouse feeders, ΔE-MEF [19]. The media used for culturing hESCs was KNOCKOUT (KO) media which contained 85% KO–DMEM supplemented with 15% KO serum replacer, 1 mM L-glutamine, 1% nonessential amino acids, 0.1 mM 2-mercaptoethanol, and 5 ng/mL of recombinant human fibroblast growth factor-2 (FGF-2) (Invitrogen). The hESC cultures were passaged as described previously [19,20]. Briefly, once the cultures reached confluency, the cells were enzymatically treated with collagenase IV (200 U/mL) and dissociated into small clumps (~100 to 1000 cells/clump) by repeated pipetting, after which the cells were reseeded at a 1:4 split ratio on fresh matrigel-coated culture dishes. Culture dishes were pre-incubated at 4^{o}C overnight with matrigel (Becton Dickinson) diluted in cold KO–DMEM (1:30 dilution).

Induced pluripotent stem cells, ESIMR90 and ES4SKIN reprogrammed from fetal lung fibroblastsand neonatal foreskin fibroblasts respectively, were obtained from Prof James Thomson [66,67]. The iPS cells were cultured as described for hESC, with the exception that 100 ng/ml of FGF-2 was supplemented to the CM instead of 5 ng/ml.

3.1.2 Mouse embryonic fibroblast and conditioned media (CM)

Monolayers of immortalized mouse embryonic fibroblast, ΔE-MEF, were grown to confluency in T-flasks and treated with 10 μg/ml mitomycin-C for 2.5-3 h. Following treatment, cells were detached with 0.25% trypsin-EDTA, seeded onto culture dishes at a density of 8 x 10^4 cells/cm^2 and incubated overnight to facilitate adhesion[20], after which the feeders were equilibrated in KO media and CM was collected every 24 h after the addition of fresh KO media [19]. The CM was clarified by filtration (0.22 μm) and supplemented with 5 ng/ml of FGF-2 prior to addition to hESC cultures.

3.1.3 IMR90 fibroblasts and Foreskin fibroblasts

IMR90 (CCL-186™) and Foreskin fibroblasts (CRL-2522™) were obtained from ATCC and were cultured in medium consisting of 90% DMEM high glucose, 10% FBS, 2mM L-glutamine, 25U/ml penicillin and 25 g/ml streptomycin (Invitrogen). Upon confluency, cells were washed in PBS, detached with 0.25% trypsin–ethylene-diamine tetraacetic acid (EDTA), and re-plated at a ratio of 1:4.

3.2 Spontaneous Differentiation of hESC

To induce hESC differentiation *in vitro*, hESCs were harvested as clumps and cultured as embryoid bodies (EB) for 8 days in EB-medium (80% KO-DMEM, 20% FCS, 25 U/ml penicillin, 25 μg/ml streptomycin, 2 mM L-glutamine, 0.1mM NEAA, and 0.1 mM 2-mercaptoethanol) on non-adherent suspension culture dishes (Corning). Subsequently, the EB were dissociated

with trypsin and plated on gelatinized culture dishes [68]. Alternatively, hESCs were cultured as described in Section 3.1.1 but in the absence of FGF-2.

3.3 Flow Cytometry Analysis

Cells were harvested as single cell suspensions using trypsin, resuspended at 2 x 10^5 cells per 10 µl volume in 1% BSA/PBS and incubated for 45 min with each mAb clone (150 µl culture supernatant or 5 µg purified mAb in 200 µl 1% BSA/PBS) or mAb to TRA-1-60 (2.5 µg in 200 µl 1% BSA/PBS, Chemicon, MAB4360), human podocalyxin (PODXL, R&D systems) and polyclonal antibody (pAb) to human PODXL (5 µg in 200 µl 1% BSA/PBS, R&D systems). Cells were then washed with cold 1% BSA/PBS, and further incubated for 15 min with a 1:500 dilution of goat α-mouse antibody FITC-conjugated (DAKO). After incubation, the cells were again washed and resuspended in 1% BSA/PBS and 1.25 mg/ml propidium iodide (PI) for analysis on a FACScan (Becton Dickinson FACS Calibur).

For analysis of TRA-1-60 and PODXL co-expression, hESCs were incubated with anti-TRA-1-60 primary antibody (10 g/ml, Chemicon) and washed with 1% BSA/PBS as described previously. Cells were then incubated for 15 min with a 1:200 dilution of goat α-mouse antibody APC-conjugated (BD Pharmingen) followed by a wash. Finally, the cells were incubated with AlexaFluor®488-labeled-mAb 84 (25 g/ml) for an additional 15 min, washed and resuspended in 1% BSA/PBS for analysis.

For triple staining of hESCs, cells were incubated with AlexaFluor®488-labeled-mAb 84 (25 g/ml) and AlexaFluor®647-labeled-TRA-1-60 for 45 min at 4^{o}C. After incubation, the cells were washed and

resuspended in 1% BSA/PBS and 1.25 mg/ml propidium iodide (PI) for analysis on a FACScan (Becton Dickinson FACS Calibur).

3.4 Conjugation of Antibodies to Alexafluor

Labeling of antibodies was carried out with AlexaFluor® 488 and AlexaFluor® 647 Monoclonal Antibody Labeling Kit (Molecular Probes). 100 µl of purified antibody (1mg/ml) was mixed with the vial of reactive dye and incubated for 1 h at room temperature. The reaction solution was subsequently loaded onto the supplied purification column and the purified AlexaFluor®488-conjugated mAb was collected in the flow through.

3.5 Cytotoxicity Assay

Cytotoxicity of mAb 84 on hESCs was evaluated using propidium iodide (PI) exclusion assays and flow cytometry. Cells were harvested as single cell suspensions using trypsin, resuspended at 2 x 10^5 cells per 10 µl volume in 1% BSA/PBS and incubated for 45 min with each mAb (150 µl culture supernatant or 5 µg purified mAb in 200 µl 1% BSA/PBS). Thereafter, cells were washed and resuspended in 1% BSA/PBS containing 1.25 mg/ml propidium iodide (PI) and analyzed on a FACScan (Becton Dickinson FACS Calibur) with detection emission in the FL-3 channel. As controls, cells were incubated either with the isotype control, mAb 85, or not treated with any antibodies. All incubations were performed at 4^{o}C unless otherwise indicated.

For hypercross-linking experiments, hESCs after primary mAb incubation were washed and further incubated with a goat α-mouse secondary antibody (5 µg in 200 µl 1% BSA/PBS, DAKO) for 45 min. The

commercially available primary antibodies used were mAb to human PODXL or pAb to human PODXL (5 µg in 200 µl 1% BSA/PBS, R&D systems). For dosage studies, hESCs were incubated with 0.1, 0.5, 1, 5 and 15 µg purified mAb 84 in 200 µl 1% BSA/PBS. For time course studies, HES-3 cells were incubated with 5 µg purified mAb 84 in 200 µl 1% BSA/PBS and harvested for analysis at 15, 30 and 45 min after addition of the mAb. As a negative control, cells were incubated with the isotype control, mAb 85. All incubations were performed at 4^{o}C unless otherwise indicated. To validate the results obtained using PI exclusion assays, viability for each sample was also determined using trypan blue exclusion.

3.6 Small Scale Purification of mAb 84 and mAb 85

mAb 84 (~100 µg) was directly captured onto Protein A PhyTip® columns (5 µl resin bed). For mAb 85 purification, biotinylated rabbit-anti-mouse-anti-IgM (1:20 dilution in PBS, Open Biosystems) was first bound to Streptavidin PhyTip® columns (5 µl resin bed) and mAb 85 (~100 µg) was subsequently captured. After washing away the unbound proteins with Wash Buffer I (10 mM NaH_2PO_4/140 mM NaCl pH 7.4), the antibodies were eluted at low pH with Elution Buffer (200 mM NaH_2PO_4/140 mM NaCl pH 2.5) and neutralized immediately with 1 M Tris-Cl pH 9.0. Total antibody concentration was quantified with DC Protein Assay (Bio-Rad Laboratories).

3.7 Immuno-precipitation

hESCs were grown to confluence in 6 cm Petri dishes (Falcon) and lysed by scraping in 2% Triton/PBS+. The cell lysate was clarified by centrifugation and used immediately for immunoprecipitation (IP). IP of the antigen was carried out using the automated MEA system (Phynexus, Inc). Briefly, mAb 84 (~100 µg) was directly captured onto Protein A PhyTip® columns (5 µl resin bed). After washing away the unbound proteins with Wash Buffer I (10 mM NaH_2PO_4/140 mM NaCl pH 7.4), clarified cell lysate from 5 x 10^6 cells was passed through the column functionalized with mAb 84. The column was further washed with Wash Buffer II (140 mM NaCl pH 7.4) and bound proteins were eluted at low pH with Elution Buffer (200 mM NaH2PO4/140 mM NaCl pH 2.5) and neutralized immediately with 1 M Tris-Cl pH 9.0. The eluate was stored at 4^oC for further analysis.

3.8 SDS–PAGE and Western Blot Analysis

Samples were separated by SDS-PAGE (NuPAGE 4-12% gradient gel, Invitrogen) under reducing conditions followed by either Western blotting or silver staining. For Western Blotting, resolved proteins were transferred onto PVDF membrane (Millipore) at 110 V for 75 min and immunoblotted with appropriately diluted antibodies in PBS containing 2.5% skim milk and 0.05% Tween 20, followed by goat α-mouse antibodies HRP-conjugated (1:10000 dilution, DAKO). Bound antibodies were detected by ECL (Amersham). Silver staining was performed using SilverQuest silver staining kit (Invitrogen) according to the manufacturer's protocol and the protein band corresponding

to the band on the Western Blot was manually excised for mass spectrometry analysis.

For cytoskeleton degradation assay, hESCs were incubated with the mAbs for 45 min, harvested and lysed with 2% Triton X-100 (Bio-Rad Laboratories) in PBS+. The lysates were clarified via centrifugation, total protein concentration quantified with DC Protein Assay (Bio-Rad Laboratories) and Western blot analysis carried out as described. For time course studies, the cells were incubated with the mAbs and at every 10 min interval, cells were harvested and lysed prior to Western blot analysis. The antibodies used for immunoblotting were anti-actin, anti-α-actinin, anti-paxillin, anti-talin, anti-vinculin, anti-integrin-β-1, anti-focal adhesion kinase (FAK) and anti-α/β-tubulin (Millipore). Anti-NHERF-1/2 and anti-ezrin were purchased from Santa Cruz and Invitrogen respectively.

3.9 Validation of Target Antigen

IP of PODXL with mAb 84 was carried out as described and Western blot analysis was subsequently performed. The primary antibodies used for validating the target antigen of mAb 84 were mAb to human PODXL or pAb to human PODXL (1:200 dilution, R&D systems).

3.10 Mass Spectrometry Analysis

The excised gel band was soaked overnight at 4^{o}C in washing solution (2.5 mM ammonium bicarbonate in 50% acetonitrile) followed by 20 min incubation at 37^{o}C after a change in washing buffer. The excised gel was then subjected to in-gel proteolysis with trypsin following reduction and s-alkylation

of cysteine residues with iodoacetamide. Extracted peptides were subjected to analysis using mass spectrometry as described but with the following modifications [69]. The analysis was performed on a QSTAR-XL (Applied Biosystems/Sciex) using Information Dependent Acquisition (IDA) mode under control of the Analyst-QS software v1.1. Each multiply-charged (2+ to 4+) parent mass ion with a threshold greater than 8 counts/sec within a mass range of 300 and 2000 amu was selected for fragmentation and subsequent MS/MS analysis using nitrogen gas at a setting of 4 and the collision energy set to automatic allowing increasing energy with increasing ion mass. Proteins were identified by searching the raw data files (*.wiff*) against the human subset of the UniProt database (EBI) using the Mascot search engine (Matrix Science).

3.11 Removal of N-link Glycans

IP of PODXL with mAb 84 was carried out as described and removal of N-link glycans was carried out with PNGase F (New England Biolabs). 20 µg of glycoprotein was denatured in 1x Glycoprotein Denaturing Buffer at 100^{o}C for 10 min. Subsequently, one-tenth volume of 10x G7 Reaction Buffer and 10% NP-40 was added and incubated with 5 µl PNGase F at 37^{o}C for an hour. Western blot analysis was carried out on the deglycosylated protein.

3.12 Removal of O-link Glycan

Removal of O-link glycans was performed with E-DEGLY kit (SIGMA). Briefly, 20 µg of purified glycoprotein was topped up with deionized water to 30 µl in a microcentrifuge tube. 10 µl of 5x Reaction Buffer and 2.5 µl of

Denaturing Solution was added and incubated at 100^{o}C for 5 min. The mixture was cooled to room temperature and 2.5 µl TRITON X-100 was added. 1 µl of α-2(3, 6, 8, 9) Neuraminidase was added and incubated for 3 h at 37^{o}C to remove terminal salic acid. Next, the mixture was incubated with 1 µl PNGase F for an additional 3 h at 37^{o}C to remove N-link glycans. Finally, the mixture was incubated for another 3 h at 37^{o}C with 1 µl O-Glycosidase, 1 µl β(1-4)Galactosidase and 1 µl β-N-Acetylglucosaminidase to remove O-link glycans. Removal of the respective glycans after each incubation step was assessed by Western blot analysis.

3.13 *In vivo* SCID mouse Teratoma Model with hESCs

To test the teratoma-forming potential of hESCs *in vivo*, cells were harvested by PBS- and treated with antibodies as described above. The single-cell suspension of hESCs (4 x 10^6 cells/per animal in a 50 µl volume) was injected directly into the quadriceps of the right hind leg of a male SCID mouse. Animal experiments were performed in accordance with NIH and NACLAR guidelines (NUS IRB protocol 05-020, Biopolis IACUC approval 050008). Teratoma formation was monitored visually using a simple grading system that was confirmed by caliper measurements: grade 0 = no visible teratoma (6.32 mm average maximal hind leg diameter), grade 1 = teratoma just detectable (10.55 mm average), grade 2 = teratoma obvious (13.2 mm average), and grade 3 = teratoma impedes locomotion (14.52 mm average).

3.14 SCID Teratoma Model with Mix Cell Population

To establish an *in vivo* model using mixed cell populations instead of undifferentied hESCs, hESCs were spontaneously differentiated to EB (as described previously) or cultured in the absence of FGF-2. Cells were subsequently harvested with trypsin and PBS- respectively to obtain a single cell suspension. Cells were then treated with antibodies as described above and was injected directly into the quadriceps of the right hind leg of a male SCID mouse (6×10^6 cells/per animal in 60 µl PBS + 30 µl Matrigel).

3.15 Induction of Apoptosis via Ultra-violet (UV) Irradiation

Confluent hESC cultures were exposed to 200 mJ of UV using a UV cross-linker (UV Stratalinker 1800) to induce apoptosis [70]. After UV exposure, the cells were maintained at 37^{o}C/5% CO_2 for 2 h before assaying them with the various apoptotic assays.

3.16 Flow Cytometric Analysis of Nuclear DNA Fragmentation

Nuclear DNA fragmentation was measured via TUNEL assay kit (Promega). Cells (1.5×10^6 cells) from each condition were washed twice with PBS+ and incubated in 4% methanol-free paraformaldehyde for 20 min on ice. Subsequently, the cells were washed, fixed and permeabilized with 5 ml of ice cold 70% ethanol and stored overnight at -20^{o}C. The cells were then centrifuged at 300 x g for 10 min at 4^{o}C and washed with 5 ml PBS+. The centrifugation step was repeated and the cells were resuspended in 1 ml buffer and transferred to a microcentrifuge tube. The cells were again centrifuged at 300 x g for 10 min at 4^{o}C and the supernatant removed. The

pellets were resuspended in 80 μl equilibration buffer and incubated at room temperature for 5 min, spun down and the supernatant removed. The pellets were then resuspended in 50 μl of rTDT incubation buffer and incubated at 37^{o}C for 1 h. During the incubation, the cells were resuspended by pipeting at 15 min intervals. The reactions were terminated by adding 1 ml of 20 mM EDTA to each sample and vortexing gently. The cells were then washed 3 times with 0.1% Triton X-100/5% ($^{w}/_{v}$) BSA in PBS and finally resuspended in 500 μl PI solution (5 μg/ml in PBS). The samples were analyzed immediately on the flow cytometer (FACScan, Becton Dickinson FACS Calibur). The green fluorescence of fluoresein-12-dUTP and PI emissions were detected in the FL-1 and FL-3 channels respectively.

3.17 Measurment of Caspases Activities

Caspase activities, namely Caspases-2/3/8/9, were measured using ApoAlert® Caspase Profiling Plate (Clontech). Modifications were made to the protocol provided by the supplier. After subjecting the cells to UV or mAb treatments, 1 x 10^{6} cells were taken from each condition and lysed with 450 μl of ice cold lysis buffer. The cell lysates were centrifuged at 13 200 x g at 4^{o}C for 5 min to pellet cellular debris. The supernatants were transferred to new microcentrifuge tubes and placed on ice. The total protein for each lysate was determined using Coomassie Blue Plus reagents. Prior to adding the samples to the assay plate, 50 μl of 2X Reaction Buffer/DTT Mix was added to each well of the assay plate and incubated at 37^{o}C for 5 min. Fifty microlitres of the appropriate cell lysate was then transferred to the wells. The plate was further incubated at 37^{o}C for 2 h and subsequently analyzed using a fluorescence

plate reader (TECAN Infinite M200) at an excitation wavelength of 380 nm and emission wavelength of 460 nm. Additional controls were also set up. Prior to induction of apoptosis or antibody incubation, cells were incubated for 30 min with ZVAD (carbobenzoxy-valyl-alanyl-aspartyl-[O-methyl]) in PBS. ZVAD is a broad spectrum inhibitor to caspases.

3.18 Annexin V Assay

Detection of phosphotidylserine on the outer leaflet of the plasma membrane during apoptosis was detected by Annexin V using the Annexin V-FITC Apoptosis detection kit (Bender MedSystems). After subjecting the cells to UV or mAb treatments, 0.5 x 10^6 cells was centrifuged at 13 200 x g for 1 min and the pellet washed with the binding buffer provided. The cells were again centrifuged and the pellet resuspended in 195 μl of binding buffer. Subsequently, 5 μl of Annexin V-FITC was added and the cells were incubated at room temperature for 10 min. The cells were then centrifuged at 13 200 x g for 1 min and the pellet washed with the binding buffer. The pellet was finally resuspended in 200 μl buffer and analyzed immediately on the flow cytometer (FACScan, Becton Dickinson FACS Calibur).

3.19 Lactate Dehydrogenase (LDH) Release

LDH released from dead cells is measured using the CytoTox 96 Non-radioactive Cytotoxicity Assay (Promega). The cells were treated with mAbs as described. After incubation with the mAbs, the cells were centrifuged at 13 200 x g for 1 min and the supernatant kept for LDH activity measurement. For total LDH measurement, untreated cells were lysed with the 10x Lysis Buffer

provided, centrifuged at 13 200 x g for 1 min to remove cellular debris and the supernatant collected. From each supernatant sample, 50 μl of supernatant was transferred to individual wells of the enzymatic assay plate and subsequently, 50 μl of reconstituted Substrate Mix was added to each sample well. The assay plate was incubated for 30 min at room temperature, protected from light. After the incubation, 50 μl of Stop Solution was added to stop all reactions and absorbance recorded at 490 nm with the TECAN Infinite M200.

3.20 Flow Cytometric Analysis of Na^+ Release

Release of intracellular sodium ions was determined using the Sodium Green™ Indicator kit according to the manufacturer's protocol (Molecular Probes). Briefly, 1 x 10^6 cells were incubated with 10 μM Sodium Green, tetra(tetramethylammonium) salt at 37°C for 35 min to allow the dye to penetrate the cells. Afterwhich, excess dye was removed after a wash with KO-media followed by 2 washes with 1% (w/v) BSA in PBS. The loaded cells were then subjected to various experimental treatments and washed. Intracellular levels of dye were analyzed on the flow cytometer (FACScan, Becton Dickinson FACS Calibur) through the FL-1 channel.

3.21 Estimation of Pore Size with Dextran Beads

Dextran conjugates of various molecular weight (3000 MW to 2 x 10^6 MW, Molecular Probes) were used to determine the size of the pores formed on the plasma membrane of the cells. The dextran conjugates were reconstituted in PBS+ according to the supplier's specification. Ten microlitres

of each dextran conjugate was added to cell suspensions (consisting of 2 x 10^5 cells) and incubated for 30 min at 37^{o}C. The cells were then washed twice with ice cold PBS+ to remove excess dextran conjugates and resuspended in 200 μl buffer. Five microlitres of PI (50mg/ml PBS) was added prior to analysis on the flow cytometer (FACScan, Becton Dickinson FACS Calibur). The dextran conjugates and PI were analyzed through the FL-1 and FL-3 channels respectively.

3.22 Visualization of Cell Surface Membrane through Scanning Electron Microscopy (SEM)

After subjecting hESCs to the various experimental conditions, cells were washed and resuspended in 2.5% glutaraldehyde in PBS and fixed at room temperature for 5 h. After fixing, the cells were washed 2x with PBS+ and post-fixed with 1% osium tetroxide (pH 7.4) for 30 min. Subsequently, the cells were washed twice with deionised water for 10 min. After the wash, the cells were dehydrated in increasing concentration of ethanol from 25% to 100%. The cells were then transferred dropwise to 1 mm diameter cover slips that were pre-coated with poly-L-lysine (PLL). Prior to SEM analysis, the prepared cells were exposed to critical point drying to purge out residual ethanol and sputtered with gold.

3.23 Visualization of Antigen Aggregation through SEM

After treatment with antibodies, the cells were washed and further incubated for 15 min with goat α-mouse antibody colloidal gold-conjugated (0.2ug/150 ul cell suspension, EY Laboratories). The cells were subsequently

fixed and prepared for SEM as described above and sputtered with carbon prior to examination.

3.24 Confocal Microscopy

Cells were treated with the various antibodies as mentioned above and washed with 1% BSA/PBS. The cells were then fixed, permeabilized (Invitrogen) and blocked with 1% BSA/PBS for 1 h. Subsequently, the cells were incubated with primary antibodies to the respective antigens overnight at 4^{o}C. The antibodies, mAb 84 and mAb 85 (both IgMs) and anti-paxillin (IgG) were used at a concentration of 25 µg/ml. The cells were washed and incubated with 1:500 dilution of FITC-conjugated goat anti-mouse IgG (γ-chain specific) antibody (SIGMA), PE-conjugated rabbit anti-mouse IgM (OPEN Biosystems) and DAPI (Molecular Probes) for 1 h at room temperature. The cells were washed and mounted onto glass slides with anti-fade reagent (Invitrogen). Localization of the proteins was visualized under a confocal microscope (Zeiss).

3.25 Calpain Inhibition

hESCs were cultured as described and incubated with the calpain inhibitors (20 nM) for 24 h. The cells were then harvested and cytotoxicity assays was carried out. All calpain inhibitors were from Calbiochem.

3.26 Statistical Analysis

Data were expressed as means ± standard error of the mean. Standard deviations were analyzed via F-test. The 2 means were compared with the Student's t-test.

CHAPTER 4 *IN VITRO* CHARACTERIZATION OF mAb 84

4.1 Introduction

In order to produce therapeutically useful cells from hESCs, it is important to characterize and understand the cellular components and pathways that govern their proliferation and differentiation [11,14,15]. One of the ways to identify the receptors or antigens involved in hESC regulation is to raise antibodies against hESCs surface markers. An additional advantage of raising antibodies specific to undifferentiated hESCs is that these antibodies can be used to separate the differentiated cells from the undifferentiated cells which potentially can form teratomas [1,11-13].

Following immunization of BALB/c mice with live cells, we generated a panel of antibodies to cell surface markers on undifferentiated hESCs. Figure 4.1 illustrates the generation of antibodies against hESC surface markers. Briefly, live undifferentiated hESCs were injected into BALB/c mice over a period of 5 weeks. Post-immunisation, serum was drawn and screened for the presence of antibodies that bind to hESCs. The mice were then sacrificed and the spleens harvested. The spleenocytes were subsequently fused with Sp2/0 myeloma cells and after hypoxanthine-aminopterin-thymidine (HAT) selection, colonies of hybridomas were isolated. Antibodies produced form the hybridomas were further screened against hESCs and various other cell types to test their specificity. From this, a panel of 10 mAbs against hESC cell markers were identified. Their reactivity to various hESC lines and other cell lines are summarized in Table 4.1. Conventional antibodies to hESCs, namely SSEA-1, TRA-1-60 and TRA-1-80 are also included for comparison.

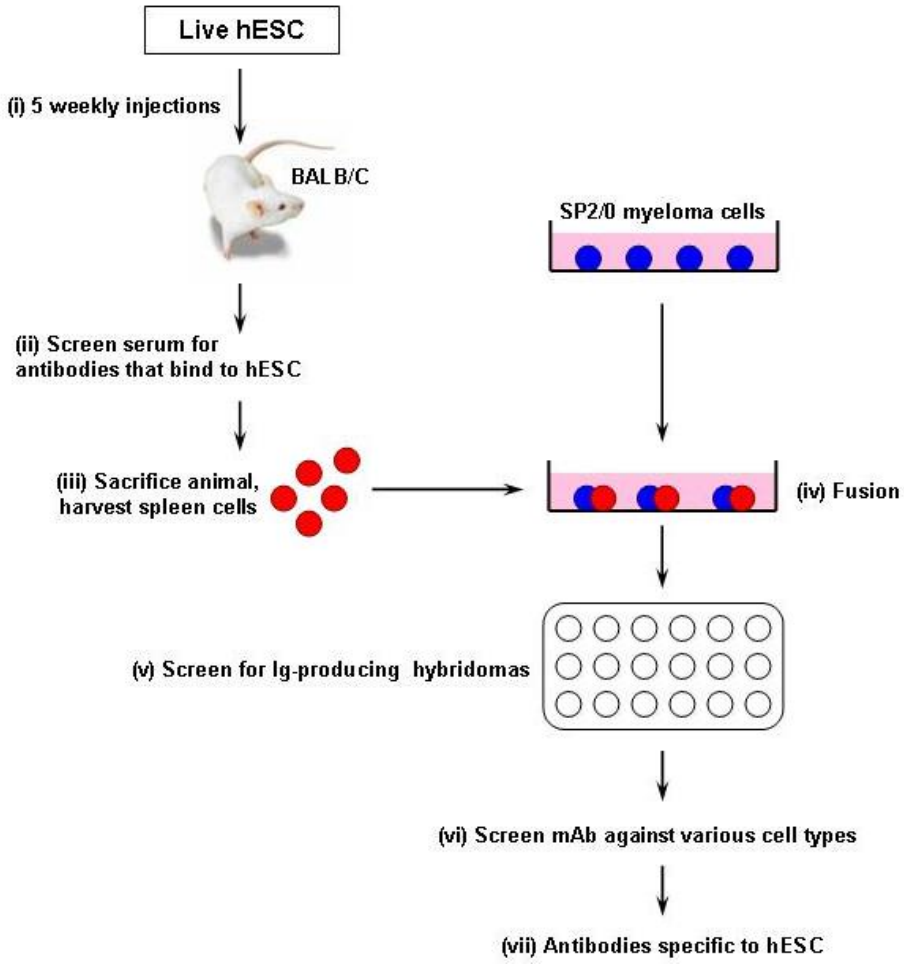

Figure 4.1 Generation of antibodies against hESC surface markers.

Table 4.1 Summary of mAb reactivity to various cell lines.

		Cell Lines											
		hESC				Feeders	mESC		EC Cells			Miscellaneous	
mAb Clone	Isotype	HES-3	HES-3 EB	HES-2	HES-4	ΔE-MEF	CS-1	E-14	Ntera	2102Ep	NCCIT	HEK-293	HeLa
84	IgM	+++	+/−	++++	++	−	−	−	−	−	+	−	−
95	IgM	++	−	++++	++	−	−	−	−	−	+/−	−	−
375	IgM	+++	−[a]	+++	n.d.	−	−	−	n.d.	−	−	−	−
432	IgM	+++	−[a]	+++	n.d.	−	−	−	n.d.	−	−	−	−
529	IgM	+++	−[a]	+++	n.d.	−	−	−	n.d.	−	−	−	−
14	IgM	++	+	++++	++	−	++	−	++	+	−	−	−
85	IgM	++	+/−	++++	++++	−	−	−	++++	+	++	−	−
8	IgG_{2a}	++++	+	++++	++	−	−	−	+	+++	+	+	+
5	IgM	+	+	+	+	−	−	−	++	+	+	+++	++++
63	IgM	++	++	+++	++	−	−	−	+++	+	+	++	++++
SSEA-4	IgG_3	+++	n.d.	++++	+++	+	+	+	+++	++	+++	+	+
TRA-1–60	IgM	+++	n.d.	++++	++++	−	−	−	++++	++	+++	−	−
TRA-1–81	IgM	+++	n.d.	++++	++++	−	−	−	++++	++	+++	−	−

[a]Day 22 EB were used instead of day 8 EB.

Abbreviations: +, represent binding; +/−, represent partial/weak binding; −, represent no binding; EB, embryoid bodies; n.d., represents not determined.

From this panel of 10 antibodies, an antibody, mAb 84, was identified that not only binds but also kills undifferentiated hESCs. mAb 84 showed strong reactivity to the undifferentiated hESC lines (HES-2, HES-3 and HES-4). However, the reactivity was significantly reduced in hESC-derived EBs, mouse ESCs, mouse feeders, human EC cells, and other human cell lines (HEK-293 and HeLa). When hESCs were incubated with mAb 84, there was a significant decrease in cell size and an increase in PI uptake, which is indicative of cell death (Figure 4.2). The ability of mAb 84 to selectively kill undifferentiated hESCs is extremely beneficial as mAb 84 can potentially be used to remove residual undifferentiated hESCs contaminating differentiated cell products prior to therapeutic applications.

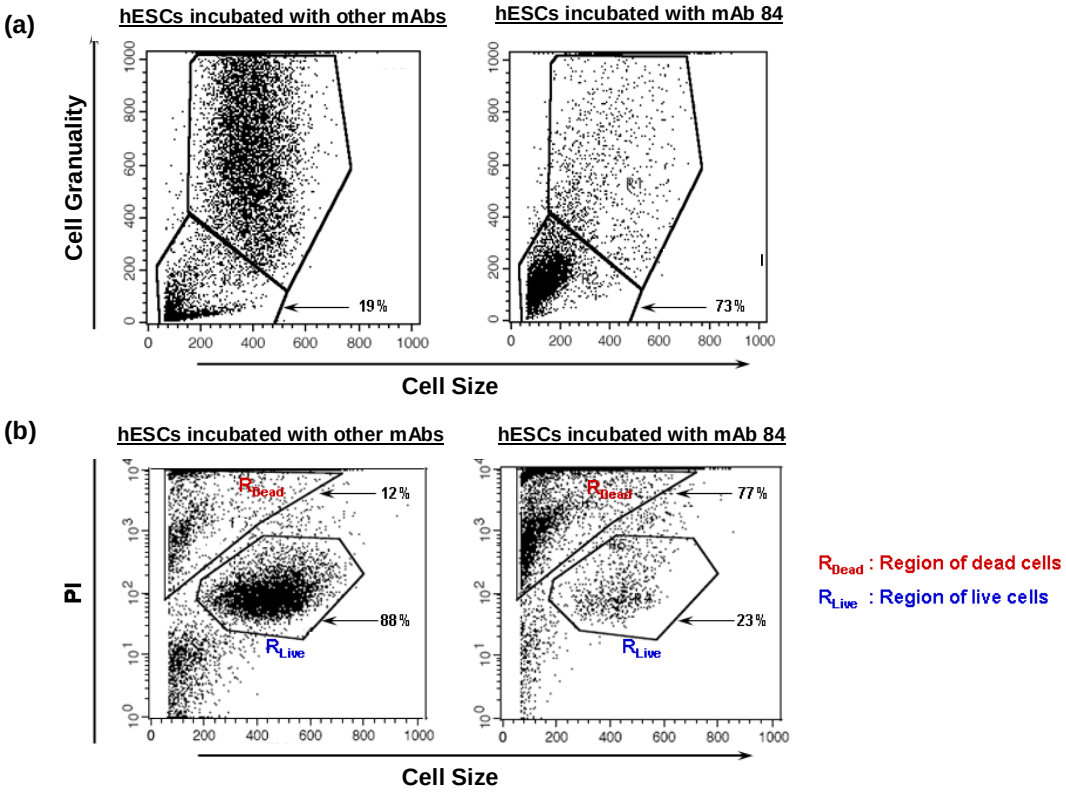

Figure 4.2 mAb 84 is cytotoxic to hESCs. (a) When hESCs were incubated with mAb 84, there was a significant decrease in cell size (from 19% to 73%) compared to hESCs incubated with other mAbs. (b) A significant increase in PI uptake was observed when hESCs were incubated with mAb 84 (from 12% to 77%).

This chapter reports the *in vitro* characterization of mAb 84. The antigen target of mAb 84 on hESCs was first identified. Next we went on to determine if the cytotoxic effect is unique to mAb 84 or is this cytotoxic effect also observed with other mAbs against the same antigen. We also investigated the effect of complement, temperature and antibody concentration on mAb 84 cytotoxicity and studied its death kinetics. Assays were also carried out to investigate if the killing ability of mAb 84 is specific to undifferentiated hESCs and to determine the type of glycan which mAb 84 binds. Studies were also carried out to determine if mAb 84 binds and kills induced pluripotent stem cells (iPS cells).

4.2 Identification of mAb 84 Target Antigen on hESC

4.2.1 Identification of Podocalyxin as the antigen target

To identify the target antigen of mAb 84, immuno-precipitation (IP) was carried out using the PhyNexus automated system. Briefly, hESC lysate was passed through a PhyTip column containing protein A resin and mAb 84. The enriched protein sample was eluted, resolved by polyacrylamide gel electropheris and immuno-blotted (IB) with mAb 84. An antigen band of ~190 kDa was detected (Figure 4.3, Lane 1). The corresponding band on a silver-stained gel was excised and analyzed by mass spectrometry (MS). From protein database search with the peptides obtained, the antigen band was identified as podocalyxin-like protein-1 precursor (PCLP1 or PODXL; Accession No. O00592).

To validate that the antigen target is PODXL, IP with mAb 84 was repeated and the eluate after PAGE and IB was probed with 2 commercially-available antibodies to PODXL (Figure 4.3, Lanes 2 and 3). From the Western blots, a band of comparable molecular weight was detected in all 3 lanes, confirming the identity of the target antigen as PODXL.

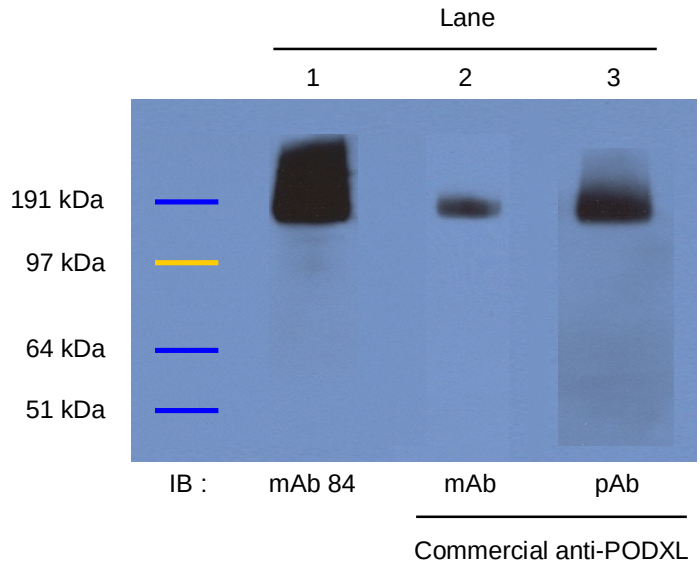

Figure 4.3 Western blot analysis of target antigen immuno-precipitated by mAb 84. Affinity purified antigen from hESC lysate using PhyTip columns containing protein A resin and mAb 84 was resolved on SDS-PAGE and subjected to Western blot. Lane 1: IB with mAb 84; Lane 2: IB with mAb to human PODXL (mAb-PODXL) and Lane 3: IB with polyclonal antibody (pAb) to human PODXL (pAb-PODXL).

4.2.2 Background of PODXL

PODXL is a heavily glycosylated type-1 transmembrane protein and belongs to the CD34 family of sialomucins, which include CD34 and endoglycan [71,72]. The human PODXL is localized on chromosome 7q32-q33 with an open reading frame that encodes for a protein of 528 amino acids [73,74]. The extracellular domain of PODXL has 5 potential sites for N-linked glycosylation and from amino acids 22 to 295, the high serine and threonine content provides numerous sites for potential O-linked glycosylation [74]. The predicted molecular weight of PODXL is 54 kDa but the apparent molecular weight is approximately 160-165 kDa, due to the extensive glycosylation [74,75].

PODXL has been reported to have diverse roles depending on the cell type. In podocytes, PODXL acts as an anti-adhesion molecule that maintains

the filtration slits open between podocyte foot processes by charge repulsion [76,77]. In high endothelial venules, PODXL acts as an adhesion molecule binding to L-selectin and mediating the tethering and rolling of lymphocytes [72].

The presence of PODXL in hESCs was also reported by Brandenberger *et. al.* [78]. In their work, they characterized hESCs at the molecular level and through expressed sequence tag (EST) frequency analysis, they found that the level of PODXL expression was down-regulated by almost 2.5 fold in 7-8 day EB and approximately 7 and 12 fold in neuroectoderm-like cells and hepatocyte-like cells respectively. Interestingly, at the protein level, Schopperle and DeWolf reported that PODXL underwent post-translational glycosylation changes during differention when 2 EC lines were exposed to retinoic acid (reduction in MW from 200 kDa to 170 kDa). The failure of the carbohydrate-binding antibodies, anti-TRA-1-60 and ati-TRA-1-81, to bind to the modified PODXL prompted them to suggest the presence of a Stem Cell PODXL (SC-PODXL) on pluripotent stem cells [79].

4.3 Cytotoxicity is Unique to mAb 84

During the characterization of the mAbs in the panel, it was identified that mAb 85 also binds to PODXL (Table 4.1). Interestingly, even though mAb 85 is also an IgM, it does not confer any cytotoxicity on hESCs (Figure 4.4). Thus, mAb 85 was consequently used as an isotype control for mAb 84.

We also proceeded to investigate whether the commercially-available antibodies to PODXL exhibited similar cytotoxic effect on hESCs. From Figure 4.4, it is apparent that although the other 3 sources of antibodies (mAb 85 and

mAb/pAb-PODXL) were specific to human PODXL on hESCs, cytotoxicity was only observed for mAb 84 and not for other anti-PODXL antibodies. This suggests that the binding of mAb 84 is epitope specific rather than antigen specific, and that the cytotoxicity is unique to mAb 84.

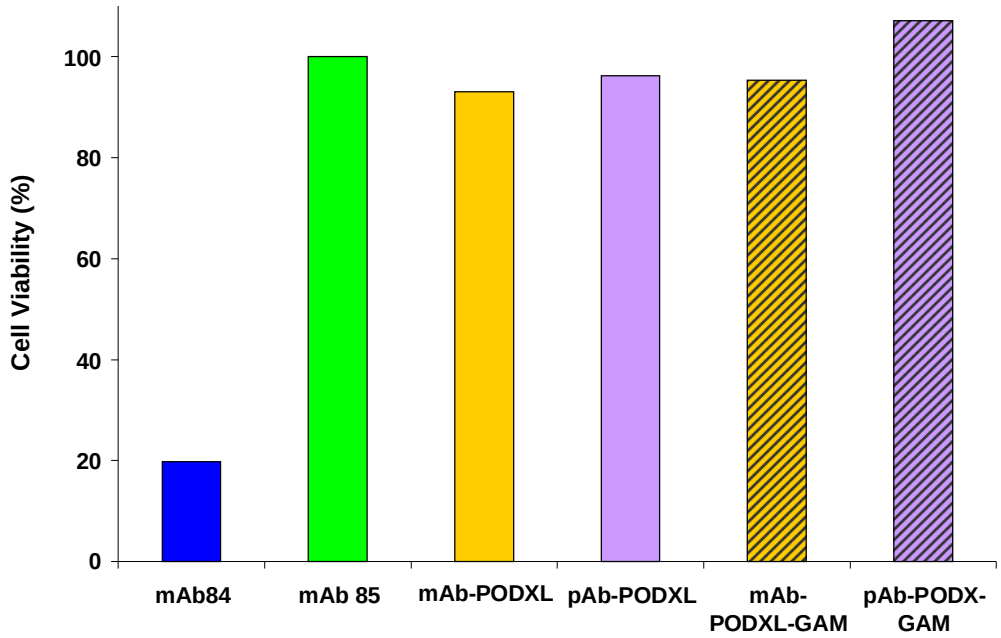

Figure 4.4 Only mAb 84 is cytotoxic to hESCs. Cytotoxicity assay was performed by incubating hESCs with 5 µg mAb 84, mAb/pAb-PODXL and mAb 85. Only mAb 84 is cytotoxicity to hESCs, as opposed to mAb 85 and the commercially available antibodies (mAb-PODXL and pAb-PODXL). When the commercially available antibodies were hyper-crosslinked with goat-anti-mouse (GAM), no cytotoxicity was observed.

Several groups have previously reported that cell death can be induced by hyper-crosslinking of primary antibodies bound to antigens on cells [32-34,80,81]. Since mAb 84 is an IgM (pentameric) whilst mAb-PODXL and pAb-PODXL are both IgG (bivalent), we investigated if hyper-crosslinking of mAb-PODXL or pAb-PODXL with goat-anti-mouse (GAM) antibodies would mimic mAb 84- mediated killing of hESCs. Incubation of hESCs with primary

antibodies followed by GAM antibodies failed to induce a similar cytotoxic effect as mAb 84 (Figure 4.4).

4.4 Cytotoxicity of mAb 84 is Independent of Complement

Next, we compared purified and non-purified (culture supernatant) mAb 84 to determine if complement in fetal bovine serum was required for cytotoxicity. We found that mAb 84 was equally cytotoxic to hESCs after purification (Figure 4.5) with a killing efficiency of more than 77% at 4^{o}C incubation. This result suggests that mAb 84-induced toxicity on hESCs was not complement-mediated. In all future experiments, purified mAb 84 was used.

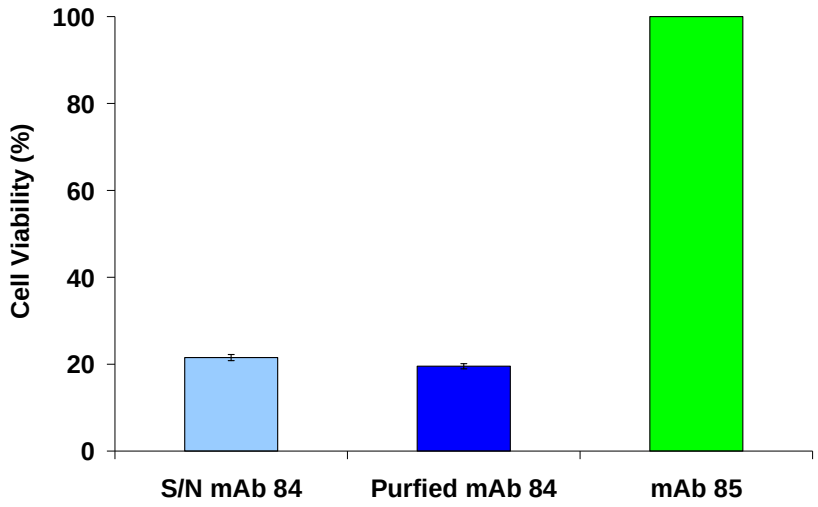

Figure 4.5 Cytotoxicity of mAb 84 is independent of complement. The killing efficiency of purified and supernatant mAb 84 (S/N mAb 84) is comparable. In both conditions, more than 77% of hESCs was killed after 45min incubation at 4^{o}C.

4.5 Cytotoxicity of mAb 84 is Independent of Temperature

As all experiments were conducted at 4^{o}C, we went on to investigate the effect of temperature on the cytotoxicity of mAb 84. hESCs were

incubated with 5 µg mAb 84 at 4°C and at 37°C (Figure 4.6). We found that the killing efficiency of mAb 84 was comparable at both temperatures and concluded that the cytotoxicity of mAb 84 is independent of temperature.

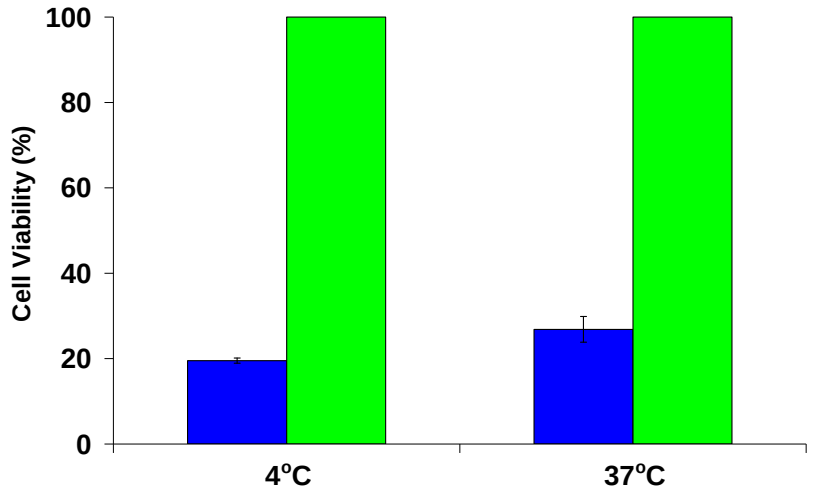

Figure 4.6 Cytotoxicity of mAb 84 is independent of temperature. The killing efficiency of mAb 84 is comparable at both 4°C and 37°C. (■) represents mAb 84-treated hESCs and (■) represents mAb 85-treated hESCs.

4.6 Cytotoxicity of mAb 84 is Dependent on Concentration

In this dose-response experiment, the concentration of mAb 84 was titrated over the range of 0.1-15 µg and added to 2 x 10^5 cells in a volume of 200 ul. It was found that the cytotoxic effect of mAb 84 on hESCs was concentration-dependent (Figure 4.7). Approximately 1 µg of purified mAb 84 was sufficient to cause more than 70% decrease in hESC viability, as indicated by the red arrow.

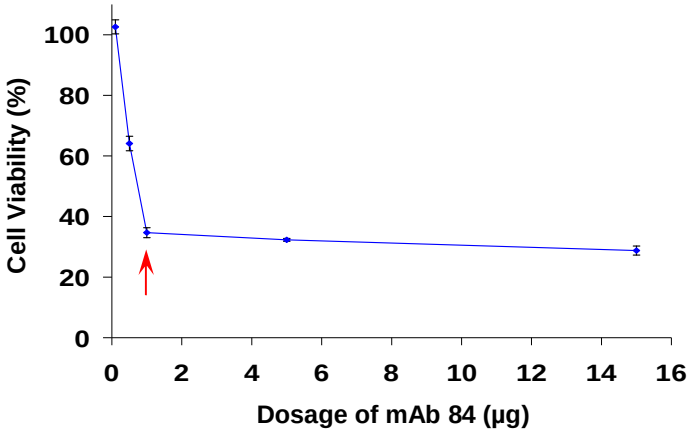

Figure 4.7 Titer experiment. Cytotoxicity of mAb 84 is dosage dependent.

4.7 Kinetics of mAb 84 Killing of hESCs

In time course studies, hESCs (2 x 10^5) were incubated with 5 µg mAb 84 or mAb 85 and the cells were harvested every 15 min for analysis by PI and trypan blue exclusion assays (Figure 4.8 a and b respectively). Through the PI exclusion assay, the cytotoxic effect of mAb 84 on hESCs was observed as quickly as 15 min after incubation with the viability dropping to 33%, with a further decrease in viability to 20% after 45 min. These results were confirmed by trypan blue exclusion assay although the cytotoxicity occurs only 30 min after incubation. This may be due to the fact that the trypan blue assay is a less sensitive assay compared to PI exclusion assay.

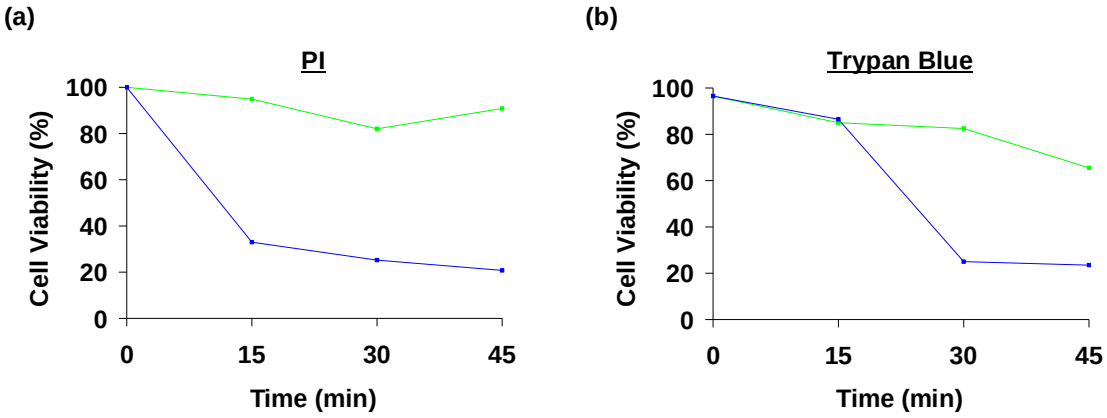

Figure 4.8 Time course assay. mAb 84 kills hESCs as fast as 15 min. (—) represents mAb 84-treated hESCs and (—) represents mAb 85-treated hESCs (a) Percentage cell viability as determined by PI exclusion assay. (b) Percentage cell viability as determined by trypan blue exclusion assay.

4.8 mAb 84 Killing is Specific to Undifferentiated hESCs

4.8.1 Cytotoxicity assay on differentiated hESCs

Table 4.1 lists the binding specificity of mAb 84 to the various cell types. It was also observed that the binding of mAb 84 to hESCs was down-regulated as the cells differentiate to 8 day old EBs. To determine if cytotoxicity of mAb 84 was specific to the undifferentiated phenotype, hESCs were induced to differentiate either by depriving the cultures of fibroblast growth factor 2 (FGF-2) or by EB formation. Differentiation was assessed based on the expression of the pluripotent marker, TRA-1-60 (Figure 4.9a). After culturing the hESCs in the absence of FGF-2 for 12 days, partial differentiation of hESCs was observed, with 49% of the cell population still expressing TRA-1-60 compared to the undifferentiated hESC culture where greater than 95% of the cell population expresses TRA-1-60. Differentiation of hESCs to EBs for 22 days yielded 99% differentiation.

When cells from these 3 conditions were incubated with mAb 84, the efficiency of cell killing corresponded closely with the percentage of TRA-1-60 positive cells (Figure 4.9b). For undifferentiated hESCs, only ~1% of cells remained viable after incubation with mAb 84. The viability increased to 69% and 99% for FGF-2 starved and EB cultures respectively concluding that the cytotoxicity of mAb 84 is indeed specific to undifferentiated hESCs.

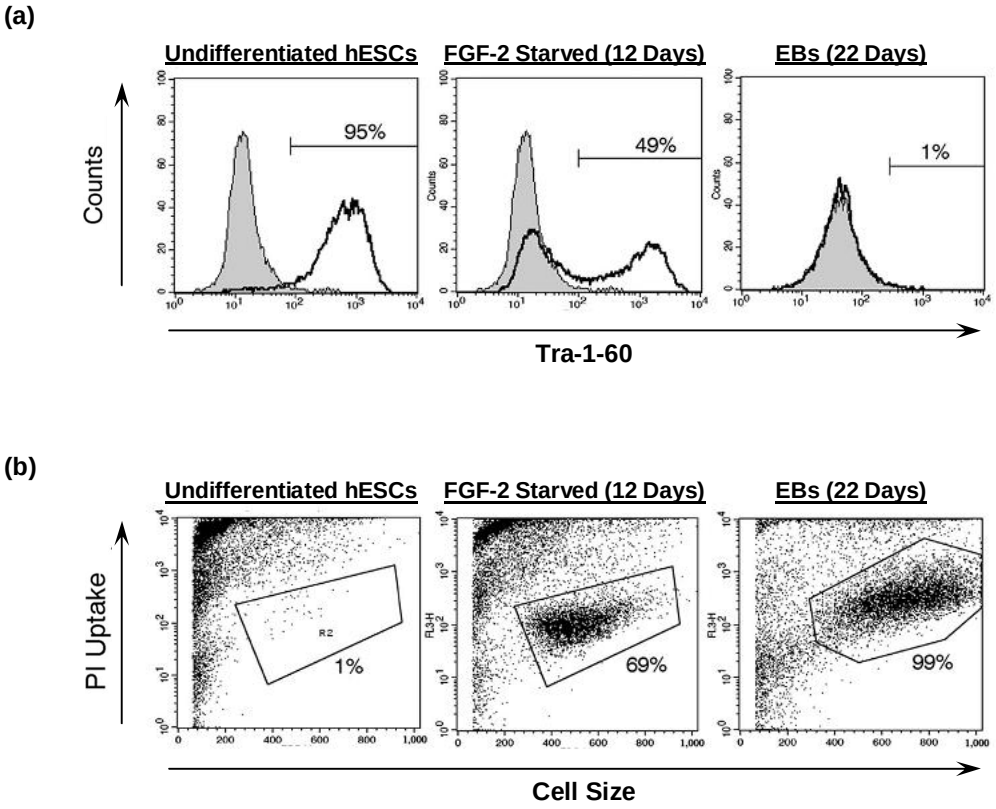

Figure 4.9 Relationship between hESC pluripotency and killing efficiency by mAb 84. (a) Cells stained with anti-TRA-1-60 and detected with a FITC-conjugated anti-mouse antibody. The shaded histogram represents staining with the negative control and open histograms represent staining with anti-TRA-1-60 mAb. (b) Incubation with mAb 84 at 4^{o}C for 45 min. Subsequently, viability of the cells were analysed by PI exclusion assay on the flow cytometer. Gated region in the scatter plot represents the viable cell population.

4.8.2 Triple staining of hESCs and differentiated cells

Using a direct approach to determine if the cytotoxicity of mAb 84 was specific only to the undifferentiated phenotype, we co-stained live hESCs and differentiating cells with mAb 84 and the pluripotent marker, TRA-1-60. At the same time, viability of the cells was analyzed via PI assay (Figure 4.10). Differentiation was achieved by culturing hESCs in the absence of FGF-2 for 12 days.

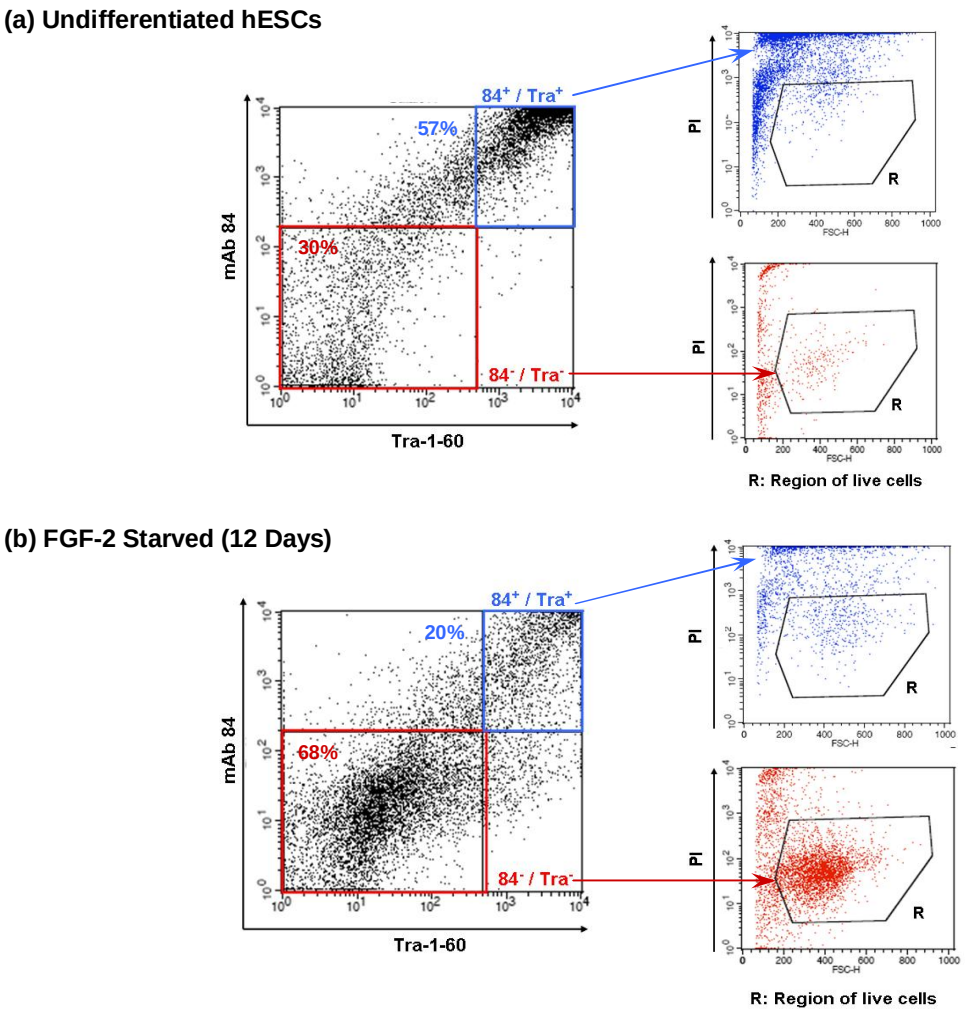

Figure 4.10 Triple staining of cells with mAb 84, TRA-1-60 and PI (a) Undifferentiated hESCs, (b) Differentiating cells cultured in the absence of FGF-2 for 12 days.

The population of double positive cells (84+/Tra+) was higher in the undifferentiated hESCs than the differentiated cells, 57% compared to 20%. These double positive cells also corresponded to cells with higher PI staining. This suggests that pluripotent cells were more susceptible to killing by mAb 84. Conversely, upon differentiation, the double negative population (84-/Tra-) increased from 30% to 68% and these cells corresponded to cells with lower PI (viable population). Taken together, this data confirms that the mAb 84-mediated is only specific to undifferentiated hESCs.

4.9 mAb 84 Binds to O-linked Glycans on PODXL

Loo *et. al.* have shown that the binding of antibody RAV12 to its antigen is associated with N-linked glycans [34]. As previously mentioned, PODXL is highly glycosylated sialomucin [74,75]. We proceeded to investigate if the binding of mAb 84 to PODXL is dependent on post-translational modifications. In general, there are 2 kinds of glycosylation, namely; N-linked and O-linked glycosylation [82]. In their work, Loo *et. al.* utilized enzymes to deglycosylate the antigen and investigated the effect on antibody binding [34]. The common enzyme used to cleave N-glycans is peptide N-glycosidase (PNGase) F [34,83,84]. Due to the complexity of O-linked glycosylation, several enzymes are utilized to cleave the various glycan residues. For example, sialidase cleaves the terminal sialic acid residues and endo-α-N-acetylgalactosaminidase (O-glycanase) is used to cleave the O-glycans post sialidase treatment [34,84].

We first investigated if the binding of mAb 84 is associated with N-linked glycans. After immuno-precipitation of PODXL by mAb 84, the eluate

was digested with PNGase F and probed with mAb 84 and commercially available anti-PODXL (Figure 4.11). From the Western blot analysis, the binding of mAb 84 was not lost after N-glycan removal with PNGase F. On the contrary, mAb-PODXL binding to PODXL is associated with N-linked glycans.

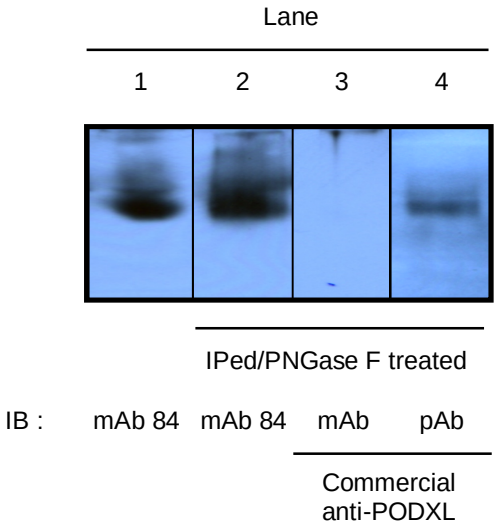

Figure 4.11 Western blot analysis of immuno-precipitated PODXL post PNGase F treatment. Affinity purified PODXL from hESC lysate using PhyTip columns containing protein A resin and mAb 84 was treated with PNGase F and resolved on SDS-PAGE and subjected to Western blot. Lane 1: Lysate (control); Lane 2: IB with mAb 84; Lane3: IB with mAb to human PODXL (mAb-PODXL) and Lane 4: IB with pAb to human PODXL (pAb-PODXL).

Next, we investigated if the binding of mAb 84 was associated with O-linked glycans. After immuno-precipitation of PODXL by mAb 84, the eluate was sequentially digested with sialidase, PNGase F and O-glycanase to remove terminal sialic acid residues, N-linked glycans and O-linked glycans respectively (Figure 4.12a). Samples were taken after each step of enzymatic digestion and probed with mAb 84 (Figure 4.12b). Binding of mAb 84 was only lost after removal of O-glycans. From this data, we concluded that mAb 84 binds to O-linked glycans on PODXL.

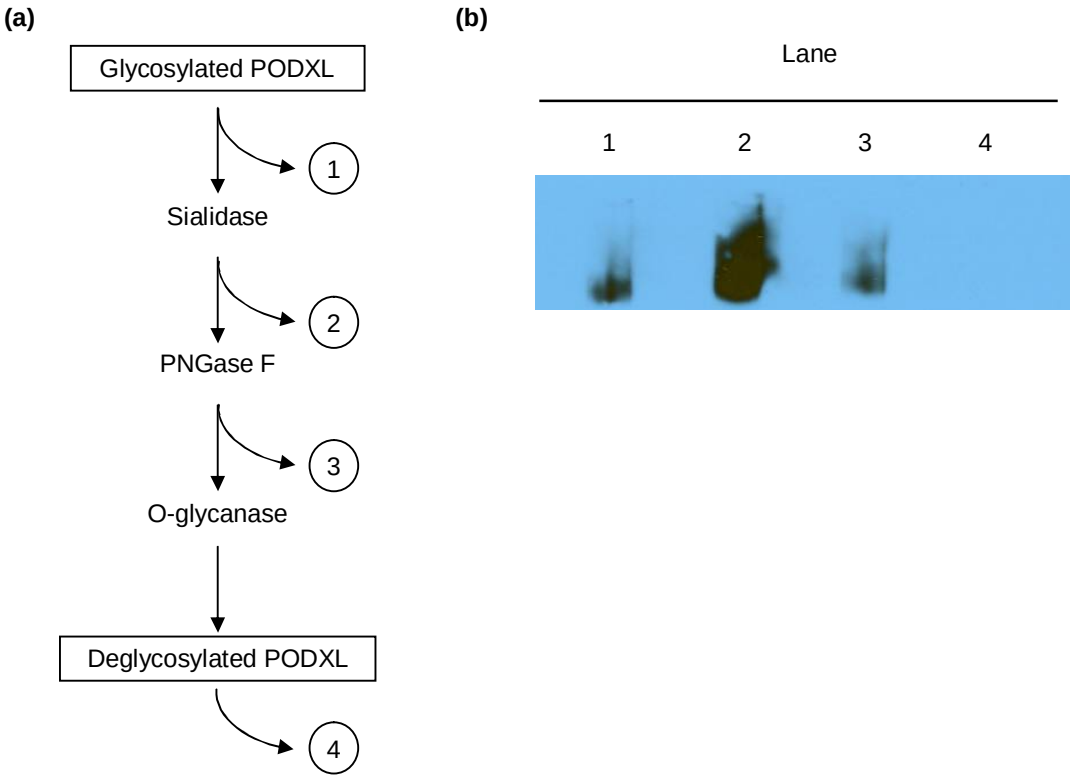

Figure 4.12 Western blot analysis of immuno-precipitated PODXL post O-glycanase treatment. (a) Affinity purified PODXL from hESC lysate using PhyTip columns containing protein A resin and mAb 84 was treated sequentially with sialidase, PNGase F and O-glycanase. Samples were taken from each step for western blot analysis. (b) Samples post enzymatic treatment were resolved on SDS-PAGE and subjected to Western blot. Lanes on the blot correspond to the samples after each enzymatic digestion step. Lane 1: IP-ed PODXL; Lane 2: Sialic acid removed; Lane3: Sialic acid and N-linked glycans removed; and Lane 4: Sialic acid, N-linked and O-linked glycans removed.

4.10 mAb 84 is Cytotoxic to Induced Pluripotent Stem Cells

Recently, the reprogramming of differentiated human somatic cells into a pluripotent state has generated enormous interest in the stem cell field. These non-pluripotent cells which are induced to express pluripotent genes,

are known as induced pluripotent stem (iPS) cells [66,84-86]. Potentially, iPS cells can overcome two important obstacles associated with the use of hESC: immune rejection after transplantation and ethical concerns regarding the use of human embryos [25,66,67]. In addition, iPS cells have been shown to be comparable to hESCs in morphology, pluripotent marker expression and differentiation potential, including teratoma formation [23,25,86]. Hence, we proceeded to investigate if mAb 84 is also cytotoxic to iPS cells.

We carried out flow cytometry analysis on 2 iPS cells which were derived by Thomson *et. al.* [66,67]. The iPS cells were derived from fetal lung fibroblasts (IMR90) and neonatal foreskin fibroblasts transfected with the pluripotent genes OCT-4, SOX-2, NANOG and LIN-28. From Figure 4.13a, mAb 84 binds to both iPS cells (ESIMR90, ES4SKIN) but not to their parental fibroblasts (IMR90 and Foreskin), indicating that PODXL is up-regulated after reprogramming of the parental fibroblasts to iPS cells. In addition, mAb 84 is cytotoxic to both iPS cells but not the parental fibroblasts (Figure 4.13b).

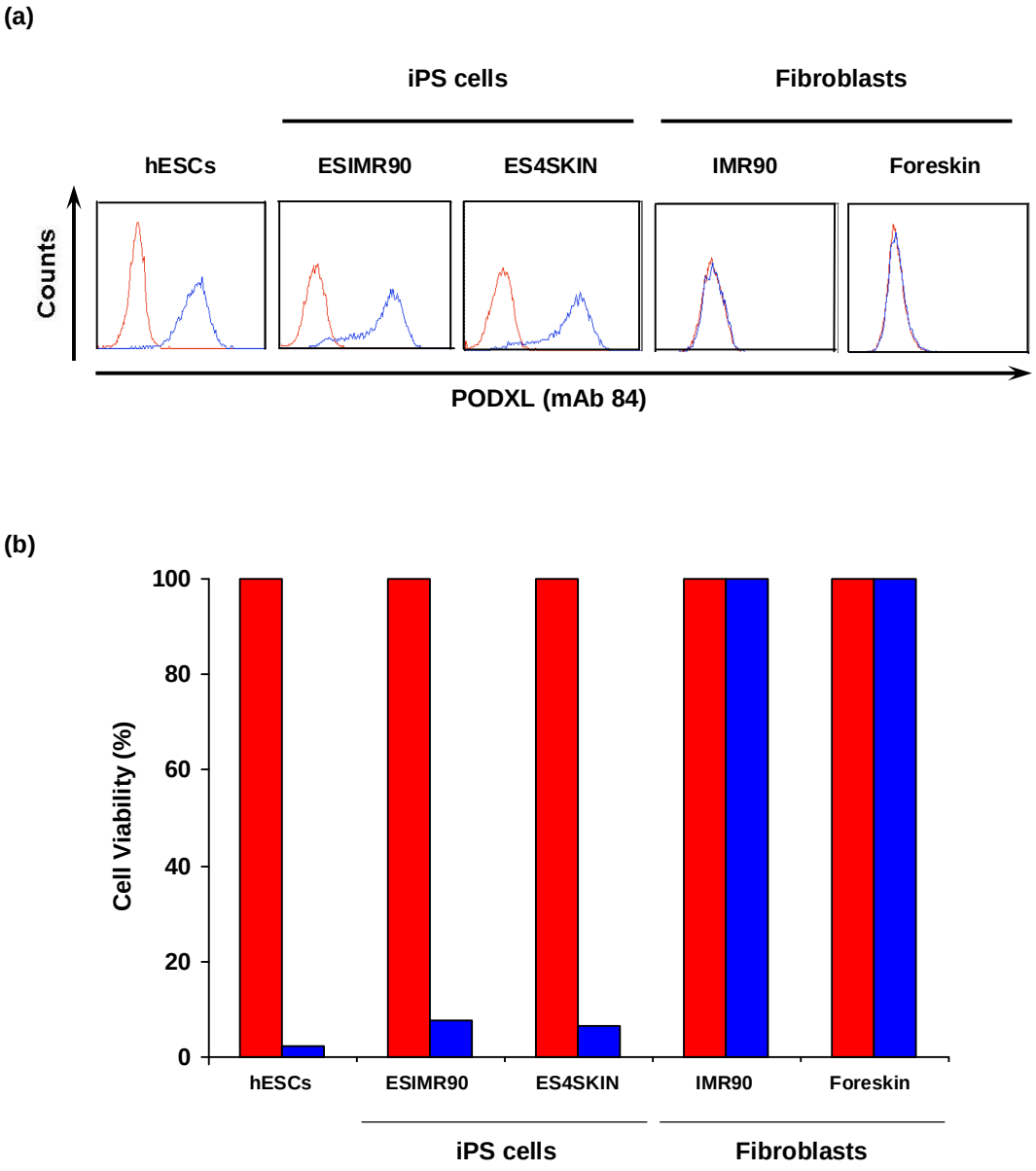

Figure 4.13 Flow cytometry analysis of mAb 84 on iPS cells. (a) mAb 84 binds to both iPS cells but not to their parental fibroblasts. (b) mAb 84 is cytotoxic to both iPS cells but not to their parental fibroblasts. (■) represents no treatment control and (■) represents mAb 84-treated cells.

4.11 Summary

This chapter details the work carried out to characterize mAb 84 in its application to kill hESCs. This characterization work entitled “Selection Against Undifferentiated Human Embryonic Stem Cells by a Cytotoxic Antibody Recognizing Podocalyxin-Like Protein-1” has been published in the journal, Stem Cells (refer to APPENDIX A).

We described a panel of antibodies that was raised against hESCs with the main objectives of identifying novel hESC surface markers that characterizes hESC populations and potentially using these mAbs to separate residual undifferentiated hESCs from differentiated cells. Uniquely, one of the clones, mAb 84, not only bound to hESCs but was also cytotoxic to the cells.

By IP and MS analysis, the target antigen of mAb 84 was identified as PODXL. Human PODXL is localized on chromosome 7q32-q33 with an open reading frame that encodes for a protein of 528 amino acids [73,74]. The calculated molecular weight of PODXL is 54 kDa but the apparent molecular weight is approximately 160-165 kDa, due to extensive glycosylation [74,75]. The presence of PODXL on undifferentiated hESCs was also reported by Brandenberger *et. al.* [78]. In addition, Schopperle and DeWolf reported the presence of a Stem Cell PODXL (SC-PODXL) on pluripotent stem cells [79].

Functionally, PODXL has been reported to have diverse roles depending on the cell type. In podocytes, PODXL acts as an anti-adhesion molecule and maintains the filtration slits open between podocyte foot processes by charge repulsion [76,77]. In high endothelial venules, PODXL acts as an adhesion molecule binding to L-selectin and mediating the tethering and rolling of lymphocytes [72]. In breast and prostate cancers,

PODXL has been implicated as an indicator of tumor aggressiveness [23,87]. Hence, it would be interesting to investigate if mAb 84 binds and kills these cancer cells.

Unlike other cytotoxic mAbs that may require either the activation of complement or hypercross-linking to induce cell death, mAb 84 mediated-killing of hESCs was found to be independent of both mechanisms and also independent of temperature [32-34,80,81,88]. In addition, mAb 84 kills hESCs in a time and concentration dependent manner. We have also shown that mAb 84 binding and cytotoxicity is specific to undifferentiated hESCs and not differentiated cells. By enzymatic deglycosylation, results show that mAb 84 binds to an O-linked glycan on PODXL. Extending our investigations to iPS cells, we observed that mAb 84 killing of iPS cells is as efficient as hESCs. Interestingly, PODXL, which is absent in the parental fibroblasts, is up-regulated upon reprogramming making the cells susceptible to mAb84.

In summary, the cytotoxic antibody, mAb 84, can be used as a cell surface marker for undifferentiated hESCs and iPS cells. In ESC therapy, mAb 84 may be applied as a death-inducing agent to kill and remove residual undifferentiated hESCs in differentiated populations, which potentially can form teratomas. The *in vivo* characterization of mAb 84 is presented in the next chapter.

CHAPTER 5 *IN VIVO* CHARACTERIZATION OF mAb 84

5.1 Introduction

The *in vitro* characterization of mAb 84 is presented in Chapter 4. We proceeded to investigate if treatment of hESCs *in vitro* with mAb 84 will eliminate its ability to form teratomas *in vivo*. This chapter details the animal studies performed with different starting cell populations and the consequence of mAb 84 treatment of them. In the first model, homogenous hESCs were treated with mAb 84 prior to transplantation into severe combined immunodeficiency (SCID) mice. We extended the model to mixed cell population where hESCs were differentiated into EBs or starved of FGF-2 during culture for 12 days. The tumorigenic potential of these cell populations *in vivo* were then evaluated.

5.2 Development of Teratoma Grading System

Teratoma formation was monitored visually using a simple grading system that was confirmed by caliper measurements: grade 0 = no visible teratoma (6.32 mm average maximal hind leg diameter), grade 1 = teratoma just detectable (10.55 mm average), grade 2 = teratoma obvious (13.2 mm average), and grade 3 = teratoma impedes locomotion (14.52 mm average). Figure 5.1 shows the grading system and sizes of the teratomas formed in the SCID mice.

Figure 5.1 Grading system for teratoma formation. Teratomas are graded according to the size.

5.3 *In Vivo* Model with Homogenous hESCs

In the first animal model, we investigated whether hESCs treated with mAb 84 *in vivo* still had the potential to form teratomas after injection into SCID mice. Single-cell suspensions of hESCs were either treated with mAb 84 or left untreated under identical conditions. When injected into the hind leg of SCID mice, all untreated transplants generated tumors (Figure 5.2), which started to form palpable and visible tumors between 6-9 weeks post-injection, and grew to full-sized tumors within 12 weeks. In contrast, when cells were treated with mAb 84 prior to injection, none of the injected animals developed tumors after 18-24 weeks.

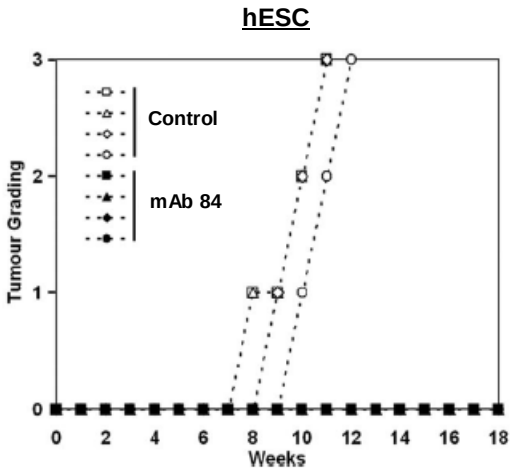

Figure 5.2. Prevention of teratoma formation by mAb 84 in SCID mice. Single-cell suspension of hESCs (4 x 10^6 cells/animal) was incubated with mAb 84 at 4^{o}C for 45 min and then injected into the right hind leg muscle of SCID mice (n = 4/group). Teratoma formation was evaluated with the grading method defined in section 5.2.

This study was extended to evaluate other mAbs in our panel to determine the specificity and uniqueness of mAb 84 to eliminate teratoma formation *in vivo*. These mAbs include mAb 85, the isotype control which binds to PODXL but is not cytotoxic to hESC, mAb 14 (IgM) and mAb 8 (IgG) which binds to other cell surface markers on hESC. Consistently, hESCs treated with mAb 84 did not form teratomas *in vivo*, while hESCs treated with other mAbs, formed teratomas as early as week 7 post-injection (Figure 5.3). From these results, we concluded that the cytotoxic properties of mAb 84 on hESC is unique to the specific epitope recognized by the antibody on PODXL and not based only on binding to PODXL or to any surface antigens on hESC (mAb 84 vs mAb 85). Also, the cytotoxicity conferred is not dependent on the class of antibody.

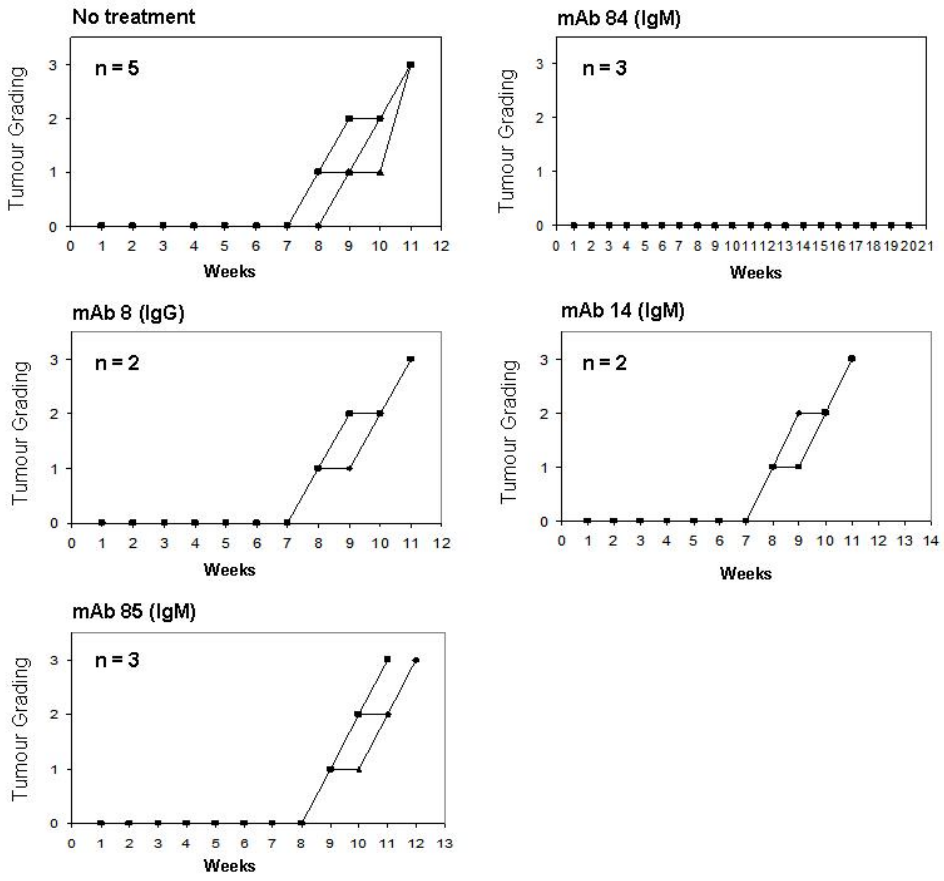

Figure 5.3 Prevention of teratoma formation is unique to mAb 84. Work was extended to other antibodies in our panel, namely; mAb8, mAb 14 and mAb 85.

5.4 *In Vivo* Model with Heterogenous Cell Population

For the second animal model, we obtained mixed cell populations of differentiated and undifferentiated hESC either by differentiating hESCs into 5 day EBs or culturing hESCs without FGF-2 for 12 days. The objective was was twofold: determine the percentage of PODXL positive cells remaining after differentiation and whether treatment of this cell mixture with mAb 84 was able to eliminate residual undifferentiated hESCs and prevent or delay the formation of tumors *in vivo*.

5.4.1 *In vivo* model with Day 5 EBs

When Day 5 EBs were trypsinized into single cells and stained with mAb 84, approximately 61% of PODXL +ve cells remained (Figure 5.4a). Although the expression of PODXL was down-regulated during differentiation to EBs, the residual PODXL +ve cell population remained susceptible to mAb 84 killing as demonstrated by the decrease in cell viability (Figure 5.4b).

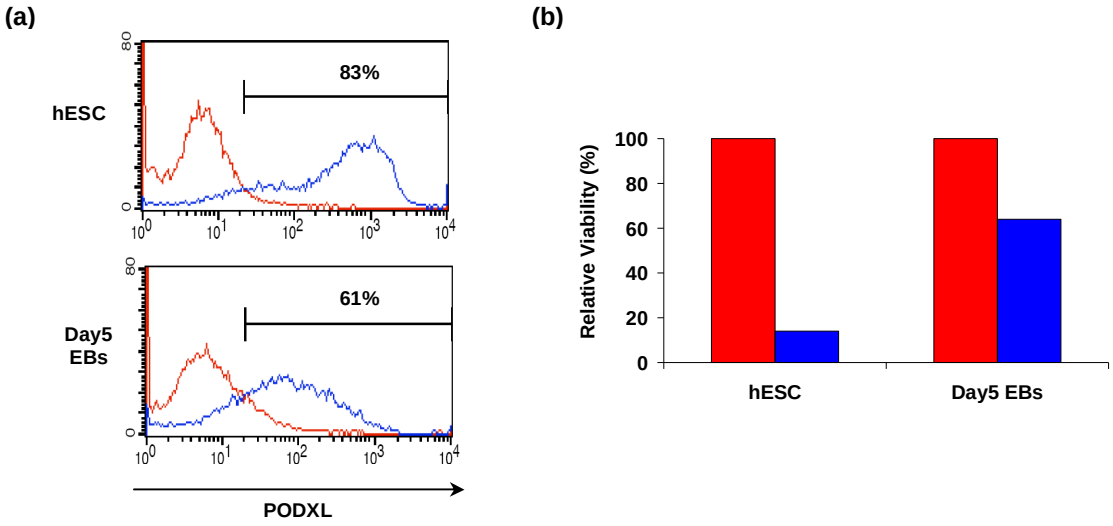

Figure 5.4 Comparison of mAb 84 binding and killing of hESC and Day 5 EBs. (a) Binding of mAb 84 to undifferentiated hESCs and Day 5 EBs. A population of undifferentiated hESC (61%) remained in Day 5 EBs. (b) Relative cell viability after mAb 84 treatment. Viability of cells was calculated with respect to the control. (■) represents untreated control, (■) represents mAb 84-treated cells. The viability of cells in Day 5 EBs dropped to 64% after mAb 84 treatment, indicative of undifferentiated cell killing.

The Day 5 EBs (both untreated and mAb 84 treated) were injected into SCID mice. However, no tumors were observed in either condition (after 24 weeks). The absence of tumors even in the untreated condition could be due to the harsh cell harvesting protocol with trypsin. However this step was necessary in order to dissociate the aggregates into a single cell suspension prior to mAb treatment and injection.

5.4.2 *In vivo* Model with hESCs cultured without FGF-2

The hESCs were cultured for 12 days in the absence of FGF-2. After differentiation, 66% of the cells were PODXL +ve and treatment with mAb 84 killed 61% of the cells. This differentiation protocol enabled us to harvest the cells into single cell suspension via a less harsh method with PBS- rather than the use of trypsin which yielded low cell viability. Preliminary data from SCID mouse model showed that differentiating cells (both untreated and mAb-84 treated) form tumors (Figure 5.5a). However, the development of tumor in the mAb 84-treated cells was much slower than that of the untreated (Figure 5.5b). In the untreated controls, tumors formed within week 10 while in the mAb 84 treated cells, formation of tumors was delayed by $3^1/_2$ months.

(a)

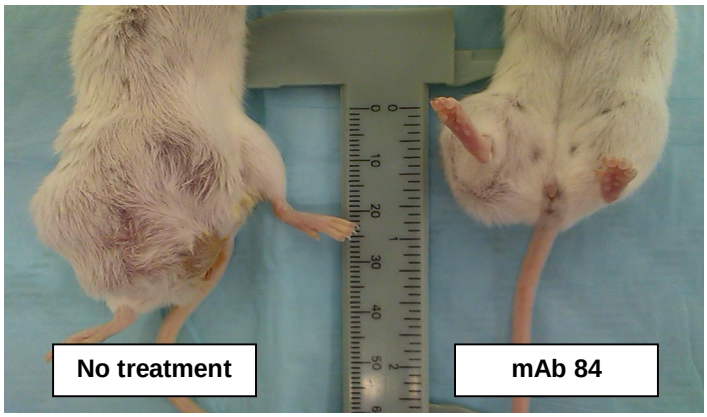

(b)

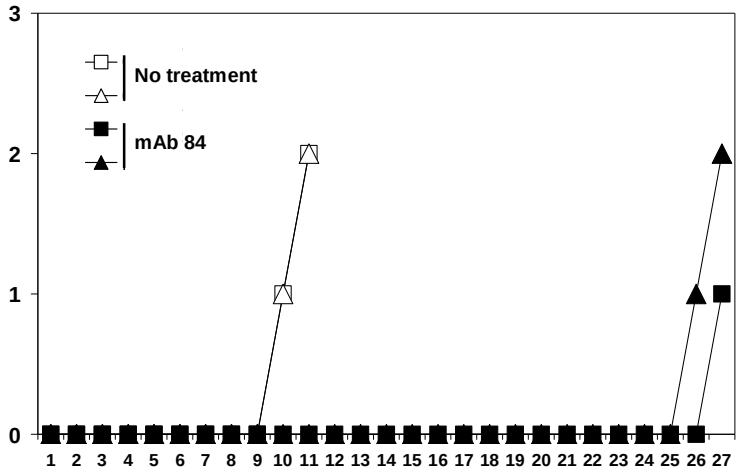

Figure 5.5 SCID mouse model with cells cultured in the absence of FGF-2 for 12 days. SCID mice were injected with differentiating cells that were either not treated with any mAb or treated with mAb 84. (a) Preliminary data shows that untreated cells form larger tumors than mAb 84 treated cells.(b) Tumor formation was delayed by $3^1/_2$ months in mAb 84 treated cells compared to untreated cells.

5.5 Summary

In the previous chapter, we demonstrated that undifferentiated hESCs can be eliminated following incubation with mAb 84 *in vitro*. Here, *in vivo* studies showed that injection of mAb 84-treated hESCs failed to form teratomas in a sensitive SCID mouse model. Extending our work to other mAbs in our panel, we showed that apart from mAb 84, treatment of hESCs with the other mAbs did not prevent teratomas and the onset was comparable to the untreated samples (as early as week 7 post-injection). We concluded that the binding and killing of hESCs by mAb 84 through PODXL is epitope specific and that the cytotoxicity is also not dependent on the class of antibody.

To date, we have demonstrated that mAb 84 is able to prevent teratoma formation by undifferentiated hESCs. However, the ultimate goal is to utilize a differentiation model which will contain a heterogenous population of both differentiated and undifferentiated hESCs. The objective of utilizing the differentiation model experiments is two-fold. The first is to investigate the ability of mAb 84 to remove residual undifferentiated hESCs from a heterogeneous cell population after differentiation and prevent the formation of tumors in SCID mouse. The second is to demonstrate functional integration of the differentiated cells after treatment with mAb 84

In addition to the mix cell model as described in section 5.4.2, we are currently investigating the application of mAb 84 in directed differentiation models. The differentiation model that we have adopted is based on the previously published protocol by Yang *et. al.* where hESCs were differentiated to chondrocytes in the presence of transforming growth factor-β3 [89]. This

differentiation protocol was shown to be robust and chondrogenic differentiation could be obtained with 2 hESC lines, H9 and HES-3. Preliminary work shows that undifferentiated hESC did not stain for Collagen-2 (Col-2), a marker for chondrocytes, while hESC-derived chondrocytes stained positive for Col-2 (Figure 5.6).

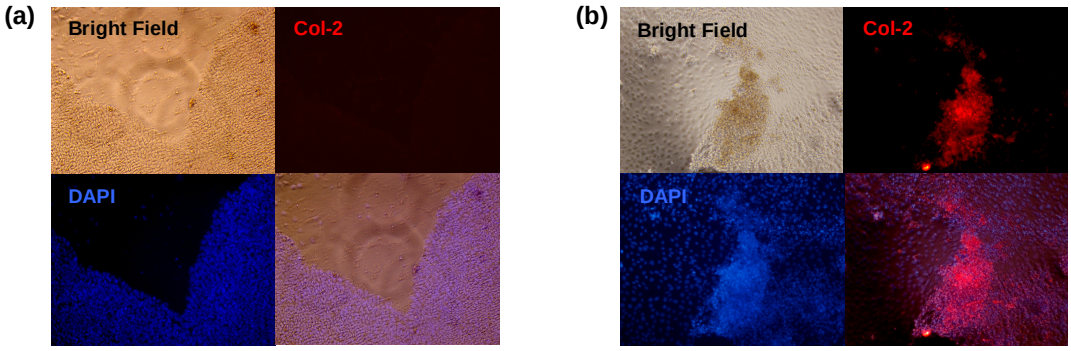

Figure 5.6 Staining for Col-2 in hESC-derived chondrocytes. (a) Undifferentiated hESC does not stain for Col-2. (b) hESC-derived chondrocytes express Col-2.

However, the differentiation of hESCs to chondrocytes is not 100% efficient. In Figure 5.7b, a population of undifferentiated hESCs was still present after chondrogenic differentiation and these cells stained positive for both Oct-4 and PODXL (as stained with mAb 84). These residual undifferentiated hESC can potentially form teratomas *in vivo*. Currently, we are establishing the *in vivo* model. Due to time constraint, data for this experiment will not be presented.

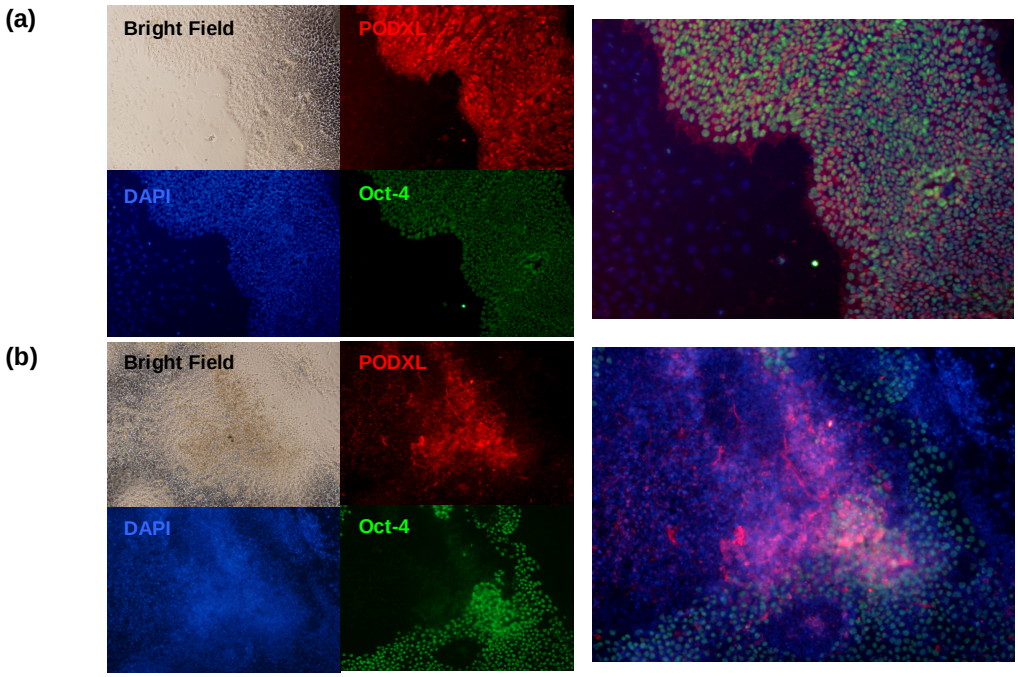

Figure 5.7 Staining for PODXL and Oct-4 in hESC-derived chondrocytes. (a) Undifferentiated hESC stained positive for PODXL and Oct-4. (b) A population of cells within the hESC-derived chondrocytes stained for PODXL and Oct-4.

Preliminary work from the mixed cell model demonstrated that although mAb 84 was able to kill PODXL +ve cells, tumor formation still occurred but the onset was significantly delayed. This result suggests that the differentiating cells (PODXL -ve) may still posses the potential to form tumors. Currently, work is in progress to separate these PODXL –ve cells from the heterogenous population for *in vivo* studies to determine if this PODXL -ve population of cells is able to form tumors.

Hence, for cell therapy utilizing hESC-derived products, we propose that several of the other hESC-specific mAbs in our panel can be used in combination with mAb 84 to ensure the complete removal of residual hESC. These mAbs, though not cytotoxic, can be conjugated to magnetic beads and used to isolate the hESCs from their differentiated progenies by magnetic cell separation technologies.

CHAPTER 6 ELUCIDATION OF DEATH MECHANISM OF mAb 84

6.1 Introduction

The previous two chapters detailed results of the *in vitro* and *in vivo* characterization of mAb 84 and its application to kill hESCs. In this chapter, the focus is to elucidate the mechanism responsible for hESC-killing by mAb 84 after binding to PODXL. Broadly, cell death can be categorized into 2 modes: apoptosis and oncosis [38,41,42,55]. Apoptosis is an organized and tightly controlled process. In most apoptosis models, cell death begins 12 to 24 h after the initiation of a trigger, with the probable activation of caspases [41,47,48,55,90]. Other characteristics of apoptosis include cell shrinkage, chromatin condensation, plasma membrane phosphatidylserine externalization, budding of the plasma membrane and the fragmentation of chromosomal DNA [38,53-55]. Oncosis, on the other hand, is typically caused by ischemia or exposure to chemical toxins [42,55]. Its mechanism is based on failure of the ionic pumps of the plasma membrane, interference with ATP generation or increase in plasma membrane permeability [38,42,55]. Early manifestations consist of plasma membrane blebbing, dilation of the ER, mitochondrial swelling, and clumping of nuclear chromatin.

6.2 Apoptosis Studies

6.2.1 Rate of killing

In most apoptosis models, cell death typically occurs within 12-24 h [41]. This suggests that the mode of mAb 84-mediated cell killing of hESCs is

unlikely through apoptosis. To demonstrate this difference in the rate of induced cell death, we performed a propidium iodide (PI) assay on mAb 84-treated and apoptosis-induced hESC (Figure 6.1). After 45 min incubation of hESCs with mAb 84, the viability relative to non-treated control dropped drastically to 9%. The viability of hESCs incubated with the isotype control, mAb 85, remained comparable to the no treatment control. On the other hand, the relative viability of apoptotic cells dropped to about 76%, even though the PI assay was carried out 2 h after the induction of apoptosis. Hence, the rate of cell death via apoptosis is much slower compared to mAb 84-mediated cell death.

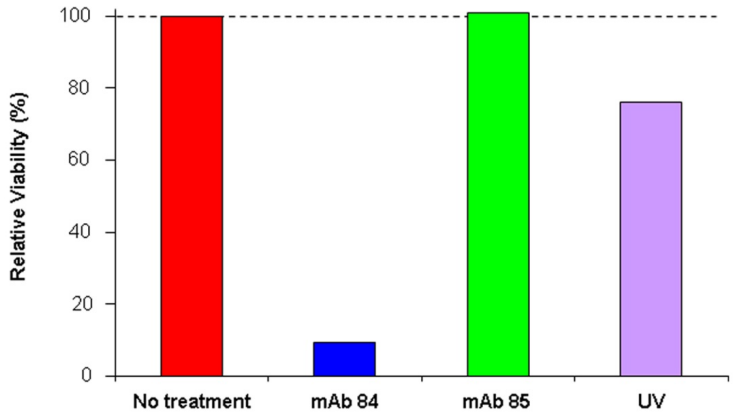

Figure 6.1 Comparison of hESC viability between mAb 84-treated cells and apoptotic hESCs. Relative viability (%) was calculated using the ratio of the viability of hESCs after mAb treatment to the viability of cells that were not treated with any antibody (No treatment control). The graph shows the relative viability of hESCs incubated with mAb 84 (■). Controls include cells incubated with isotype control, mAb 85 (■) and apoptotic cells that were induced by UV irradiation and incubated for 2 h (■). Viability was determined via PI stain on a flow cytometer.

6.2.2 TUNEL assay

This observation is further reiterated by 2 complementary biochemical assays for apoptosis. The first assay was to measure the extent of DNA

fragmentation via TUNEL assay [42,53,54].[43] From Figure 6.2, mAb 84-treated cells did not exhibit significant elevation in the level of DNA fragmentation compared to the isotype control, mAb 85. On the contrary, apoptotic hESC exhibited a significant elevation in the level of DNA fragmentation.

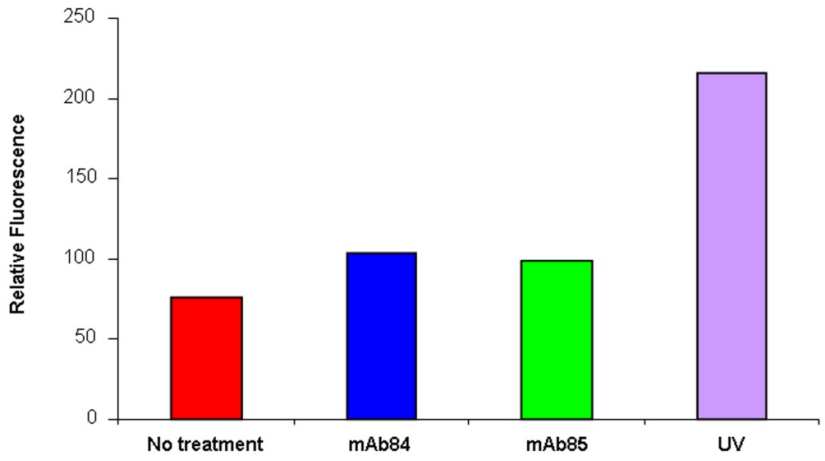

Figure 6.2 Degree of DNA fragmentation measured by TUNEL via flow cytometry.

6.2.3 Caspase activation

Next, we compared the activity of several caspases between mAb 84-treated and apoptotic hESCs (Figure 6.3). Results showed that the activity of caspases measured were at minimal basal levels for mAb 84-treated hESCs. In contrast, apoptosis-induced hESCs exhibited significantly higher caspase activities, in particular, caspases 2 and 3. The activities of these caspases were significantly reduced in cells that were incubated with ZVAD, an inhibitor to these capases. Hence, both results suggest that the mode of mAb 84-mediated cell death is unlikely to be apoptosis.

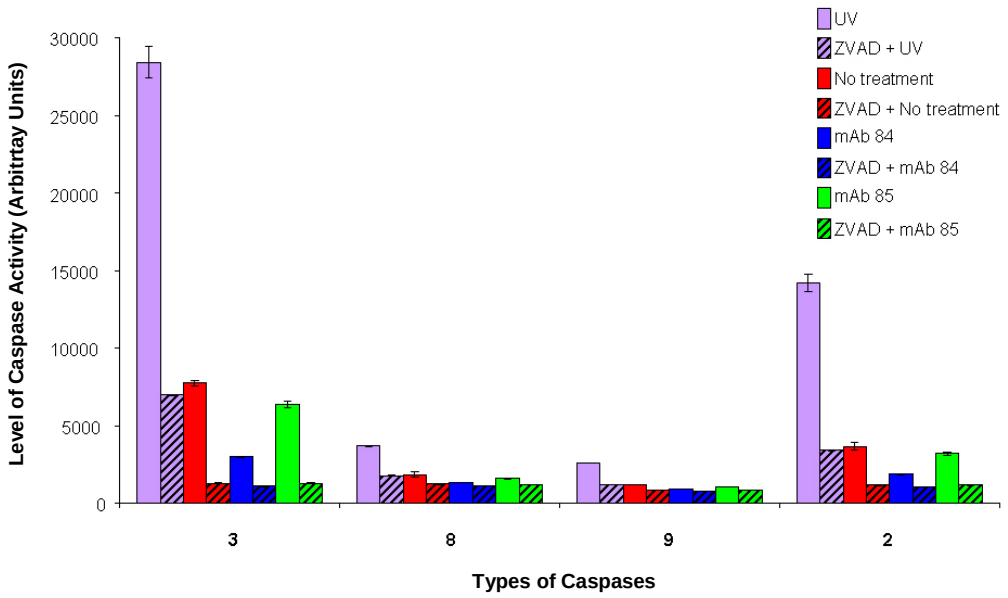

Figure 6.3 Measured caspase activities. Error bars represent standard error of the mean of duplicate samples.

6.2.4 Annexin staining

Another characteristic of apoptosis is the exposure of the phospholipid, phosphatidylserine (PS), on the external surface of the cell. The detection of PS has been widely accepted as a hallmark of apoptosis and is detected by Annexin V [50,51,91-94].[95-99] In our experiments, surprisingly PS was detected by Annexin V in both apoptotic cells and mAb 84-treated cells (Figure 6.4 a and b). However, it is likely that the latter result is an artifact and not due to the exposure of PS on the external surface of the mAb 84-treated cells[55,56]. We speculate that because the membrane becomes permeable after mAb 84 treatment (increase in PI uptake), Annexin V is detecting intracellular PS instead. To validate this, hESCs were fixed, permeabilized and incubated with Annexin V (Figure 6.4c). Similar to mAb 84-treated hESCs, fixed and permeabilized hESCs had an elevated binding of annexin V

but to intracellular PS. Due to the mechanism which mAb 84 kills the cells, we are not able to utilize this assay.

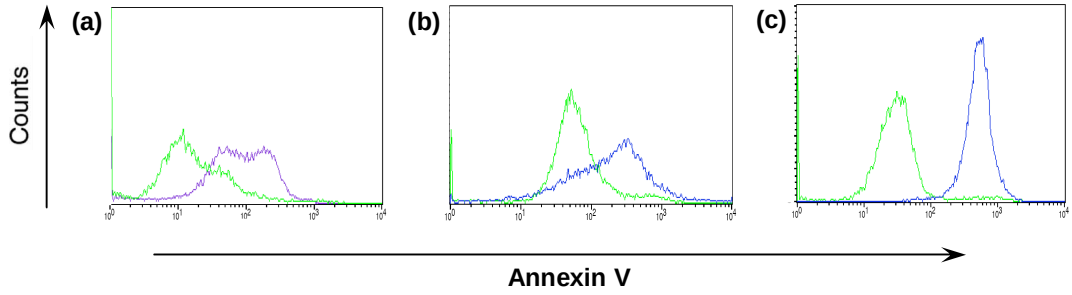

Figure 6.4 Detection of PS via annexin staining. (a) Non-apoptotic cells (green) versus apoptotic cells (purple). (b) mAb 84-treated cells (blue) versus mAb 85-treated cells (green). (c) Live cells (green) versus fixed and permeabiilzed cells (blue).

6.3 Oncotic Studies

6.3.1 mAb 84 induces plasma membrane damage

Alternatively, we investigated oncosis as the probable mode of mAb 84-mediated cell death. Oncosis is characterized by an increase in cell membrane permeability and altered membrane morphology due to damage to the plasma membrane [42,57-62].[47-50] The increase in membrane permeability of the cells can be assessed by the leakage of intracellular lactate dehydrogenase (LDH) and Na^+ from the cells and entry of dextran beads into the cells [52,53,57-62,100-102].

6.3.1.1 Leakage of LDH out of cells

LDH leakage has been used as a marker for increase membrane permeability during cell death [57-59,62]. Human ESCs were incubated for 45 min either with mAb 84, the isotype control mAb 85 or untreated (No

treatment control). Subsequently, the clarified supernatant was collected and assayed for LDH activity (Figure 6.5).

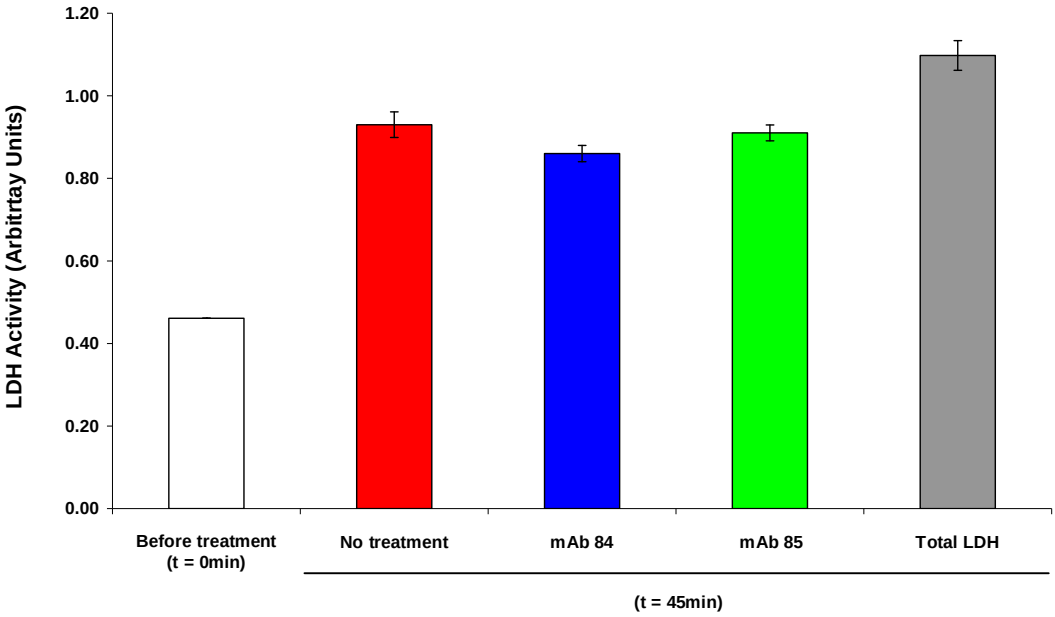

Figure 6.5 Measurement of LDH activity in the supernatant after treatment of hESC with antibodies. Cells were incubated with antibodies for 45 min and LDH activity measured. (□) represents sample at t = 0 min. (■) represents untreated control, (■) represents mAb 84-treated cells, (■) represents mAb 85-treated cells, (■) represents total LDH (leaked LDH in the supernatant and LDH that remains in the cells).

Interestingly, there were no significant differences in the LDH activity between the untreated control, mAb 84- and mAb 85-treated cells despite the increase in membrane permeability of mAb 84-treated hESCs compared to the controls. This was probably due to the high percentage of dead cells after harvesting with trypsin resulting in the elevated basal LDH levels into the supernatant. This consequently masked any changes to the LDH activity after incubating the hESCs with mAb 84.

6.3.1.2 Leakage of Na^+ out of cells

Alternatively, the increase in membrane permeability of the cells can be assessed by the leakage of intracellular Na^+ from the cells [52,53,100-102]. The fluorescence level within the cells increased upon irreversible coupling of intracellular Na^+ with a fluorescence dye (Figure 6.6). When these cells were treated with mAb 85, the fluorescence level remained as high as the non-treated control. However, upon incubation with mAb 84, the fluorescence level within the cells decreased, suggesting the leakage of intracellular Na^+ out of the cells as a result of increased membrane permeability.

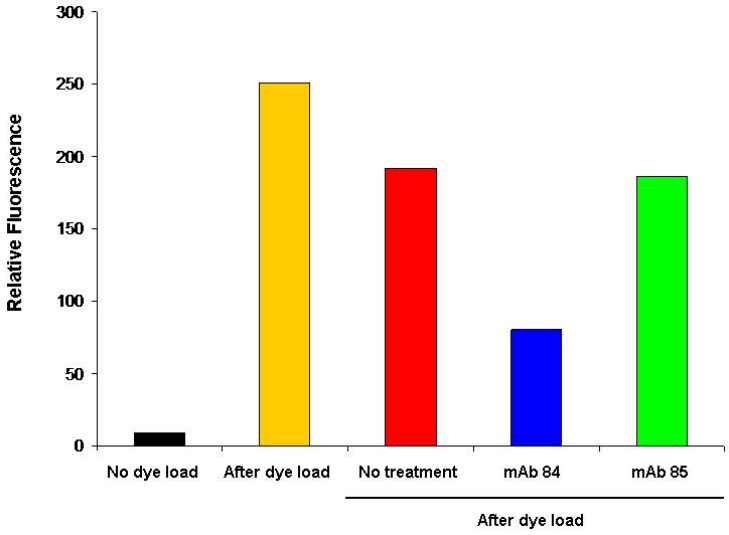

Figure 6.6 Coupling of intracellular Na^+ with fluorescence dye. Fluorescence level of hESCs (loaded with fluorescence dye) after incubation with mAb 84 and mAb 85, compared with the 'no treatment' control.

6.3.1.3 Entry of dextran beads into cells

Studies have shown that plasma membrane damage in oncotic cells is caused by the formation of pores on the cell surface [36]. The sizes of these pores can be estimated with dextran beads of varying molecular weight [49,50,58,60,61]. From Figure 6.7, it was observed that both 3 and 2,000 kDa

dextran beads were able to diffuse into mAb 84-treated hESC, leading to an increase in fluorescence level comparable to fixed and permeabilized cells (positive control). This data suggest that the pores formed on the plasma membrane were greater than 2,000 kDa in size. In contrast, diffusion of dextran beads varying between 3 to 2,000 kDa into the cells for both controls (non-treated and mAb 85) were minimal (Figure 6.7). The percentage of cells that had higher fluorescence in the controls was attributed to the background of dead cells after cell harvest and incubation. In addition, based on our calculation, we estimated the diameter of the 2,000 kDa dextran beads to be approximately 20 ηm. This suggests that the size of the pores formed on the surface of the mAb 84-treated hESCs were larger than 20 ηm.

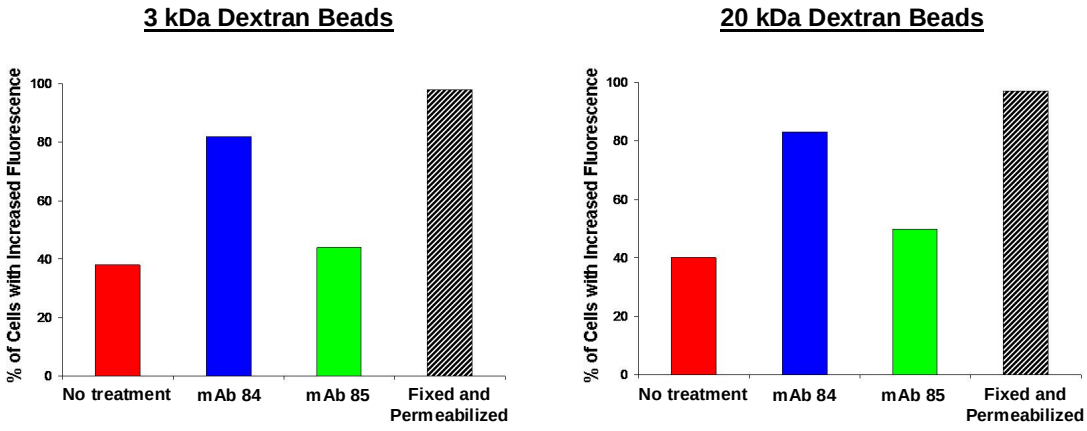

Figure 6.7 Determination of pore size with 3kDa and 2,000 kDa dextran beads respectively. Cells were incubated with mAb 84, mAb 85, or not treated with any antibodies followed by fluorescent dextran beads. As a positive control, cells were fixed and permeabilized. Increase in intracellular fluorescence is correlated with the entry of dextran beads into the cells. The population of cells with high fluorescence were gated and the percentages are represented in the graph.

6.3.1.4 Visualization of cell surface with scanning electron microscopy (SEM)

To further investigate the cytotoxic effects of mAb 84 on hESCs, we examined the cell surfaces for structural changes via SEM (Figure 6.8). Characteristically, pronounced clumping of hESCs after incubation with mAb 84 was observed (Figure 6.8 B). Morphologically, these cells displayed a loss of surface microvilli, with the formation of membrane blebs and surface wrinkles. Most importantly, numerous pores were formed on the plasma membrane (Figure 6.8 E). The sizes of these pores were heterogeneous with diameters as large as 0.5 μm (white arrows). This observation explains the entry of the 2,000 kDa dextran beads. In contrast, cells in both controls did not aggregate and preserved uniform morphology with normal cell surface structures (Figures 6.8 A, C, D and F). Our findings are similar to a previous study by Zhang *et. al*. and these results suggest that the mode of mAb 84-mediated cell death is through oncosis [44].

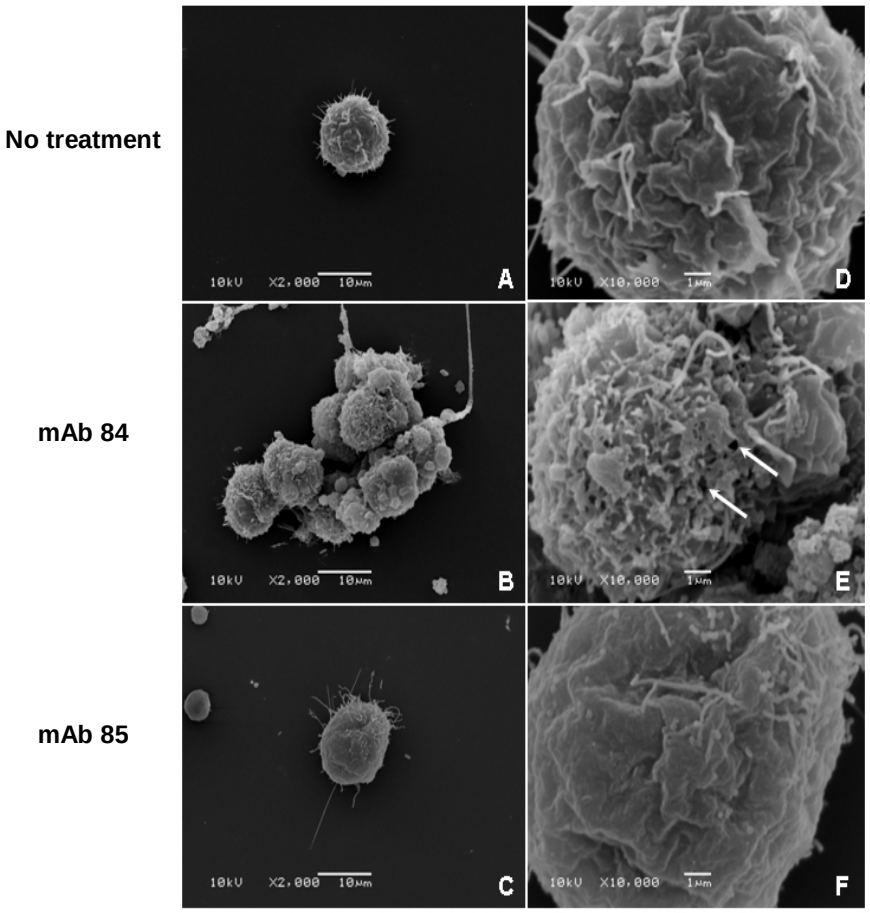

Figure 6.8 Observation of cell surface via SEM. (A-C) Magnifications are at x 2,000 (bar = 10 μm). (D-F) Magnifications are at x 10,000 (bar = 1 μm).

6.3.2 mAb 84-mediated oncosis involves changes in cytoskeleton proteins

6.3.2.1 mAb 84-mediated oncosis causes the degradation of some cytoskeletal proteins

Liu *et. al.* previously found that the increase in plasma membrane permeability of oncotic cells is closely correlated to modifications in structural proteins, namely, α-actinin, paxillin, talin and vinculin [62]. In particular, degradation of paxillin resulted in membrane permeability during oncosis [55]. In mAb 84-mediated oncosis, significant degradation was observed with

cytoskeleton-associated proteins, α-actinin, paxillin and talin, compared to the controls (Figure 6.9). There was however no change in the levels of vinculin after mAb 84 treatment.

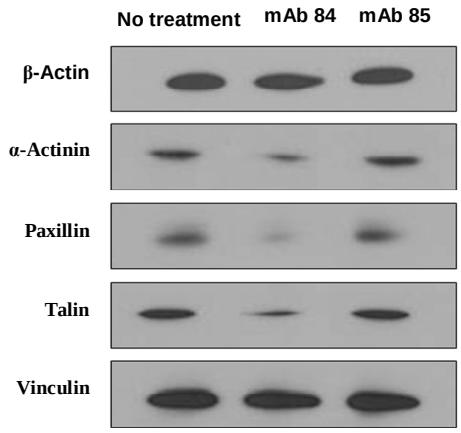

Figure 6.9 Degradation of cytoskeleton-associated proteins. mAb 84-mediated oncosis leads to degradation of α-actinin, paxillin and talin.

By immunocytochemistry and confocal microscopy, paxillin was found to localize at the periphery of the cell membrane after treatment with mAb 84 (white arrows) as opposed to treatment with control mAb 85 where the staining of paxillin was diffuse within the cytoplasm (Figures 6.10 a and b respectively). Taken together, these results demonstrate a close association of the reorganization of cytoskeleton-associated α-actinin, paxillin and talin with mAb 84-mediated oncosis.

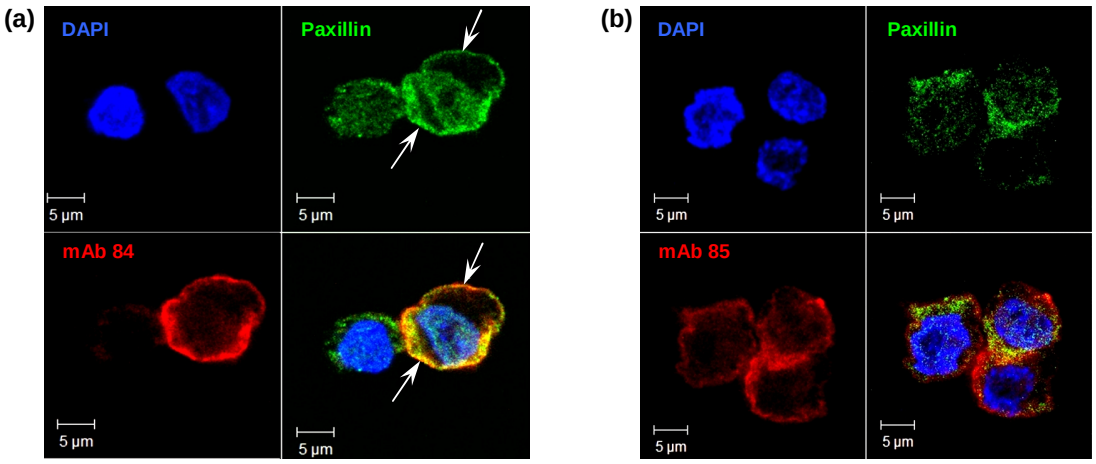

Figure 6.10 Confocal microscopy of hESC after treatment with mAb 84 and mAb 85. (a) Co-localization of paxillin (green) at the periphery of the cell membrane with mAb 84 (red) as indicated by the white arrows. The nuclei are stained with DAPI (blue). Magnification is at x 2520 (bar = 5 µm). (b) Diffuse staining of paxillin (green) within the cells after treatment with mAb 85 (red). The nuclei are stained with DAPI (blue). Magnification is at x 2520 (bar = 5 µm).

Takeda *et. al.* and Schmieder *et. al.* have shown that PODXL is connected to the actin filaments through the Na^+/H^+-exchanger regulatory factor 2 (NHERF2)/ezrin complex [76,103]. In a report by Lebart and Bentamin, the complex interaction between actin, numerous cytoskeleton proteins and integrins was mapped [104,105]. Piecing these data together, PODXL interacts with various cytoskeleton proteins and integrins. Hence, we proceeded to investigate if mAb 84-mediated oncosis causes the degradation of other cytoskeleton proteins apart from α-actinin, paxillin and talin. From Figure 6.11, mAb 84 treatment of cells causes the degradation of focal adhesion kinase NHERF -1 and -2, ezrin, α- and β- tubilin. However, integrin β-1 was not degraded during mAb 84-mediated oncosis.

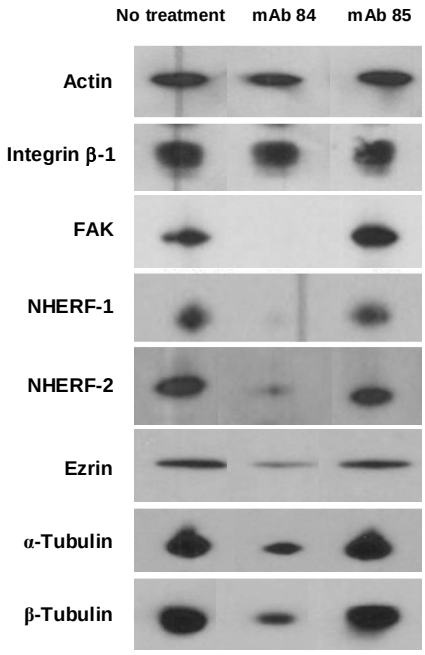

Figure 6.11 Degradation of other cytoskeleton-associated proteins during mAb 84-mediated oncosis. Integrin β-1 was not degraded after mAb 84 treatment.

Confocal microscopy was also carried out to investigate if there was re-organization of the actin filaments during mAb 84-mediated oncosis. From Figure 6.12, no apparent re-arrangement of the actin filaments was observed in mAb 84 treated cells compared to the controls. This was probably due to the fact that the cells had to be treated with the antibodies as a single cell suspension. The cells circularize and any morphology change in actin is not apparent.

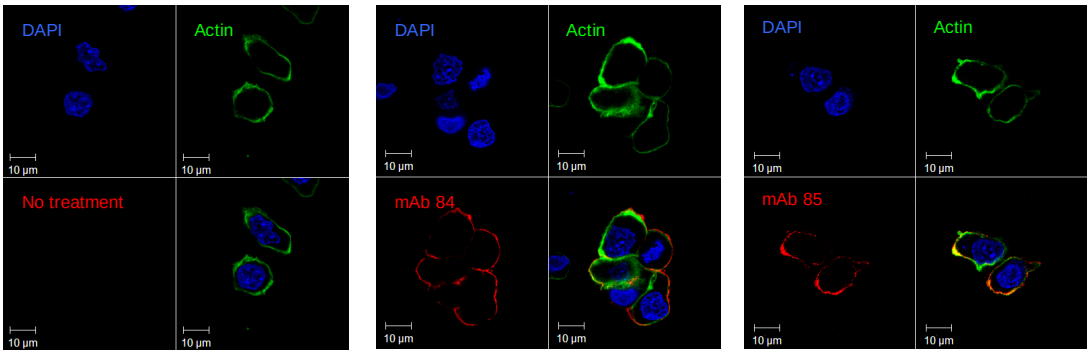

Figure 6.12 Confocal microscopy to investigate changes in actin filament during mAb 84-mediated oncosis.

6.3.2.2 Degradation of cytoskeletal proteins during mAb 84-mediated oncosis occurs rapidly

When we tracked the degradation of α-tubulin with time, we found that the protein degraded within 10 min post mAb 84 treatment (Figure 6.13). This result was consistent with the time course experiment whereby significant hESC was killed as fast as 15 min (Figure 4.8).

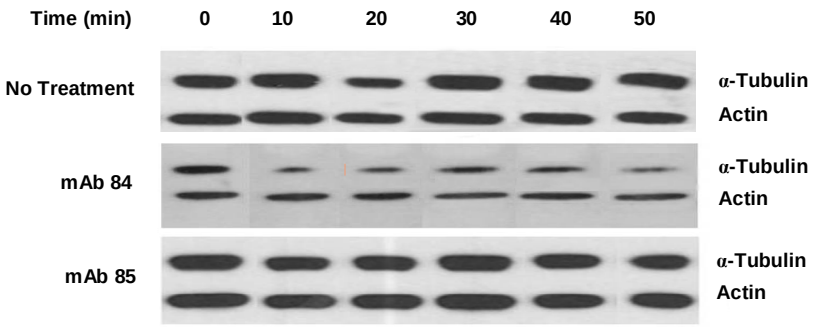

Figure 6.13 Degradation of α-tubilin is time-dependent during mAb 84-mediated oncosis. The degradation of α-tubilin occurs as fast as 10min after the cells were treated with mAb 84.

6.3.2.3 Degradation of cytoskeletal proteins during mAb 84-mediated oncosis is not caused by calpains

Increase in membrane permeability is a characteristic of oncosis. However, the mechanism underlying this increase in membrane permeability during oncosis is poorly understood [62]. Growing evidence indicates that the protease, calpain, plays a critical role in the process [55,62,106]. Calpain belongs to a family of 14 Ca^{2+}-activated neutral cysteine proteases [55,107]. However, the biochemistry of most calpains and the specific roles of the different calpains in physiology and pathology remains to be determined. Various studies have identified a number of calpain substrates in cellular systems. These calpain substrates include numerous cytoskeleton proteins [63,107-111]. Studies also suggest that calpains mediate the increase in plasma membrane permeability and the progressive breakdown of the membrane during oncosis through the proteolysis of cytoskeletal and plasma membrane proteins [55,62,106].

We proceeded to investigate if calpain is responsible for increase in membrane permeability and degradation of cytoskeleton proteins observed in mAb 84-mediated oncosis (Sections 6.3.1 and 6.3.2). Calpain inhibitors have been successfully used to demonstrate calpain involvement in several studies [55,62,65,106]. In these studies, the authors showed that they were able to prevent the hydrolysis of cytoskeletal proteins, minimize membrane permeability and significantly improve cell viability during oncosis when they treated the cells with calpain inhibitors prior to trigger of oncosis [62,106]. Here, hESCs were pre-incubated for 24 h with an array of calpain inhibitors

before treatment with mAb 84. From Figure 6.14, it was observed that none of the calpain inhibitors were able to prevent mAb 84-mediated cell death.

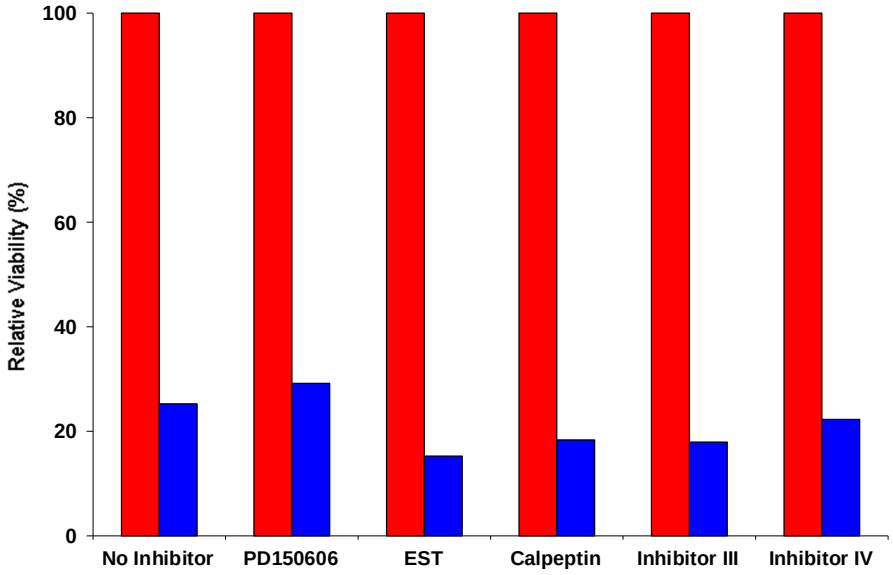

Figure 6.14 An array of calpain inhibitors was tested to prevent mAb 84-mediated oncosis. Cells in culture were pre-incubated with the inhibitors for 24 h prior to mAb 84 treatment. (■) represents untreated control, (■) represents mAb 84-treated cells. None of the inhibitors was able to inhibit mAb 84-mediated oncosis.

6.3.3 mAb 84-mediated oncosis involves oligomerization of antigens

We also hypothesized that the degradation of these cytoskeleton-associated proteins increases the mobility of the cell surface proteins, thus permitting PODXL to oligomerize following binding to the pentameric mAb 84. This perturbation of the cell membrane consequently leads to pore formation on hESCs. This phenomenon of PODXL oligomerization was visualized via SEM following tagging of mAb 84 and mAb 85 with secondary antibodies conjugated to colloidal gold. From Figure 6.15, no non-specific binding of the secondary antibody to the cells was observed in the non-treated control. For mAb 84-treated cells, large clusters of antibodies were detected as opposed to mAb 85-treated cells, where the antibody binding was distributed

throughout the cells in small clusters. An important point to note was that the cells were sputtered with carbon, instead of gold, to allow the differentiation of the secondary gold particles from the cells for SEM visualization. However using this counter stain method, it was not possible to simultaneously visualize pore formation and antibody-antigen aggregation. Thus, the data in Figures 6.8 and 6.15 suggest that the oligomerization of antigens occurs following mAb 84 treatment on hESCs, consequently forming pores on the plasma membrane.

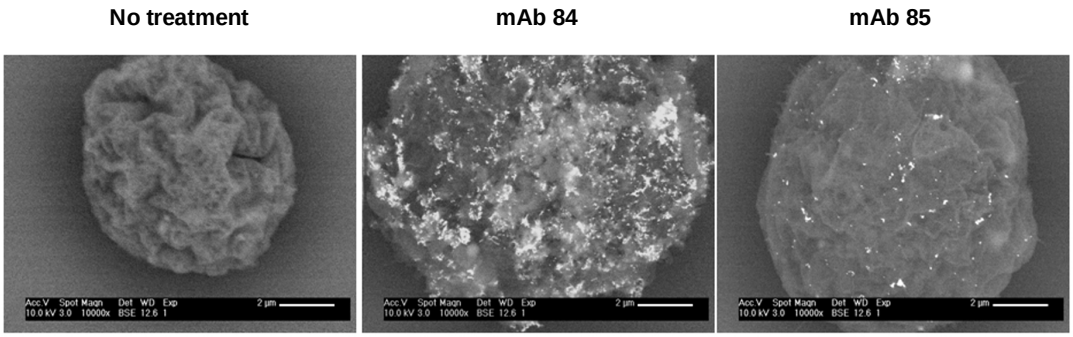

Figure 6.15 Aggregation of antigens upon incubation of hESCs with mAb 84. Antigen aggregation as visualized by SEM. Magnification is at x 10,000 (bar = 2 μm).

6.4 Summary

In this chapter, we elucidated the death mechanism of mAb 84 killing. The work reported here was published in Stem Cells, entitled “mAb 84, a Cytotoxic Antibody that Kills Undifferentiated Human Embryonic Stem Cells via Oncosis” (refer to APPENDIX A). We showed that mAb 84 is unlikely inducing hESC killing via apoptosis based on TUNEL and caspase activity assays. Instead, from our observations, we concluded that cell death is mediated via a process similar to oncosis. Many of our findings are consistent with previous work carried out by Zhang *et. al.* where an antibody, anti-

Porimin, kills Jurkat cells via a process similar to oncosis [36]. Both mAb 84 and anti-Porimin bind to antigens that are highly glycosylated, with cell death observed as fast as 20 min. In addition, both antibodies mediate cell death that was preceded by rapid cell aggregation, pore formation on the plasma membrane, cell swelling and membrane blebbing. The similarities between anti-Porimin and mAb 84 are summarized in Table 6.1.

Although oncosis and apoptosis are 2 different cell-death processes, the characteristics between apoptosis and oncosis are not distinct. One such characteristic is the exposure of the phospholipid, phosphatidylserine (PS), on the external surface of the cell. The detection of PS has been widely accepted as a hallmark of apoptosis and is detected by Annexin V [50,51,91-99]. However, Lecoeur *et. al.* demonstrated that the exposure of PS is not limited to apoptosis but is also associated with oncosis [56]. In our experiments, PS was also detected by Annexin V staining on the flow cytometer in mAb 84-treated cells. However, this detection of PS was not due to its exposure on the external surface of the mAb 84-treated cells. Instead, the pores (> 2,000 kDa) formed on hESC after mAb 84 treatment were sufficiently large for Annexin V (~33 kDa) to enter the cells and bind to the intracellular PS [55,56,112-114]. Intracellular PS was also detected in healthy cells that were fixed and permeabilized to allow the entry of Annexin V into the cells. Hence, due to the unique mechanism of mAb 84-mediated cell killing, the use of Annexin as an absolute marker to demonstrate apoptosis is questionable.

Table 6.1 Similarities between anti-Porimin and mAb 84.

Characteristic	Anti-Porimin	mAb 84
Not apoptosis	No DNA fragmentation/laddering	No DNA fragmentation Low caspase activities
Antigen - highly glycosylated	Calculated MW ~ 21.5 kDa Apparent MW ~ 55-110 kDa	Calculated MW ~ 55 kDa Apparent MW ~ 200 kDa
Cell death	Occurs ~ 20 min	Occurs ~ 15-20 min
Increase membrane permeability	PI	PI, Trypan blue, Na^+
Aggregation of cells	Yes	Yes
Pore formation	Visualized through SEM	Visualized through SEM

Consistent with past work on oncosis, we also observed the degradation of cytoskeleton-associated proteins, such as α-actinin, paxillin and talin, and the degradation of these proteins was found to be time-dependent [62]. Previous studies have identified the role of a calcium-dependent protease, calpain, in the hydrolysis of these cytoskeleton-associated proteins [55,62,63,104-110,115-117]. Interestingly, these calpain substrates can be linked to PODXL. It has been reported that PODXL complexes with erzin and Na^+/H^--exchanger regulatory factor (NHERF) which interacts with actin and these cytoskeleton-associated proteins [103,104,118-

122]. However, we failed to elucidate the role of calpain in mAb 84-mediated oncosis.

Putting our data together, a model is proposed to illustrate the events that occur in mAb 84-mediated oncosis of hESCs (Figure 6.16). When mAb 84 binds to the highly glycosylated PODXL, it causes the degradation of cytoskeleton-associated proteins. Hydrolysis of these proteins increases the mobility of PODXL, resulting in the clustering of antigens on the cell surface due to crosslinking by the pentameric mAb 84. Consequently, the oligomerization of the antigens results in the formation of pores on the plasma membrane. To our knowledge, this is the first study on antibody-mediated oncosis which utilizes hESCs as a model.

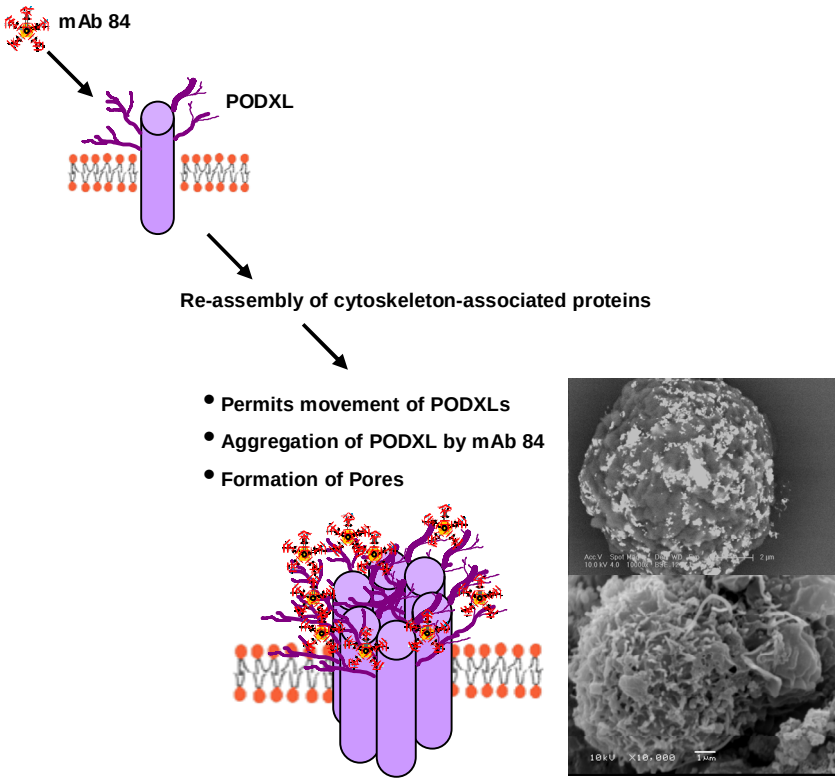

Figure 6.16 Proposed model for mAb 84-mediated oncosis.

CHAPTER 7 CONCLUSION AND FUTURE WORK

7.1 Conclusion

A panel of antibodies was raised against hESCs with the aim of identifying novel hESC surface markers, characterizing hESC populations and using these mAbs to separate residual undifferentiated hESCs from differentiated cells. One of the mAbs from this panel, mAb 84, not only binds to but also kills hESCs. *In vitro* characterization of mAb 84 found that:

(1) mAb 84 specifically kills undifferentiated hESCs and not differentiated cells.

(2) By IP and MS analysis, the antigen which mAb 84 binds to on hESCs was identified as podocalyxin-like protein-1 precursor (PODXL). The protein is highly glycosylated with an apparent molecular weight of ~200 kDa.

(3) mAb 84 mediated-killing of hESC is independent of complement and temperature.

(4) mAb 84 mediated-killing of hESCs occurs rapidly. Based of PI exclusion assay, the cytotoxic effect of mAb 84 on hESCs was observed as quickly as 15 min after incubation with the viability dropping to 33%, with a further decrease in viability to 20% after 45 min.

(5) Efficiency of mAb 84 mediated-killing of hESCs is dose dependent. In our experiments, when 2 x 10^5 cells was resuspended in 200 µl buffer, more than 70% of cells was killed by 1ug of mAb 84.

(6) The binding of mAb 84 to PODXL is via O-linked glycans.

(7) mAb 84 is also cytotoxic to iPS cells.

From *in vivo* characterization of mAb 84, we demonstrated that the *in vitro* treatment of homogenous populations of hESCs with mAb 84 eliminated teratoma formation in SCID mouse models. Extending the work to other hESC-specific mAbs in our panel, we showed that only hESCs treated with mAb 84 did not form teratomas *in vivo*. Treatment with the other mAbs failed to prevent the onset of teratoma formation which occurred as early as 7 weeks post-injection. From this, we concluded that the binding and killing of hESCs by mAb 84 is epitope specific and that the cytotoxicity is probably not dependent on the class of antibody.

We also extended these animal model studies to a heterogenous population of undifferentiated hESCs and differentiated cells generated by spontaneously differentiating the cells in the absence of FGF-2 for 12 days. From this preliminary work, we found that although mAb 84 treatment failed to prevent the formation of teratomas *in vivo*, it was able to delay the onset of teratoma formation compared to the non-mAb84 treated control. We speculate that the differentiating cells may still possess the potential to form teratomas however this requires more detailed investigation. Currently, work is in progress to separate the PODXL –ve cells from the heterogenous population for *in vivo* studies to determine if the PODXL -ve cell population is able to form teratomas. For cell therapy utilizing hESC-derived products, we propose that several of the other hESC-specific mAbs in our panel can be used in combination with mAb 84 to ensure the complete removal of residual hESCs. These mAbs, though not cytotoxic, can be conjugated to magnetic

beads and used to isolate the hESCs from their differentiated progenies by magnetic cell separation technologies.

We also elucidated the mechanism responsible for hESC killing following mAb 84 binding. It was determined that binding of mAb 84 induced oncosis in hESCs and a model was proposed to illustrate the series of events that occur. Following mAb 84 binding to the highly glycosylated PODXL, it causes the degradation of several cytoskeleton-associated proteins such as α-actinin, paxillin and talin. Hydrolysis of these proteins increases the mobility of PODXL, resulting in the aggregation of PODXL on the cell surface due to crosslinking by the pentameric mAb 84. Consequently, the oligomerization of the PODXL results in the formation of pores on the plasma membrane.

This is the first study on antibody-mediated oncosis which utilizes hESCs as a model. The significance of these findings is that this antibody can be used to eliminate contaminating hESCs and iPS cells from the differentiated cell population prior to clinical applications because teratoma formation *in vivo* would severely compromise the success of the transplant. This “clean-up” step prior to transplantation will increase the safety of this procedure and alleviate concerns over the use of hESCs and iPS cells as the starting cell population for cell therapy.

7.2 Future Work

7.2.1 *In vitro* characterization of mAb 84

For *in vitro* characterization of mAb 84, it would be interesting to investigate if mAb 84 binds and kills other cancer cells apart from the embryonal carcinoma cell line, NCCIT. It has been reported that the antigen

PODXL is found in breast and prostate cancers and has been implicated as an indicator of tumour aggressiveness [23,87].

7.2.2 *In vivo* characterization of mAb 84

Based on our preliminary results, we have shown that mAb 84 is able to significantly delay the onset of tumor formation in heterogenous cell population where the cells were spontaneously differentiated in the absence of FGF-2 for 12 days. This result suggests that the differentiating cells (PODXL -ve) may still possess the potential to form tumors. Currently, work is in progress to separate the PODXL –ve cells from the heterogenous population for *in vivo* studies to determine if these cells are able to form teratomas.

Studies are also being carried out with directed differentiated model. The differentiation model that we have adopted is based on the previously published protocol by Yang *et. al.* where hESCs were differentiated to chondrocytes in the presence of transforming growth factor-β3 [89]. The objective of these experiments is two-fold. The first is to investigate the ability of mAb 84 to remove residual undifferentiated hESC from a heterogeneous cell population after differentiation and prevent the formation of tumors in SCID mouse. The second is to demonstrate functional integration of the differentiated cells after treatment with mAb 84 at the injury site.

Preliminary work on the hESC-derived chondrocytes showed that undifferentiated hESCs did not stain for Collagen-2 (Col-2), a marker for chondrocytes, while the hESC-derived chondrocytes stained positive for Col-2. However, the differentiation of hESCs to chondrocytes is not 100%

efficient. A population of undifferentiated hESCs was still present after chondrogenic differentiation and these cells stained positive for both Oct-4 and PODXL. These residual undifferentiated hESCs can potentially form tumorss *in vivo*. Currently, we are establishing the *in vivo* model for the hESC-derived chodrocytes. In addition to chondrogenic differentiation, other directed differentiation protocols may also be explored, e.g. cardiomyocytes. This will enable us to demonstrate the generic utility of mAb 84 to eliminate contaminating hESCs from different cell populations and more importantly, demonstrate that the differentiated cells remain functional after treatment with mAb 84.

In addition to hESCs, we would like to expand the *in vivo* work to iPS cells since patient-specific iPS cells are also a valuable source of cells for therapy and drug screening. The *in vivo* models for iPS cells would be similar to that for hESCs, namely; homogenous iPS cells, heterogeneous mix cell population and differentiation models with iPS cells.

7.2.3 Elucidation of death mechanism of mAb 84

A model has been proposed to describe the mechanism of mAb 84-induced oncosis. As mAb 84 kills hESCs rapidly, we would like to investigate the possible role of calcium ions as second messengers upon antibody binding to PODXL [123]. Studies have also shown that Ca^{2+} is involved in many cell signaling processes including cell death [123,124]. Recently, it was also suggested that F-actin and actin-binding proteins may modulate the release of Ca^{2+} [125,126]. As described, PODXL complexes with erzin and Na^{+}/H^{-}-exchanger regulatory factor (NHERF) which interacts with actin [103].

Hence, it will be interesting to investigate any perturbation in Ca^{2+} concentration upon mAb 84 binding to PODXL which ultimately leads to pore formation on the plasma membrane. Such perturbation in Ca^{2+} concentration can be studied via patch clamp [127,128]. Currently, preliminary studies are being carried out in collaboration with Prof Soong (Physiology NUS) leveraging on his expertise in patch clamping.

ABBREVIATIONS

APC	Allophycocyanin
ATP	Adenosine-5'-triphosphate
BSA	Bovine serum albumin
CAD	Caspase-activated DNAse
CM	Condition media
CO_2	Carbon dioxide
CoI-2	Collagen 2
DMEM	Dulbecco's modified Eagle's medium
DNA	Deoxyribonucleic acid
DTT	Dithiothreitol
dUTPs	Deoxynucleotide triphosphates
EB	Embryoid bodies
EC	Embryonal carcinoma
EDTA	Ethylenediaminetetraacetic acid
ESI	ES Cell International
EST	Expressed sequence tag
Fab	Fragment, antigen binding
FAK	Focal adhesion kinase
FGF-2	Fibroblast growth factor-2
FITC	Fluorescein isothiocyanate
GAH	Goat-anti-human
GAM	Goat-anti-mouse
HAT	Hypoxanthine-aminopterin-thymidine

hESC	Human embryonic stem cell
HPC	Hematopoietic progenitor cells
HRP	Horseradish peroxidase
IB	Immuno-blot
iCAD	Inhibitor of caspase activated DNAse
IDA	Information dependent acquisition
IgG	Immunoglobin G
IgM	Immunoglobin M
IP	Immuno-precipitation
iPS cells	Induced pluripotent stem cells
KO	Knockout
LDH	Lactate dehydrogenase
mAb	Monoclonal antibody
MDCK	Madin-darby canine kidney
MS	Mass spectrometry
MW	Molecular weight
NaH_2PO_4	Sodium dihydrogen phosphate
NEAA	Non-esential amino acids
NHERF	Na^+/H^+ exchanger regulatory factor
pAb	Polyclonal antibody
PBS	Phosphate buffer saline
PE	Phycoerythrin
PI	Propidium iodide
PLL	Poly-L-lysine
PODXL	Podocalyxin

PS	Phosphotidylserine
PVDF	Polyvinylidene fluoride
RPT	Renal proximal tubules
S/N	Supernatant
SCID	Severe combined immunodeficiency
SC-PODXL	Stem cell podocalyxin
SEM	Scanning electron microscopy
SSEA-3	Stage-specific embryonic antigen-3
SSEA-4	Stage-specific embryonic antigen-4
TDT	Terminal deoxynucleotidyl transferase
TGFB3	Transforming growth factor beta-3
TRA-1-60	Tumour rejection antigen-1-60
TRA-1-61	Tumour rejection antigen-1-81
TUNEL	Terminal deoxynucleotidyl transferase dUTP nick end labeling
UV	Ultra-violet
ZVAD	Carbobenzoxy-valyl-alanyl-aspartyl-[O-methyl]
ΔE-MEF	Immortalized mouse embryonic fibroblasts

REFERENCE

1. Bongso A, Richards M. History and perspective of stem cell research. Best.Pract.Res.Clin.Obstet.Gynaecol. 2004;18:827-842.

2. Gerecht-Nir S, Itskovitz-Eldor J. Cell therapy using human embryonic stem cells. Transpl.Immunol. 2004;12:203-209.

3. He JQ, Ma Y, Lee Y et al. Human embryonic stem cells develop into multiple types of cardiac myocytes: action potential characterization. Circ.Res. 2003;93:32-39.

4. Snir M, Kehat I, Gepstein A et al. Assessment of the ultrastructural and proliferative properties of human embryonic stem cell-derived cardiomyocytes. Am.J.Physiol Heart Circ.Physiol 2003;285:H2355-H2363.

5. Assady S, Maor G, Amit M et al. Insulin production by human embryonic stem cells. Diabetes 2001;50:1691-1697.

6. D'Amour KA, Bang AG, Eliazer S et al. Production of pancreatic hormone-expressing endocrine cells from human embryonic stem cells. Nat.Biotechnol. 2006;24:1392-1401.

7. Efrat S. Cell replacement therapy for type 1 diabetes. Trends Mol.Med. 2002;8:334-339.

8. Pankratz MT, Li XJ, Lavaute TM et al. Directed neural differentiation of human embryonic stem cells via an obligated primitive anterior stage. Stem Cells 2007;25:1511-1520.

9. Schulz TC, Palmarini GM, Noggle SA et al. Directed neuronal differentiation of human embryonic stem cells. BMC.Neurosci. 2003;4:27.

10. Reubinoff BE, Itsykson P, Turetsky T et al. Neural progenitors from human embryonic stem cells. Nat.Biotechnol. 2001;19:1134-1140.

11. Hentze H, Graichen R, Colman A. Cell therapy and the safety of embryonic stem cell-derived grafts. Trends Biotechnol. 2007;25:24-32.

12. Hentze H, Soong PL, Wang ST et al. Teratoma formation by human embryonic stem cells: Evaluation of essential parameters for future safety studies. Stem Cell Res. 2009.

13. Shih CC, Forman SJ, Chu P et al. Human embryonic stem cells are prone to generate primitive, undifferentiated tumors in engrafted human fetal tissues in severe combined immunodeficient mice. Stem Cells Dev. 2007;16:893-902.

14. Stewart R, Stojkovic M, Lako M. Mechanisms of self-renewal in human embryonic stem cells. Eur.J.Cancer 2006;42:1257-1272.

15. Brivanlou AH, Gage FH, Jaenisch R et al. Stem cells. Setting standards for human embryonic stem cells. Science 2003;300:913-916.

16. Kannagi R, Cochran NA, Ishigami F et al. Stage-specific embryonic antigens (SSEA-3 and -4) are epitopes of a unique globo-series ganglioside isolated from human teratocarcinoma cells. EMBO J. 1983;2:2355-2361.

17. Badcock G, Pigott C, Goepel J et al. The human embryonal carcinoma marker antigen TRA-1-60 is a sialylated keratan sulfate proteoglycan. Cancer Res. 1999;59:4715-4719.

18. Thomson JA, Itskovitz-Eldor J, Shapiro SS et al. Embryonic stem cell lines derived from human blastocysts. Science 1998;282:1145-1147.

19. Choo A, Padmanabhan J, Chin A et al. Immortalized feeders for the scale-up of human embryonic stem cells in feeder and feeder-free conditions. J.Biotechnol. 2006;122:130-141.

20. Choo AB, Padmanabhan J, Chin AC et al. Expansion of pluripotent human embryonic stem cells on human feeders. Biotechnol.Bioeng. 2004;88:321-331.

21. Alper J. Geron gets green light for human trial of ES cell-derived product. Nat.Biotechnol. 2009;27:213-214.

22. Keirstead HS, Nistor G, Bernal G et al. Human embryonic stem cell-derived oligodendrocyte progenitor cell transplants remyelinate and restore locomotion after spinal cord injury. J.Neurosci. 2005;25:4694-4705.

23. Takahashi K, Tanabe K, Ohnuki M et al. Induction of pluripotent stem cells from adult human fibroblasts by defined factors. Cell 2007;131:861-872.

24. Yu J, Vodyanik MA, Smuga-Otto K et al. Induced pluripotent stem cell lines derived from human somatic cells. Science 2007;318:1917-1920.

25. Yamanaka S. A fresh look at iPS cells. Cell 2009;137:13-17.

26. Liu SP, Fu RH, Huang YC et al. Induced pluripotent stem (iPS) cell research overview. Cell Transplant. 2011;20:15-19.

27. Zaehres H, Scholer HR. Induction of pluripotency: from mouse to human. Cell 2007;131:834-835.

28. Wakitani S, Takaoka K, Hattori T et al. Embryonic stem cells injected into the mouse knee joint form teratomas and subsequently destroy the joint. Rheumatology.(Oxford) 2003;42:162-165.

29. Nussbaum J, Minami E, Laflamme MA et al. Transplantation of undifferentiated murine embryonic stem cells in the heart: teratoma formation and immune response. FASEB J. 2007;21:1345-1357.

30. Fujikawa T, Oh SH, Pi L et al. Teratoma formation leads to failure of treatment for type I diabetes using embryonic stem cell-derived insulin-producing cells. Am.J.Pathol. 2005;166:1781-1791.

31. Amariglio N, Hirshberg A, Scheithauer BW et al. Donor-derived brain tumor following neural stem cell transplantation in an ataxia telangiectasia patient. PLoS.Med. 2009;6:e1000029.

32. Bazil V, Brandt J, Tsukamoto A et al. Apoptosis of human hematopoietic progenitor cells induced by crosslinking of surface CD43, the major sialoglycoprotein of leukocytes. Blood 1995;86:502-511.

33. Zhang N, Khawli LA, Hu P et al. Generation of rituximab polymer may cause hyper-cross-linking-induced apoptosis in non-Hodgkin's lymphomas. Clin.Cancer Res. 2005;11:5971-5980.

34. Loo D, Pryer N, Young P et al. The glycotope-specific RAV12 monoclonal antibody induces oncosis in vitro and has antitumor activity against gastrointestinal adenocarcinoma tumor xenografts in vivo. Mol.Cancer Ther. 2007;6:856-865.

35. Roque-Navarro L, Chakrabandhu K, de Leon J et al. Anti-ganglioside antibody-induced tumor cell death by loss of membrane integrity. Mol.Cancer Ther. 2008;7:2033-2041.

36. Zhang C, Xu Y, Gu J et al. A cell surface receptor defined by a mAb mediates a unique type of cell death similar to oncosis. Proc.Natl.Acad.Sci.U.S.A 1998;95:6290-6295.

37. Zong WX, Thompson CB. Necrotic death as a cell fate. Genes Dev. 2006;20:1-15.

38. Van Cruchten S, Van Den BW. Morphological and biochemical aspects of apoptosis, oncosis and necrosis. Anat.Histol.Embryol. 2002;31:214-223.

39. Trump BF, Berezesky IK, Chang SH et al. The pathways of cell death: oncosis, apoptosis, and necrosis. Toxicol.Pathol. 1997;25:82-88.

40. Kane AB. Redefining cell death. Am.J.Pathol. 1995;146:1-2.

41. Hockenbery D. Defining apoptosis. Am.J.Pathol. 1995;146:16-19.

42. Majno G, Joris I. Apoptosis, oncosis, and necrosis. An overview of cell death. Am.J.Pathol. 1995;146:3-15.

43. Kanduc D, Mittelman A, Serpico R et al. Cell death: apoptosis versus necrosis (review). Int.J.Oncol. 2002;21:165-170.

44. Strasser A, O'Connor L, Dixit VM. Apoptosis signaling. Annu.Rev.Biochem. 2000;69:217-245.

45. Elmore S. Apoptosis: a review of programmed cell death. Toxicol.Pathol. 2007;35:495-516.

46. Hengartner MO. The biochemistry of apoptosis. Nature 2000;407:770-776.

47. Nicholson DW. Caspase structure, proteolytic substrates, and function during apoptotic cell death. Cell Death.Differ. 1999;6:1028-1042.

48. Shi Y. Mechanisms of caspase activation and inhibition during apoptosis. Mol.Cell 2002;9:459-470.

49. Bratton DL, Fadok VA, Richter DA et al. Appearance of phosphatidylserine on apoptotic cells requires calcium-mediated

nonspecific flip-flop and is enhanced by loss of the aminophospholipid translocase. J.Biol.Chem. 1997;272:26159-26165.

50. Koopman G, Reutelingsperger CP, Kuijten GA et al. Annexin V for flow cytometric detection of phosphatidylserine expression on B cells undergoing apoptosis. Blood 1994;84:1415-1420.

51. Ravanat C, Archipoff G, Beretz A et al. Use of annexin-V to demonstrate the role of phosphatidylserine exposure in the maintenance of haemostatic balance by endothelial cells. Biochem.J. 1992;282 (Pt 1):7-13.

52. Bortner CD, Oldenburg NB, Cidlowski JA. The role of DNA fragmentation in apoptosis. Trends Cell Biol. 1995;5:21-26.

53. Enari M, Sakahira H, Yokoyama H et al. A caspase-activated DNase that degrades DNA during apoptosis, and its inhibitor ICAD. Nature 1998;391:43-50.

54. Gavrieli Y, Sherman Y, Ben Sasson SA. Identification of programmed cell death in situ via specific labeling of nuclear DNA fragmentation. J.Cell Biol. 1992;119:493-501.

55. Liu X, Van Vleet T, Schnellmann RG. The role of calpain in oncotic cell death. Annu.Rev.Pharmacol.Toxicol. 2004;44:349-370.

56. Lecoeur H, Prevost MC, Gougeon ML. Oncosis is associated with exposure of phosphatidylserine residues on the outside layer of the

plasma membrane: a reconsideration of the specificity of the annexin V/propidium iodide assay. Cytometry 2001;44:65-72.

57. Ma F, Zhang C, Prasad KV et al. Molecular cloning of Porimin, a novel cell surface receptor mediating oncotic cell death. Proc.Natl.Acad.Sci.U.S.A 2001;98:9778-9783.

58. Chen J, Liu X, Mandel LJ et al. Progressive disruption of the plasma membrane during renal proximal tubule cellular injury. Toxicol.Appl.Pharmacol. 2001;171:1-11.

59. Kern JC, Kehrer JP. Acrolein-induced cell death: a caspase-influenced decision between apoptosis and oncosis/necrosis. Chem.Biol.Interact. 2002;139:79-95.

60. Pan C, Bai X, Fan L et al. Cytoprotection by glycine against ATP-depletion-induced injury is mediated by glycine receptor in renal cells. Biochem.J. 2005;390:447-453.

61. Nishimura Y, Lemasters JJ. Glycine blocks opening of a death channel in cultured hepatic sinusoidal endothelial cells during chemical hypoxia. Cell Death.Differ. 2001;8:850-858.

62. Liu X, Schnellmann RG. Calpain mediates progressive plasma membrane permeability and proteolysis of cytoskeleton-associated paxillin, talin, and vinculin during renal cell death. J.Pharmacol.Exp.Ther. 2003;304:63-70.

63. Perrin BJ, Huttenlocher A. Calpain. Int.J.Biochem.Cell Biol. 2002;34:722-725.

64. Huang Y, Wang KK. The calpain family and human disease. Trends Mol.Med. 2001;7:355-362.

65. Sorimachi H, Ishiura S, Suzuki K. Structure and physiological function of calpains. Biochem.J. 1997;328 (Pt 3):721-732.

66. Yu J, Hu K, Smuga-Otto K et al. Human induced pluripotent stem cells free of vector and transgene sequences. Science 2009;324:797-801.

67. Zhang J, Wilson GF, Soerens AG et al. Functional cardiomyocytes derived from human induced pluripotent stem cells. Circ.Res. 2009;104:e30-e41.

68. Heins N, Lindahl A, Karlsson U et al. Clonal derivation and characterization of human embryonic stem cell lines. J.Biotechnol. 2006;122:511-520.

69. Seth G, Philp RJ, Denoya CD et al. Large-scale gene expression analysis of cholesterol dependence in NS0 cells. Biotechnol.Bioeng. 2005;90:552-567.

70. Lim SF, Chuan KH, Liu S et al. RNAi suppression of Bax and Bak enhances viability in fed-batch cultures of CHO cells. Metab Eng 2006;8:509-522.

71. Sassetti C, Van Zante A, Rosen SD. Identification of endoglycan, a member of the CD34/podocalyxin family of sialomucins. J.Biol.Chem. 2000;275:9001-9010.

72. Sassetti C, Tangemann K, Singer MS et al. Identification of podocalyxin-like protein as a high endothelial venule ligand for L-selectin: parallels to CD34. J.Exp.Med. 1998;187:1965-1975.

73. Kershaw DB, Wiggins JE, Wharram BL et al. Assignment of the human podocalyxin-like protein (PODXL) gene to 7q32-q33. Genomics 1997;45:239-240.

74. Kershaw DB, Beck SG, Wharram BL et al. Molecular cloning and characterization of human podocalyxin-like protein. Orthologous relationship to rabbit PCLP1 and rat podocalyxin. J.Biol.Chem. 1997;272:15708-15714.

75. Schopperle WM, Kershaw DB, DeWolf WC. Human embryonal carcinoma tumor antigen, Gp200/GCTM-2, is podocalyxin. Biochem.Biophys.Res.Commun. 2003;300:285-290.

76. Takeda T, McQuistan T, Orlando RA et al. Loss of glomerular foot processes is associated with uncoupling of podocalyxin from the actin cytoskeleton. J.Clin.Invest 2001;108:289-301.

77. Takeda T, Go WY, Orlando RA et al. Expression of podocalyxin inhibits cell-cell adhesion and modifies junctional properties in Madin-Darby canine kidney cells. Mol.Biol.Cell 2000;11:3219-3232.

78. Brandenberger R, Wei H, Zhang S et al. Transcriptome characterization elucidates signaling networks that control human ES cell growth and differentiation. Nat.Biotechnol. 2004;22:707-716.

79. Schopperle WM, DeWolf WC. The TRA-1-60 and TRA-1-81 human pluripotent stem cell markers are expressed on podocalyxin in embryonal carcinoma. Stem Cells 2007;25:723-730.

80. Chaouchi N, Vazquez A, Galanaud P et al. B cell antigen receptor-mediated apoptosis. Importance of accessory molecules CD19 and CD22, and of surface IgM cross-linking. J.Immunol. 1995;154:3096-3104.

81. Shan D, Ledbetter JA, Press OW. Apoptosis of malignant human B cells by ligation of CD20 with monoclonal antibodies. Blood 1998;91:1644-1652.

82. Van den SP, Rudd PM, Dwek RA et al. Concepts and principles of O-linked glycosylation. Crit Rev.Biochem.Mol.Biol. 1998;33:151-208.

83. Alvarez-Manilla G, Warren NL, Atwood J, III et al. Glycoproteomic analysis of embryonic stem cells: identification of potential glycobiomarkers using lectin affinity chromatography of glycopeptides. J.Proteome.Res. 2010;9:2062-2075.

84. Carpenter GH, Proctor GB. O-linked glycosylation occurs on basic parotid salivary proline-rich proteins. Oral Microbiol.Immunol. 1999;14:309-315.

85. Winkler T, Cantilena A, Metais JY et al. No evidence for clonal selection due to lentiviral integration sites in human induced pluripotent stem cells. Stem Cells 2010;28:687-694.

86. Nakagawa M, Koyanagi M, Tanabe K et al. Generation of induced pluripotent stem cells without Myc from mouse and human fibroblasts. Nat.Biotechnol. 2008;26:101-106.

87. Somasiri A, Nielsen JS, Makretsov N et al. Overexpression of the anti-adhesin podocalyxin is an independent predictor of breast cancer progression. Cancer Res. 2004;64:5068-5073.

88. Casey G, Neville PJ, Liu X et al. Podocalyxin variants and risk of prostate cancer and tumor aggressiveness. Hum.Mol.Genet. 2006;15:735-741.

89. Yang Z, Sui L, Toh WS et al. Stage-dependent effect of TGF-beta1 on chondrogenic differentiation of human embryonic stem cells. Stem Cells Dev. 2009;18:929-940.

90. Kroemer G, Martin SJ. Caspase-independent cell death. Nat.Med. 2005;11:725-730.

91. Matsukawa H, Kanai T, Naganuma M et al. A novel apoptosis-inducing monoclonal antibody (anti-LHK) against a cell surface antigen on colon cancer cells. J.Gastroenterol. 2005;40:945-955.

92. Cartee L, Kucera GL, Willingham MC. Induction of apoptosis by gemcitabine in BG-1 human ovarian cancer cells compared with

induction by staurosporine, paclitaxel and cisplatin. Apoptosis. 1998;3:439-449.

93. Alkhalaf M, El Mowafy A, Renno W et al. Resveratrol-induced apoptosis in human breast cancer cells is mediated primarily through the caspase-3-dependent pathway. Arch.Med.Res. 2008;39:162-168.

94. Zappala G, Elbi C, Edwards J et al. Induction of apoptosis in human prostate cancer cells by insulin-like growth factor binding protein-3 does not require binding to retinoid X receptor-alpha. Endocrinology 2008;149:1802-1812.

95. Nagata S. Apoptosis by death factor. Cell 1997;88:355-365.

96. Ashkenazi A, Dixit VM. Death receptors: signaling and modulation. Science 1998;281:1305-1308.

97. Desagher S, Martinou JC. Mitochondria as the central control point of apoptosis. Trends Cell Biol. 2000;10:369-377.

98. Gross A, Jockel J, Wei MC et al. Enforced dimerization of BAX results in its translocation, mitochondrial dysfunction and apoptosis. EMBO J. 1998;17:3878-3885.

99. Cecconi F. Apaf1 and the apoptotic machinery. Cell Death.Differ. 1999;6:1087-1098.

100. Amorino GP, Fox MH. Intracellular Na+ measurements using sodium green tetraacetate with flow cytometry. Cytometry 1995;21:248-256.

101. Minta A, Tsien RY. Fluorescent indicators for cytosolic sodium. J.Biol.Chem. 1989;264:19449-19457.

102. Zhang GH, Melvin JE. Na+-dependent release of Mg2+ from an intracellular pool in rat sublingual mucous acini. J.Biol.Chem. 1996;271:29067-29072.

103. Schmieder S, Nagai M, Orlando RA et al. Podocalyxin activates RhoA and induces actin reorganization through NHERF1 and Ezrin in MDCK cells. J.Am.Soc.Nephrol. 2004;15:2289-2298.

104. Lebart MC, Benyamin Y. Calpain involvement in the remodeling of cytoskeletal anchorage complexes. FEBS J. 2006;273:3415-3426.

105. Schoenwaelder SM, Burridge K. Bidirectional signaling between the cytoskeleton and integrins. Curr.Opin.Cell Biol. 1999;11:274-286.

106. Liu X, Rainey JJ, Harriman JF et al. Calpains mediate acute renal cell death: role of autolysis and translocation. Am.J.Physiol Renal Physiol 2001;281:F728-F738.

107. Carragher NO, Frame MC. Calpain: a role in cell transformation and migration. Int.J.Biochem.Cell Biol. 2002;34:1539-1543.

108. Inomata M, Hayashi M, Ohno-Iwashita Y et al. Involvement of calpain in integrin-mediated signal transduction. Arch.Biochem.Biophys. 1996;328:129-134.

109. Dedieu S, Poussard S, Mazeres G et al. Myoblast migration is regulated by calpain through its involvement in cell attachment and cytoskeletal organization. Exp.Cell Res. 2004;292:187-200.

110. Bhatt A, Kaverina I, Otey C et al. Regulation of focal complex composition and disassembly by the calcium-dependent protease calpain. J.Cell Sci. 2002;115:3415-3425.

111. Kwak KB, Kambayashi J, Kang MS et al. Cell-penetrating inhibitors of calpain block both membrane fusion and filamin cleavage in chick embryonic myoblasts. FEBS Lett. 1993;323:151-154.

112. Schlaepfer DD, Mehlman T, Burgess WH et al. Structural and functional characterization of endonexin II, a cal. Proc.Natl.Acad.Sci.U.S.A 1987;84:6078-6082.

113. Kobayashi R, Nakayama R, Ohta A et al. Identification of the 32 kDa components of bovine lens EDTA-extractable protein as endonexins I and II. Biochem.J. 1990;266:505-511.

114. Pula G, Bianchi R, Ceccarelli P et al. Characterization of mammalian heart annexins with special reference to CaBP33 (annexin V). FEBS Lett. 1990;277:53-58.

115. Schmidt JM, Zhang J, Lee HS et al. Interaction of talin with actin: sensitive modulation of filament crosslinking activity. Arch.Biochem.Biophys. 1999;366:139-150.

116. Kulkarni S, Saido TC, Suzuki K et al. Calpain mediates integrin-induced signaling at a point upstream of Rho family members. J.Biol.Chem. 1999;274:21265-21275.

117. Dourdin N, Bhatt AK, Dutt P et al. Reduced cell migration and disruption of the actin cytoskeleton in calpain-deficient embryonic fibroblasts. J.Biol.Chem. 2001;276:48382-48388.

118. Tan PC, Furness SG, Merkens H et al. Na+/H+ exchanger regulatory factor-1 is a hematopoietic ligand for a subset of the CD34 family of stem cell surface proteins. Stem Cells 2006;24:1150-1161.

119. Takeda T. Podocyte cytoskeleton is connected to the integral membrane protein podocalyxin through Na+/H+-exchanger regulatory factor 2 and ezrin. Clin.Exp.Nephrol. 2003;7:260-269.

120. Meder D, Shevchenko A, Simons K et al. Gp135/podocalyxin and NHERF-2 participate in the formation of a preapical domain during polarization of MDCK cells. J.Cell Biol. 2005;168:303-313.

121. Weinman EJ. New functions for the NHERF family of proteins. J.Clin.Invest 2001;108:185-186.

122. Denker SP, Barber DL. Cell migration requires both ion translocation and cytoskeletal anchoring by the Na-H exchanger NHE1. J.Cell Biol. 2002;159:1087-1096.

123. Berridge MJ. Inositol trisphosphate and calcium signalling mechanisms. Biochim.Biophys.Acta 2009;1793:933-940.

124. Orrenius S, Zhivotovsky B, Nicotera P. Regulation of cell death: the calcium-apoptosis link. Nat.Rev.Mol.Cell Biol. 2003;4:552-565.

125. Santella L, Puppo A, Chun JT. The role of the actin cytoskeleton in calcium signaling in starfish oocytes. Int.J.Dev.Biol. 2008;52:571-584.

126. Chun JT, Santella L. Roles of the actin-binding proteins in intracellular Ca2+ signalling. Acta Physiol (Oxf) 2009;195:61-70.

127. Margolis DJ, Gartland AJ, Euler T et al. Dendritic calcium signaling in ON and OFF mouse retinal ganglion cells. J.Neurosci. 2010;30:7127-7138.

128. Faria RX, Cascabulho CM, Reis RA et al. Large-conductance channel formation mediated by P2X7 receptor activation is regulated through distinct intracellular signaling pathways in peritoneal macrophages and 2BH4 cells. Naunyn Schmiedebergs Arch.Pharmacol. 2010;382:73-87.

APPENDIX A PUBLICATIONS

(1) Selection against undifferentiated human embryonic stem cells by a cytotoxic antibody recognizing podocalyxin-like protein-1.

Choo AB, **Tan HL**, Ang SN, Fong WJ, Chin A, Lo J, Zheng L, Hentze H, Philp RJ, Oh SK, Yap M.

Stem Cells. 2008 Jun;26(6):1454-63. Epub 2008 Mar 20.

(2) mAb 84, a cytotoxic antibody that kills undifferentiated human embryonic stem cells via oncosis.

Tan HL, Fong WJ, Lee EH, Yap M, Choo A.

Stem Cells. 2009 Aug;27(8):1792-801.

APPENDIX B POSTERS

(1) International Society for Stem Cell Research (ISSCR), 2007.

A cytotoxic antibody that kills human embryonic stem cells by inducing membrane damage.

Heng Liang Tan, Sheu N'go Ang, Angela Chin, Eng Hin Lee, Miranda Yap, Andre Choo.

(2) International Society for Stem Cell Research (ISSCR), 2008.

A cytotoxic antibody that kills human embryonic stem cells by inducing membrane damage.

Heng Liang Tan, Eng Hin Lee, Miranda Yap, Andre Choo

(3) International Society for Stem Cell Research (ISSCR), 2009.

A cytotoxic antibody that kills human embryonic stem cells by inducing membrane damage.

Heng Liang Tan, Wey Jia Fong, Eng Hin Lee, Miranda Yap, Andre Choo

(4) Singapore Stem Cell Consortium (SSCC), 2010

Methods to Eliminate Human Embryonic Stem Cells

Tan Heng Liang, Fong Wey Jia and Andre Choo